On the circadian organization of nitrogen and sulphur metabolism in *Neurospora crassa*

by

Karène Jacques Jensen

Thesis submitted in fulfilment of
the requirements for the degree of
PHILOSOPHIAE DOCTOR
(PhD)

Faculty of Science and Technology
Department of Mathematics and Natural Science
2012

University of Stavanger
N-4036 Stavanger
Norway
www.uis.no

ISBN 978-82-7644-487-2
ISSN 1890-1387

Acknowledgements

I would first of all like to thank my supervisor Professor Dr. Peter Ruoff, for his support during my work with this thesis. I appreciate his expertise and valuable comments.

Secondly, I would like to express my sincere appreciation of my friends and colleagues here at CORE. The days would have been ever so dull without all of you! Dr. Amr Kataya, Behzad Heidari Ahootapeh, Nemie-Feyissa Dugassa, Dr. Else Muller Jonassen, Dr. Ingeborg Knævelsrud, Ingunn Westvik Jolma, and Dr. Kristin Grøsvik. A special thanks goes to Dr. Kristine Marie Olsen for being the best laboratory engineer in the world, ever!

The third mention most definitely belongs to my friends who have put up with me during this process: Marit Svåsand-Ørestrand: I look forward to finally catching up! Monica Hongrø Solbakken and Lars Erik Hamre: I can hardly wait for our celebration at Valle Hovin! \m/. Anette Ulvøy Helland: I owe you some serious Bøker&Børst time!

To Gry Sivertsen and Thor Egil and Eilén Olsen: thank you for being here showing you support!

To my mother and brother, Anne Karin and Kristian Jensen: thank you for your love, support and tolerance!

Last, but definitely not least, to my chauffeur, my chef, my butler, my best friend and partner in crime, Jonny Pollestad Olsen: I would not be here today if not for you! Words do not suffice! Thank you!

Abstract

The purpose of this thesis was to study the circadian organization of the nitrogen and sulphur metabolism in the filamentous fungi *Neurospora crassa*. *Neurospora* is an important model organism used in genetics and circadian rhythm research. Its sporulation rhythm is an easily assayed output of the circadian clock, and is generally used to study properties of the clock. The period length of the sporulation rhythm is temperature compensated and is approximately 22 h when *Neurospora* is grown in constant darkness at 15-30°C. The sporulation rhythm in *Neurospora* has been shown to be dependent on the *frequency* (*frq*) gene, which encodes a negative acting element in the so-called FRQ/WCC (Frequency/White Collar Complex) feedback loop. The FRQ/WCC loop is a negative feedback in which the FRQ protein inhibits its own transcription, and is the assumed core oscillator in the *Neurospora* circadian clock.

Nitrogen is an essential nutrient in all organisms as it is an integral part of proteins and nucleic acids. As nitrogen is often a limiting factor in the environment, many organisms possess complex control systems for its regulation. Nitrate is a secondary source of nitrogen in *Neurospora*. Nitrate assimilation is repressed when preferable nitrogen sources such as ammonium and glutamine are available. In the absence of preferable nitrogen sources, activation of the nitrate assimilation pathway requires the de-repression of the assimilatory pathway. The assimilation of nitrate requires the enzymes nitrate reductase (NR), nitrite reductase (NiR) and glutamine synthetase (GS). The *Neurospora* NR enzyme is highly regulated, and the NR system can be considered as an autonomous negative feedback oscillator.

Endogenous oscillations in NR activity with a period length of approximately 24 h have been found in the *Neurospora* wild-type (wt) strain, as well as in several mutants in which putative key components

of the FRQ/WCC core circadian oscillator were knocked out. In order to further study the nature of the NR activity rhythm, *Neurospora luciferase* (*luc*) reporter strains were constructed. The *luc* gene from the firefly *P. pyralis* had been codon-optimized for *Neurospora*, and was used in the construction of reporter strains in which the promoter of the NR structural gene, *nit-3*, drove the *luc* activity. The NR activity assay and quantitative real-time PCR (qPCR) was used to study the oscillations in NR activity and in *nit-3* mRNA levels. The *luc* activity in the *nit-3-luc* reporter strains was shown to oscillate. However neither the period lengths, nor the phase of the oscillations coincided with activity and transcript measurements obtained from qPCR/activity experiments. Moreover, the *luc* reporter signal was observed in a negative control strain in which the *luc* gene was expressed in the absence of a promoter. Results indicate that nitrogen, molecular oxygen, and metabolic intermediates from intracellular processes appear to modulate the *luc* reporter activity.

The NMR protein has been implicated in the repression of NR activity. NR activity levels were measured for the *nmr-1* mutant, in which the negative feedback of the NR system is removed. As expected, the overall NR activity levels were elevated, but, surprisingly, an oscillatory response with a period length of approximately 24 h was also observed. The oscillations in NR activity levels had been shown to be independent of *frq*, and it was therefore hypothesized that the oscillations in NR activity would be abolished in *frq* and *nmr* double knock-out (KO) strain. Because an oscillatory response in NR could in principle still be mediated via FRQ, Δ*frq*Δ*nmr* KO strains were constructed and the NR activity levels and *nit-3* mRNA expression measured. Surprisingly, oscillations in NR activity with period of approximately 24 h were still observed, suggesting additional control mechanisms other than repression by NMR.

The sporulation rhythm in a Δ*frq*Δ*nmr* KO strain was assayed at 20°, 25°, and 30°C, both under sole nitrate conditions and in the presence of

ammonium. The rhythm persisted at all temperatures under nitrate conditions, but showed poor temperature compensation. This was also found to be the case in a *frq* single KO strain (*frq*^{10}), and in the wt strain. In both cases, a difference in the period length of the sporulation rhythm in nitrate and ammonium was observed. Results therefore indicate that nitrate may exert an effect on the sporulation rhythm of *Neurospora*, and that *frq* appears to be important for the temperature compensation of the sporulation rhythm.

The regulation of the *Neurospora crassa* sulphur circuit is similar to that of nitrate. It is assumed that transcriptional/translational feedback loops involving the positive acting transcription factor CYS-3 as well as the negative acting protein SCON-2, ensure transcription of genes needed for the uptake of sulphur in the form of sulphate. It was therefore hypothesized that CYS-3 and SCON-2 would show periodic oscillations on a circadian time scale. A reaction kinetic model of the *Neurospora* sulphur circuit was tested, and results indicated that CYS-3 and SCON-2 protein concentrations oscillated with a period length of approximately 22 ½ h. To further study the regulation of the sulphur circuit, *cys-3*- and *scon-2 luc*-reporter strains were constructed. Oscillations in *luc* activity were observed for both *cys-3* and *scon-2*, both under nitrate and ammonium conditions. qPCR showed that *cys-3* mRNA was expressed in a rhythmic manner in nitrate. However, a difference in period length was observed when qPCR and the *luc* reporter data were compared. Interestingly, the oscillations observed in the *cys-3-luc* reporters under ammonium conditions, had the same phase and period length (22 h) as *cys-3* levels determined by qPCR.

Abbreviations

APS	adenosine-5’-phosphosulphate
ARS	arylsulfatase
bd	*band*
CCD	charge-coupled device
ccg	*clock controlled gene*
CK	casein kinase
CSA	choline sulphatase
CSN	COP9 signalosome
cys	*cysteine*
DD	constant darkness
DD conditions	constant darkness, 25°C
FFC	FRQ-FRH complex
FGSC	Fungal Genetics Stock Center
fl	*fluffy*
FLO	*frq*-less oscillator
FRH	*frq*-interacting RNA helicase
frq	*frquency*
FWD-1	F-box/WD40-repeat
GS	glutamine synthetase
his	*histidine*
hph	*hygromycin B phosphotransferase*
k	rate constant
K_{diss}	dissociation constant
KO	knock-out
LD	light/dark
Leu	leucine
LL	constant light
LL conditions	constant light, 30°C
luc	*luciferase*
NAT	natural antisense transcript
NiR	nitrite reductase
nit	*nitrate non-utiliser*
nmr	*nitrogen metabolite repressor*
NR	nitrate reductase
ORF	open reading frame

PAPS	3’-phosphoadenosine-5’-phosphosulphate
PAS	Per-Arnt-Sim
PKA/C	protein kinase A/C
PLRE	proximal light-regulated element
PP4	protein phosphatase 4
ROI	region of interest
ROS	reactive oxygen species
SCF	Skp1p/Cdc53p/F-box
SCN	suprachiasmatic nuclei
scon	*sulphur controller*
THX	thioredoxin
Thr	threonine
vvd	*vivid*
wc	*white collar*
WCC	white collar complex
WD	ß-transducin
wt	wild-type

List of figures

List of tables

Contents

1 Introduction

"For centuries man believed that the sun revolves around the earth. Centuries later, he still thinks that time moves clockwise"

- Robert Brault.

1.1 Circadian rhythms and endogenous clocks

The daily rhythms of work and family life during the development of today's modern industrial society have gone through significant changes as a result of technological advances due to modern inventions. Examples include the invention of high precision clocks, and the light bulb in factories, both essential factors to the introduction of shift work that allow production to continue both day and night with the slogan: "time is money". The world has gotten smaller in the sense that air travel is now commonplace and as a result, we are now able to travel rapidly across time zones. These and other technological advances have led to increased research around the human biological clock and how we adapt to abrupt environmental changes. Moreover, advances in medical research have begun to show the importance of understanding the daily changes in metabolic and cellular processes occurring in our bodies, in order for certain drugs to be administered at the optimal times to ensure optimal efficiency and the use of their full potential. Thus, understanding how we, and other organisms, adapt to variations in our environment, for example by sleep and wakefulness, appears essential.

1.1.1 Endogenous clocks

All organisms need to deal with changes in their environment caused by our rotating planet through both daily and seasonal adaptations. The ability to tell the time of day and to respond to environmental cues is therefore essential. Biological rhythms provide organisms with the ability to anticipate the environmental changes arising from the earth's rotation. The rhythmicity is generated by an internal clock that controls a broad spectrum of biological processes. The clock regulates important molecular, physiological and social aspect of biology, preparing an organism for daily or seasonal events. Fungi, for example, release their spores during a clock regulated window of time [1], and plants regulate photosynthesis, stomata opening, leaf movement and growth based on signals from the clock [2]. In mammals, the sleep hormone melatonin is known to show both daily and seasonal variations. The production of melatonin occurs during the night and its regulation is mostly a result of the clock mechanism [3].

The mechanisms controlling these biological rhythms are called the "circadian clock". The name "circadian" is derived from the Latin words *circa* (about) and *dias* (day), and the term depicts an endogenous rhythm with a period length of approximately one day. Circadian clocks have been found in nearly all eukaryotes, including insects, fungi, and mammals. Furthermore, at least one prokaryote, the cyanobacteria *Synecococcus*, has also been shown to have a functioning circadian rhythm. The first circadian rhythm discovered in a cyanobacterium was that of nitrogen fixation, a process whose rate is regulated by the circadian clock to be maximal in the night phase [4,5].

Circadian rhythms manifest at all levels of tissue organization, yet they are found at the level of each individual cell [6]. Understanding the underlying mechanisms of circadian rhythms is essential, and both biochemical, genetic as well as physiological research is being carried out. Results of circadian clock studies are important for many fields,

including human pathology and medication, human physiological health, agriculture and environmental work. The first human clock gene, *hper2*, was identified in 2001 [7]. *Hper2* is a homologue of the *period* (*per*) gene in the fruit fly *Drosophila melanogaster*, and was identified in a family with advanced sleep phase syndrome. Affected individuals carry a missense mutation in *hper2*. Further study of the *hper2* gene may increase the possibility to treat jet lag and sleep problems in adolescents, elderly and shift workers. Bipolar disorder is also thought to be the result of a defect clock [8]. Lithium has long been used in treatment of bipolar disease, although the mechanism through which it works has been unclear. It has been shown that lithium affects the clock, for some individuals, by extending the period length and thereby correcting the defect. This is thought to happen through inhibition of a key kinase GSK3-β, which is inhibited by lithium [8]. Additional indications supporting this view were published by Jolma *et. al.* in 2006. The study concerned the role of lithium in the *Neurospora crassa* circadian clock. Lithium is seen to increase the stability of the FRQ protein, one of the core proteins of the clock, thus leading to an increase in period length [9]. Furthermore, a role for the circadian clock in drug metabolism and detoxification has been shown [10], and functional polymorphisms of circadian regulatory genes have been associated with colorectal cancer survival rate [11].

1.1.2 General properties of circadian rhythms

The complexity of the biological clock varies greatly from organism to organism, but certain basic characteristics have evolved. Traditionally, the circadian system is divided into three functional components (Figure 1.1):

- The input pathway. The input transmits signals from external cues to the oscillator.
- The oscillator. A self-sustained rhythm generator.

- Output rhythms.

The input variables are environmental cues that can affect the oscillator. Input variables can give information to the oscillator and do not necessarily drive it. Environmental cues are also referred to as “zeitgebers” (from German meaning “time givers”). The most common form of input into a circadian system is light. Other zeitgebers include temperature and pH. While the input pathway allows the clock to set itself according to external cues, the output rhythms have characteristics based on the inherited traits of the oscillator. Humans have over one hundred registered output rhythms, the most obvious being the sleep/wake cycle.

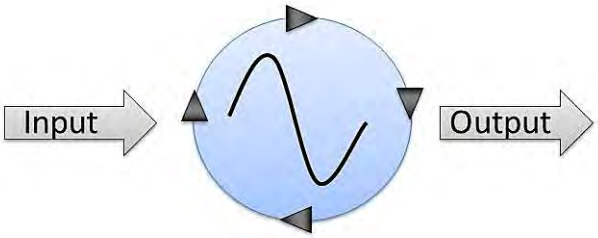

Figure 1.1. A simple model of a circadian oscillator. The input pathway transmits signals (zeitgebers) from external cues to the oscillator. The oscillator generates a self-sustained rhythmicity and regulates various output pathways.

By definition, for an oscillator to be considered circadian, it must fulfil the following requirements [12]:

i. Persistence of the rhythm under constant conditions.
ii. The period length of the oscillator under free-running conditions is approximately 24 h.
iii. The rhythm is entrainable by external cues.
iv. The rhythm is resettable by brief interruptions.
v. The rhythm is compensated so that the period length varies only slightly under different ambient temperature, pH and nutrition.

Circadian rhythms are self-sustained, persisting even in the absence of environmental cues. When the rhythms are observed under constant conditions, they are called free-running rhythms. Circadian rhythms are often studied under free-running conditions, although this is not the normal situation for the organism. An example is asexual spore formation in the filamentous fungi *Neurospora crassa* in darkness [13].

Furthermore, the period length of the oscillator under free-running conditions is approximately 24 h. Circadian rhythms are also entrainable, which refers to the synchronization of circadian rhythms by external cues. The most common cues are light and temperature [14,15]. Light and temperature are constantly fluctuating in nature, so the ability to adapt its internal period length to the external light/dark cycle is critical to an organism's survival. In experiments done with the cyanobacteria *Synecococcus*, mutants with altered entrainment abilities showed a much lower survival rate than mutants with altered period lengths [16].

A circadian oscillator also has to compensate for environmental fluctuations, for example in temperature, salinity, pH or nutrient supply. The circadian system is therefore said to be compensated over a physiological range for environmental parameters. Circadian rhythms have a stable period length in different nutritional conditions and over a given temperature range, thus preserving endogenous timing despite large changes in metabolic rates. Temperature compensation is the most often stated circadian criterion, however pH compensation has also been observed in *Neurospora crassa* [17].

1.1.3 The concept of a core circadian oscillator

The ability of an organism to show endogenous circadian rhythms is often associated with a central molecular clock. This core oscillator is comprised of components whose main purpose is the function of the clock. It has been commonly assumed that this core oscillator is

responsible for driving the physiological systems that rely on timekeeping for their function [18]. Presumably, the general system driving the mechanistic core of the circadian clock is based transcriptional-translational negative feedback oscillators with both positive and negative acting elements. Experimental results from *Neurospora*, *Drosophila*, mammals and cyanobacteria have all contributed a similar picture of the workings of the clock. Central to these systems, are negative feedback loops where the core "clock genes" inhibit their own transcription, together with the positive transcription and translation processes [19]. Such a system is depicted in Figure 1.2.

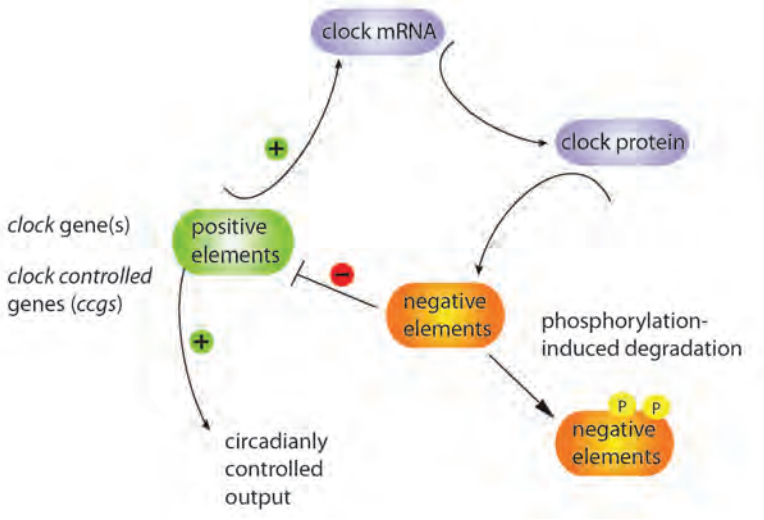

Figure 1.2. A simple transcriptional/translational negative feedback oscillator. The protein products of the negative elements (clock genes) block the activity of the positive elements and turn off their transcription. In addition, the clock protein products promote the expression of the positive elements. Degradation of the negative elements releases the positive elements and transcription starts again.

There is a high degree of conservation between the circadian oscillators of *Neurospora*, *Drosophila* and mammals, which is primarily seen on two major levels: conservation of mechanisms and conservation of regulation methods and components [20]. In terms of mechanisms, the

circadian oscillators of all studied organisms consist of negative feedback loops (Figure 1.2). The positive elements ensure transcription of the negative elements, and the negative elements then inhibit the activities of the positive elements, turning off their transcription and closing the negative feedback loop. In all studied organisms, the negative feedback is in addition interlocked with positive feedback loops, and they share a role in promoting robustness and stability of the clocks. When it comes to the second level of conservation; regulation, it has been found that posttranslational regulation through phosphorylation is important for all studied eukaryotic circadian systems. Phosphorylation is essential for the translocation of the negative acting elements from the cytosol to the nucleus where they can inhibit the positive elements, repressing their own transcription. In addition, the core proteins of the circadian system are progressively phosphorylated, ultimately leading to degradation through the ubiquitin/proteasome pathway. Degradation of the negative elements releases the positive elements, and transcription starts again. As well as determining the subcellular localization of the clock proteins, the phosphorylation status also regulates the level of the positive and negative acting elements. Moreover, the components involved in the post-translational regulation through phosphorylation are highly conserved indicating the importance of the phosphorylation process in circadian timekeeping [20].

Whether or not all organisms have a single, core circadian oscillator that functions as a pacemaker for each clock-controlled output is of current discussion. In *Neurospora*, oscillators that can generate rhythms independently of the assumed core pacemaker have been found (described in section 1.3.3). In mammals, many individual clocks exist, and these multiple-cell, autonomous, circadian clocks are synchronized by a core clock oscillator found in the suprachiasmatic nuclei (SCN) in the brain [21]. The SCN was for a long time viewed as a master regulator, imposing its rhythm onto the “slave” peripheral clocks. The

current view is that the SCN acts as a reference clock used by the peripheral clocks for synchronization and fine-tuning. This leads to coordinated circadian outputs that regulate the expressed rhythms [2,22]. Emerging evidence seems to support this type of multi-oscillator model for the function of the circadian system, and similar systems have also been proposed in *Drosophila* and mice [23]. How these multiple oscillators are connected might differ from organism to organism [24], and the mode of communication between oscillators as well as their coordination is of current interest. The answer might lie within the circadian organization, perhaps a result from evolution, as there seems to be a tendency towards increase in circadian complexity with increasing tissue diversity [25].

1.2 Neurospora crassa as a model organism for the study of circadian systems

1.2.1 The biology of Neurospora crassa

Neurospora crassa is a filamentous fungus more commonly known as red bread mould. It was studied extensively in France in the 1840's when it caused an epidemic infestation of bakeries [26]. *Neurospora* is also the fermenting agent in a soybean or peanut cake common in Indonesia. *Neurospora* is found in moist tropical and subtropical areas, and penetrates many temperate zones, especially in connection with human agriculture and commercial activity [27]. The fungus is often the first colonist in areas of burned-over vegetation. *Neurospora* is an ascomycete and depending on conditions, it propagates asexually or reproduces sexually. The fungus exists mainly as a haploid. The diploid zygote stage immediately undergoes meiosis and generates haploid spores. The asexual and the sexual life cycles of *Neurospora* are depicted in Figure 1.3 and described in sections 1.2.1.1 and 1.2.1.2, respectively.

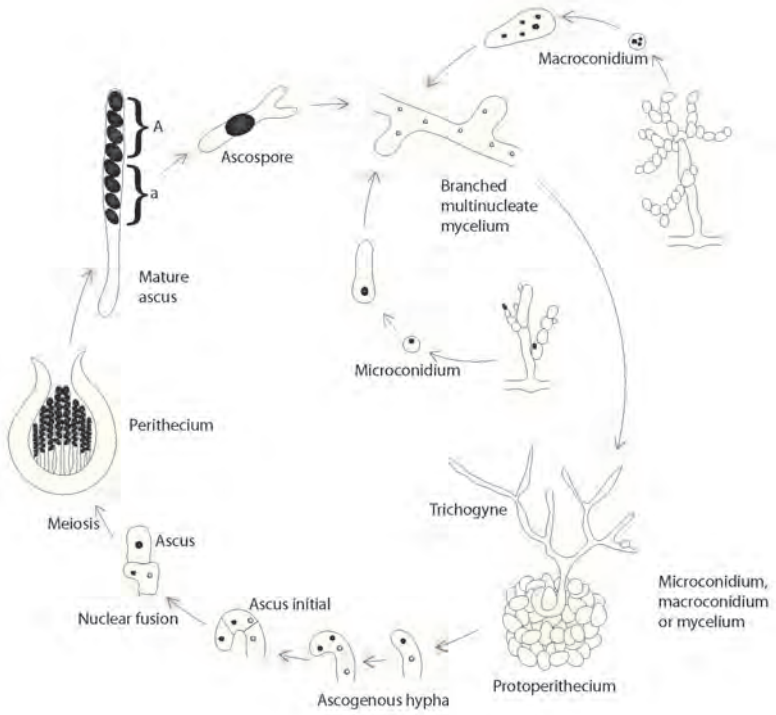

Figure 1.3. The life cycle of *Neurospora crassa*. The asexual cycle (smaller sequence) depicts the formation of macroconidia from aerial hyphae, and their germination to form new mycelium. Microconidial formation is also shown. The sexual cycle (large sequence) is shown with the formation of the protoperithecium, its fertilization via its trichogyne by a conidium of the opposite mating type, and the later events culminating in the formation of ascospores.

1.2.1.1 Asexual cycle

In its asexual stage, *Neurospora* forms a mycelium. Mycelia consist of hyphae, tubular filaments with multiple nuclei (Figure 1.4, panel B). The asexual cycle also includes the formation of macroconidia, formed on aerial hyphae (Figure 1.4, panel C). The macroconidia (or simply conidia) have one to several haploid nuclei, with two nuclei being the most frequent. Genetically different haploid nuclei may coexist in a single conidia or mycelia and such strains are called heterokaryons. The conidia develop an intense orange, carotenoid pigment in the light,

accounting for their pinkish-orange colour (Figure 1.4, panel A). Conidia germinate to form a hypha, which continues to grow by tip extension and by branching out to form a typical mycelium. *Neurospora* also produces uninucleate microconidia. The microconidia usually form singly and are extruded directly from the cells of microconidiophores [28]. Microconidia generally germinate poorly on most standard media, and might have evolved as fertilizing agents in crosses.

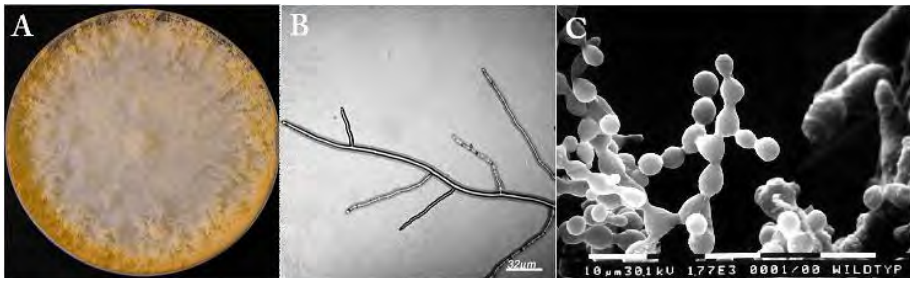

Figure 1.4. Growth and morphology of *Neurospora crassa* during asexual propagation. Photograph A: *Neurospora* wild-type strain grown for 5 days on minimal medium at 25°C. Photograph B: Micrograph of hyphae grown between sheets of cellophane for 24-48 h at 25°C. Photograph C: SEM micrograph of conidia. Photographs A and B are taken by Dr. A. J. F. Griffiths, and photograph C by M. Springer. The pictures are printed with permission from the Fungal Genetics Stock Center (FGSC).

1.2.1.2 Sexual cycle

The sexual cycle (Figure 1.3) of *Neurospora* requires that parents be of different mating types. Mating type is determined by alternative forms of the mating type region, *mat A* or *mat a*. Either strain may act as a female parent by forming a specialized multicellular structure (protoperithecium) containing the female gamete (asgogonium). Fertilization occurs through specialized hyphae (trichogynes), which emerge from the gametic cell. The trichogynes respond to a pheromone emitted by conidia of the opposite mating type, and grow towards them until contact and cell fusion occurs. The fertilizing agent is normally a conidium, however hyphae can also serve as the male element. Upon fusion, a nucleus of the conidium travels through the trichogyne to the

ascogonial cell in the protoperithecium. In the protoperithecium, the male and female nuclei divide several times in a mass of ascogenous hyphae. Nuclei of the opposite mating types fuse, and undergo simultaneous meiosis. At the same time, the protoperithecium enlarges and forms a thick-walled, mature perithecium around the ascogonium. The ascogenous hyphae form asci with eight sexual ascospores (four *mat A* and four *mat a*). Mature asci shoot the ascospores away from the perithecium. The ascospores mature 2-3 days after being shot, and germinate upon heat activation. Dormant ascospores survive in the soil for long periods of until activated by fire or by certain chemicals [29].

1.2.2 Circadian rhythms in Neurospora crassa

The study of circadian rhythms requires model organisms that display an easily assayed output. For *Neurospora*, an easy assay for circadian rhythmicity is the rhythm of asexual spore formation (conidiation). Conidiation is regulated by the *Neurospora* circadian system in concert with environmental factors, including light. In constant darkness (DD), conidia accumulate in dense bands, one per 22 h, showing a free-running circadian rhythm [30]. When grown on minimal medium in so-called “race tubes”, or “growth tubes” conidial banding is clearly visible and easily assayed. Race tubes are long glass tubes, curved slightly at the ends. Figure 1.5 shows an example of a race tube experiment. In constant light (LL), band formation is absent, and conidia are produced continuously. In light-dark (LD) cycles of 24 h, conidia are produced within a precise temporal window that is related to the LD cycle [31]. The *Neurospora* conidiation rhythm is in practise expressed in nearly all strains however one mutant, *band* (*bd*) exhibits the rhythm much more clearly and under more varied conditions than the wild-type (wt) strains [32].

Figure 1.5. Example of a race tube experiment showing the conidial banding in *Neurospora crassa*. The *Neurospora bd* strain was grown on 25 mM nitrate medium, in DD at 25°C. The picture is printed with the permission of P. Ruoff.

Since the discovery of the *bd* strain, nearly all circadian clock experiments have been carried out using this mutant. The *bd* mutant displays all of the characteristic properties of the circadian clock (described in section 1.1.2), and it has been shown that the mutation responsible for the *bd* phenotype is a mutation in the *ras-1* gene [33]. Due to its haploid stage the phenotypes of *Neurospora* mutants are immediately visible and new mutations easily selected. The first clock mutant was reported by Feldman and Hoyle (1973), and bore mutations in the *frequency* (*frq*) gene [34]. The sequencing of the *Neurospora* genome was completed in 2003 [35], and genomic data is available from the Broad Institute database[1]. In addition, the Fungal Genetics Stock Center (FGSC)[2] maintains numerous single- and multiple mutant strains, keeping them readily available to the *Neurospora* community. Substantial genetic and molecular information has also been obtained about species differences and intraspecific variations, building on the efforts by Dr. David D. Perkins (1919-2007) [36]. He sampled strains from all over the world, and this collection is also available from FGSC. It was in fact *Neurospora* that led to the discovery of the one-

[1] http://www.broadinstitute.org/annotation/genome/neurospora/MultiHome.html
[2] http://www.fgsc.net/

gene-one-enzyme hypothesis by Beadle and Tatum [37], and it was the first organism to be used for studying conditional biological mutants. *Neurospora* has even been to space in order to test the functioning of circadian rhythms removed from periodicities of the earth's 24 h rotation [38]. The significant insights we have today into *Neurospora*'s life cycle, behaviour and genetics combined with modern experimental tools and approaches, make *Neurospora* an ideal organism for circadian rhythm studies.

1.3 The current understanding of the FRQ/WCC oscillator of the Neurospora crassa circadian clock

The assumed main circadian oscillator in *Neurospora crassa* is known to consist of a core Frequency/White Collar Complex (FRQ/WCC) autoregulatory transcriptional/translational negative feedback loop where two positive elements function to activate the transcription of a negative element, and the negative element acts to repress its own transcription by inhibiting the activity of the positive elements [39]. In addition, it has been found that the FRQ/WCC oscillator contains multiple feedback loops important for the precision and flexibility of the system [18]. Moreover, the existence of oscillators operating independent of FRQ and potentially also *white collar-1* (WC-1) (section 1.3.3), suggests a multi-oscillator model for the *Neurospora* circadian clock.

Figure 1.6 shows a current model for the molecular network of the *Neurospora crassa* circadian oscillator. The core components of the *Neurospora* circadian oscillator are FRQ, a FRQ-interacting RNA helicase (FRH), WC-1 and WC-2. The positive elements are the WC-1 and WC-2 transcription factors. Both proteins are GATA-type zinc finger DNA-binding proteins. GATA factors serve as transcriptional activators in a wide variety of eukaryotic organisms and bind to

consensus HGATAR (H = A, T, or C, and R = A or C) DNA motifs. The DNA-binding domain is comprised of a zinc finger domain and a successive basic region. In addition to their DNA-binding capacity, most GATA family members can form protein-protein complexes, and these interactions appear to allow for specific regulation of DNA-binding [40]. WC-1 and WC-2 form the heterodimeric WCC via their Per-Arnt-Sim (PAS) domains [39,41-43].

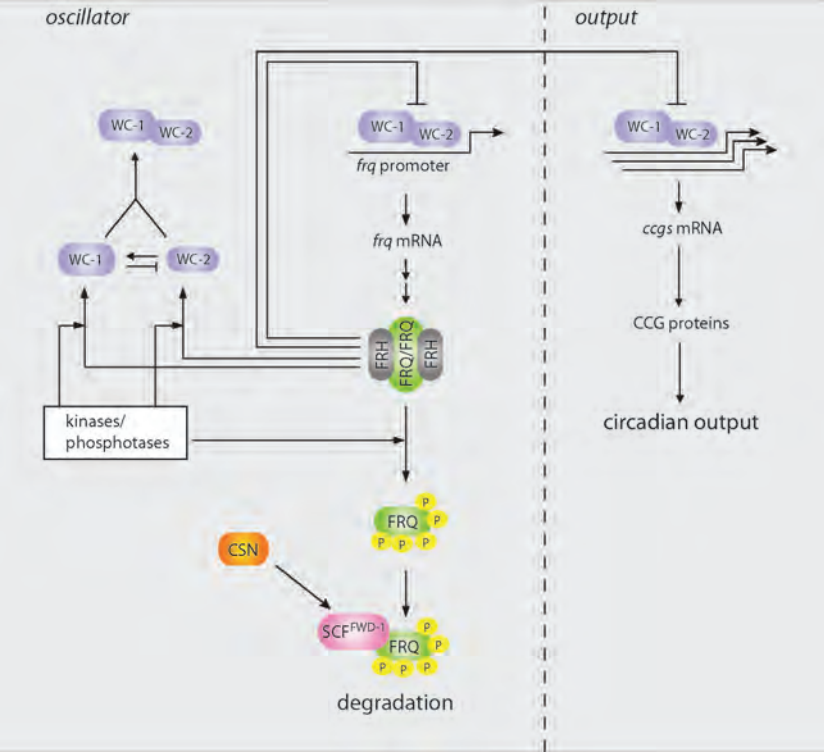

Figure 1.6. Model of the *Neurospora crassa* circadian oscillator. The positive elements WC-1 and WC-2 form a heterodimer that acts as a transcriptional activator for the *frq* gene as well as clock output genes (*ccgs*). The FRQ protein inhibits the WCC thus inhibiting its own transcription and the transcription of the output genes.

The WCC binds to the clock-box (C-box) in the *frq* promoter activating *frq* mRNA transcription [39,44-46]. *frq* mRNA is translated to FRQ protein, the key negative element of the oscillator, which self-associates to form a homodimer through the coiled-coil region near its N-terminus

[47]. The FRQ homodimer then forms a complex with FRH [42], and the FRQ-FRH complex (FFC) enters the nucleus and dissociates WCC from the *frq* promoter by promoting phosphorylation of WCC through the recruitment of several kinases [39,48]. This results in the suppression of *frq* transcription and closing of the negative feedback loop [39,49]. After its synthesis, FRQ undergoes progressive phosphorylation and highly phosphorylated FRQ is degraded by the ubiquitin/proteasome pathway [50,51]. This liberates WCC to once again initiate *frq* transcription. The cyclic activation, repression and reactivation of *frq* expression generate the endogenous circadian rhythmicity, which controls expression of *clock-controlled genes* (*ccgs*) [39]. A more detailed account of the components essential for a functioning clock in *Neurospora crassa* is given in section 1.3.1 and 1.3.2.

1.3.1 The WC-1 and WC-2 proteins

The two positive elements in the *Neurospora* circadian negative feedback loop, WC-1 and WC-2, are both GATA-type zinc finger DNA-binding proteins, which form the WCC. Heterodimerization is mediated by the C-terminal PAS domain of WC-1 and the single PAS domain of WC-2 [39]. WC-1 and WC-2 are found *in vivo* as a heterodimer in at least two different forms, one formed with a one to one relationship of the proteins [52,53], and one with two WC-1 proteins and one WC-2 protein [54]. The ability of WC-1 and WC-2 to form a heterodimer is essential for full activation of transcription [52,54]. WC-1 and WC-2 bind to promoter regions of *frq* and other light inducible genes. Essential for the transcription of the *frq* gene is a *cis*-acting sequence called the C-box, as well as proximal light-regulated element (PLRE) [55]. The C-box contains two GATN-repeats (section 1.3) required for the expression of *frq*. These repeats can be bound by both WC-1 and WC-2, and the binding of the WCC to the C-box is rhythmic [55,56]. WC-1 is also considered to be the main blue-

light photoreceptor for *Neurospora* [52], and all known blue-light responses in the organism have been shown to require functioning WC-1 and WC-2 proteins. Photoresponses include conidiation, entrainment of the circadian clock, and carotenoid synthesis [57-61].

Expression of the *wc-1* gene is driven by three promoters: P_{dist}, P_{prox} and P_{int}. P_{dist} is dependent on WCC. P_{prox} however, is independent of WCC in darkness but inducible by light in a manner depending on WCC. P_{int} is located within the *wc-1* open reading frame (ORF), and promotes expression of an N-terminal truncated WC-1 isoform which function remains unknown. Expression of *wc-1* by P_{dist} or P_{prox} alone affects both light response as well as the phase of circadian conidiation [62]. The roles of the different WC-1 isoforms in the circadian clock are currently under closer investigation [18]. The *wc-2* promoter also contains several transcription initiation sites, which result in the expression of full-length WC-2 as well as an N-terminally shortened isoform, sWC-2. WC-2 and sWC-2 are expressed in an antagonistic manner as an apparent fail-safe mechanism maintaining WC-2 levels above a threshold [63].

Regulation of the WC proteins is achieved on several levels. The WCC is post-transcriptionally regulated by the FRQ protein which inhibits WCC activity by promoting WCC phosphorylation. The kinases mediating the phosphorylation include casein kinase 1 and 2 (CK1 and CK2), as well as protein kinase A and C (PKA and PKC) [39]. Phosphorylation of the WC proteins inhibits their DNA-binding activity. There are five major *in vivo* WC-1 phosphorylation sites (serine sites) located immediately downstream of the DNA-binding domain. Phosphorylation of the sites is a sequential process starting with FRQ-independent phosphorylation at Ser-990 by PKA. This converts the rest of the serine sites into good CK1 or CK2 sites [64]. Phosphorylation of the WC proteins is also reversibly regulated by phosphatases. Protein phosphatase 4 (PP4) has been shown to dephosphorylate the WC proteins, thereby stimulating their activity by

promoting the nuclear entry of the WCC. In the nucleus the WCC binds to DNA, activating the transcription of target genes such as *frq* and *ccgs* [65,66]. The inhibition of WCC transcriptional activity by FRQ-dependent phosphorylation closes the circadian negative feedback loop [39].

Other interconnected feedback loops also contribute to the regulation of the WC proteins: FRQ positively promotes the accumulation of WC-1 and WC-2 (section 1.3.2), and in addition, the WC proteins regulate their own expression. In this interconnected feedback loop, WC-1 negatively regulates WC-2 at the transcriptional level by indirectly inhibiting *wc-2* expression through interaction with a putative repressor [39,54], and WC-2 stabilizes WC-1 by forming the WCC [54,67]. Moreover, recent studies indicate a possible role for WC-1 in *frq*-less oscillators (FLOs) [68-70].

1.3.2 The FRQ and FRH proteins

The FRQ protein is the key negative element of the *Neurospora* circadian oscillator. As described in section 1.3.1, the *frq* gene is regulated through the WCC, which binds to the *frq* promoter C-box and activates *frq* mRNA transcription. The FRQ protein self-associates to form homodimers, which form a complex with FRH. The FFC then promotes phosphorylation of WCC, inhibiting its binding to the *frq* promoter, and thus negatively regulating its own activity. *frq* mRNA and FRQ protein cycle throughout the circadian day. When FRQ is at a minimum, *frq* transcription begins, and then formed FRQ represses *frq* transcription until it disappears from turnover [27].

Essential for clock function is the formation of the FRQ homodimers through the coiled-coil domains in the highly conserved N-terminal region. Deletion of this region eliminates FRQ-FRQ dimerization and inhibits all binding of FRQ to the WCC [47]. In addition, the downregulation of FRH completely abolishes circadian rhythmicity

indicating that FRH is also an essential clock component [42]. Moreover, FRH has also been shown to be necessary for the positive feedback from WC-1, activating expression of *wc-2* (section 1.3.1) [39].

Full-length FRQ contains 989 amino acid residues [71]. Two isoforms exist, one large, lFRQ, and one small, sFRQ, which differ by 100 amino acids at the N-terminus. The isoforms are due to alternative splicing. sFRQ has been shown to be predominant at lower temperatures (<22°C), while lFRQ is the dominant form at higher temperatures (>26°C). The alternative splicing of *frq* functions to tune the period length and reset the clock in response to ambient temperature [72-75]. The *frq* locus also transcribes natural antisense transcript (NAT). This small mRNA does not encode a protein, yet shows low amplitude rhythmicity in anti-phase to *frq* mRNA. The *frq* NAT appears to contribute to the light entrainment of the clock [76].

FRQ is post-translationally regulated by phosphorylation. This controls the FRQ/WCC negative feedback and is important for the clock, especially in terms of period length [42,77]. After its synthesis, FRQ is progressively phosphorylated, becoming extensively phosphorylated before its degradation [74]. Over 75 phosphorylated residues have been identified [78]. Five kinases (CK-1a, CK2, calmodulin kinase 1 (CAMK-1), PKA, and checkpoint kinase 2 (chk2/PRD-4)) have all been shown to phosphorylate FRQ, where CK-1a and CK2 contribute most to the FRQ phosphorylation events [39]. CK-1a and CK2 also mediate the FRQ-dependent phosphorylation of WC-1 and WC-2 which inhibits the WCC activity in order to close the negative feedback loop (described in section 1.3.1) [48,49]. In addition, CK2 regulates temperature compensation of the *Neurospora* clock, allowing it to function precisely at different temperatures [79]. PKA mediates the phosphorylation of both FRQ and the WC proteins [64], and, in contrast to the function of the casein kinases, phosphorylation of FRQ by PKA, results in stabilization of FRQ. It is possible that the

phosphorylation by PKA at certain sites of FRQ can inhibit the efficient ubiquitilation or phosphorylation of FRQ that leads to degradation [39]. Moreover, FRH can also indirectly regulate the phosphorylation profile of FRQ most likely by regulating the protein-protein associations between FRQ and its kinases [39]. The phosphorylation of FRQ as well as the WC proteins is reversibly regulated by several phosphatases [39]. These phosphatases stabilize FRQ and the WC proteins, antagonizing the functions of the kinases. The combined effects of the kinases and phosphatases set the phosphorylation status and thus determine the stability of FRQ. Regulation of the degradation of FRQ is mediated through the progressive phosphorylation of FRQ, and the ubiquitin/proteasome pathway controls this turnover process. The ubiquitination and subsequent degradation of FRQ is dependent on FWD-1, the F-box/WD40-repeat-containing adaptor protein of a Skp1p/Cdc53p/F-box (SCF)-type ubiquitin ligase. Moreover, it has been found that the COP9 signalosome (CSN) plays a role in modulating the clock by regulating the stability of the SCF^{FWD-1} complex [50,51,79] (see Figure 1.6).

Shortly after synthesis, FRQ enters the nucleus to fulfil its role in repressing the WCC function through phosphorylation. In addition, FRQ functions to support the level of WC proteins, forming a positive feedback. The progressive phosphorylation of FRQ appears to trigger a switch of FRQ from a nuclear repressor to a cytoplasmic activator of WC-1 accumulation [80,81]. This positive feedback is thus interlocked with the negative loop, and is suggested to confer stability and robustness to the FRQ/WCC oscillator. FRQ also regulates the levels of *wc-2* mRNA through a yet unknown mechanism [18,44].

1.3.3 frq-less oscillators

The conidiation rhythm in the *frq*-null mutant, frq^9 [82], and the *frq* knock-out (KO) mutant, frq^{10}, indicate a model for the *Neurospora*

clock involving multiple oscillators, termed FLOs. A study by Correa and colleagues used microarray technology to provide molecular evidence for the existence of the FLO, and three *ccgs* were found to be rhythmically expressed in a *frq*-null strain [23]. A later study by de Paula and colleagues, demonstrated that one of these *ccgs*, *ccg-16*, is regulated by a temperature compensated circadian FLO, dependent of the WC proteins [68]. Other WC-dependent FLOs (WC-FLOs) have also been described. It has been found that the conidiation rhythm under constant light conditions in a *vivid* (*vvd*) mutant was dependent of WC-1, but not FRQ [70]. A study on the effect of *Neurospora period* (*prd*) circadian clock mutants on FLOs, proposed a model of the *Neurospora* circadian system in which a single WC-FLO oscillator drives conidiation and interacts with the FRQ/WCC feedback loop [69]. de Paula and colleagues speculate that the interaction between the FRQ/WCC and WC-FLO oscillators occur through the WC proteins [68].

When nitrate is the only nitrogen source, the *Neurospora* nitrate reductase (NR) enzyme shows endogenous oscillations in its activity on a circadian time-scale under both light and dark conditions. Such oscillations have also been found in the frq^9 and frq^{10} mutants, as well as in a *wc-1* KO mutant [83,84]). de Paula and colleagues suggest that the *Neurospora crassa* circadian system is composed of three oscillators: i) the FRQ-based FRQ/WCC oscillator, ii) the FRQ/WCC-independent FLOs [83,84], and iii) the WC-FLOs [68-70]. Li and colleagues suggest that the FRQ/WCC oscillator is a component of a larger system where it interacts with a single FLO. They identified a mutation that disrupts two FLO rhythms and also affects the main FRQ/WCC oscillator. They propose that single FLOs might interact with the main oscillator in a circadian architecture similar to that of cyanobacteria, where the core pacemaker is coupled with a transcriptional/translational feedback loop. They conclude that the simplest model for the architecture of the *Neurospora* circadian system

is a single FLO that mutually interacts with, and is required to support the FRQ/WCC feedback loop [85].

There is an on-going debate concerning the organization of the *Neurospora* circadian system, however accumulating evidence seems to support a multi-oscillator model of interconnected feedback loops. The core clock might be organized as a network of coupled oscillators, which on their own might be less robust. Evidence also suggests the existence of genetically distinct circadian oscillators that function as core oscillators to regulate specific outputs [18].

1.4 Nitrogen metabolism in Neurospora crassa

Nitrogen is an essential nutrient for all organisms as it is an integral part of proteins and nucleic acids. All organisms require nitrogen for their function. Nitrogen is often a limiting factor in the environment, and many organisms therefore have a complex regulatory system for its metabolism. *Neurospora* is capable of utilizing several different secondary nitrogen sources, including nitrate and nitrite salts as well as nucleic acids and proteins. However, *Neurospora*'s preferable nitrogen sources are ammonium salts and glutamine. Ammonium is transported into the cell by two highly specific systems, suggestive of two transporters with different affinities. Once in the cell, ammonium is further assimilated into organic form. In the first system, glutamate dehydrogenase (NADP-GDH) converts α-ketoglutarate and ammonium to glutamate using NADPH as the reducing agent. The second ammonium assimilating system is effective at low concentrations, and consists of a cycle of two enzymes. One is glutamine synthetase (GS) and the other glutamate synthase. GS synthesises glutamine form glutamate, whereas glutamate synthase transfers the amide nitrogen of glutamine to α-ketoglutarate, yielding two molecules of glutamate.

Glutamate and glutamine are the primary nitrogen donors of the cell, and upon nitrogen limitation, the synthesis of glutamine increases.

In the presence of glutamine, the genes involved in the pathway allowing assimilation of nitrate and nitrite are repressed [86,87]. Glutamine appears to be the critical metabolite, which exerts nitrogen catabolite repression. Still unknown however, is the identity in the signal pathway that senses the presence of repressing levels of glutamine [87]. In the absence of ammonium when nitrate or nitrite is present, nitrate repression is lifted (de-repressed), and nitrate is transported into the cell. Nitrate transport is performed by the recently characterized NIT-10 high affinity, transporter protein, encoded by the *nitrate nonutiliser-10* (*nit-10*) structural gene. NIT-10 is a nitrate permease of 541 amino acids and is responsible for the active transport of nitrate across the plasma membrane [88,89].

The use of nitrate requires two enzymes, nitrate reductase (NR) and nitrite reductase (NiR). The presence of nitrate in the cell triggers the transcription of the NR and NiR structural genes, *nit-3* and *nit-6*. *Neurospora* requires de-repression as well as induction through the presence of nitrate to activate transcription of the *nit-3* gene [86,90]. The conversion of nitrate into nitrite is the first step in the enzymatic stepwise reduction of nitrogen from nitrate to glutamine (Figure 1.7). In the second step nitrite is further reduced to ammonium by NiR.

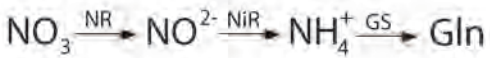

Figure 1.7. The first steps of the nitrate assimilation pathway. Nitrate is reduced to nitrite by NR, and NiR catalyses the reduction of nitrite to ammonium. Ammonium is further incorporated into glutamine by GS.

NR is a large homodimeric multi-redox protein and contains three separate domains separated by hinge regions. Each domain contains a cofactor essential for the catalytic activity of the enzyme. *Neurospora* uses NADPH as a reducing agent and electrons from NADPH are

transferred to a C-terminal flavin domain, which contains a FAD cofactor, then to a central heme-containing domain, and finally to an N-terminal molybdopterin-containing domain where the reduction of nitrate to nitrite takes place [27,87,91]. The NR and NiR structural genes are, although unlinked, regulated in a parallel fashion [92].

1.4.1 A transcriptional/translational negative feedback loop regulates nitrate assimilation in Neurospora crassa

In *Neurospora*, both positive and negative regulator elements make up the transcriptional/translational negative feedback loop regulating the assimilation of nitrate. The genes *nit-2* and *nit-4* comprise the positive transcriptional activators. *nit-2* encodes a Cys_2/Cys_2-type zinc finger DNA-binding protein which is a member of the GATA family of transcriptional activators [93-95] (section 1.3.1) The global acting NIT-2 is involved in the activation of transcription of many of the unlinked the structural genes of the nitrate assimilatory circuit, including *nit-3*, *nit-6*, and *nit-10* [86,89,96]. As is the case for *nit-3*, *nit-6* is regulated at the transcriptional level and eight potential binding sites for NIT-2 are located upstream of *nit-6* [86,92].

The activation of the nitrate assimilatory genes also requires a functional NIT-4 protein. The *nit-4* gene product is a pathway-specific transcriptional activator, and contains a putative DNA-binding domain consisting of an N-terminal Cys_6/Zn_2-type zinc finger motif, and a C-terminal leucine-rich activation domain [97]. The NIT-4 protein is a member of the GAL4 family of fungal transcription factors [98]. The protein is expressed constitutively, but *nit-4* transcript is found in low abundance [99]. It has been shown that the cooperative actions of NIT-2 and NIT-4 are required for the activation of *nit-3* [100,101], and the expression of *nit-10* has also been found to require both proteins [89]. NIT-2 and NIT-4 form a heterodimer, and protein analysis indicates

that the zinc finger DNA-binding domain of NIT-2 as well as both the DNA-binding domain and the C-terminal coiled-coiled activation domain of NIT-4, are sufficient and essential for the interaction [100]. The *nit-3* promoter contains three binding sites for NIT-2, as well as two for NIT-4. All binding sites have been shown to be required for full *nit-3* expression. A study performed by Chiang and Marzluf, revealed that the NIT-2 binding sites contain a varying number of GATA elements necessary for the binding of NIT-2 to the *nit-3* promoter [102]. According to Mo and Marzluf, the most distal NIT-2 binding site is located -1240 bp upstream from the transcription start point, and contains three GATA elements. The two next sites at -1090 bp and -180 bp, contain only one, and four GATA elements, respectively [101]. Both of the distal binding sites showed comparable binding capacity for NIT-2, despite a difference in core elements. They are also clustered with the two binding sites for NIT-4 [102]. Figure 1.8 shows an overview of the NIT-2 and NIT-4 binding sites in the *nit-3* promoter.

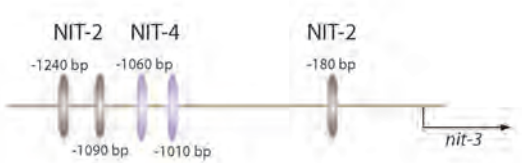

Figure 1.8. Model of the promoter region of the *nit-3* gene. Dark regions indicate NIT-2 binding sites; light regions indicate NIT-4 binding sites. The locations of the binding sites are taken from the study by Mo and Marzluf [101].

Production of NR sets off a series of reactions whereby nitrate is reduces to nitrite, then to ammonium, and finally to glutamine. The accumulation of ammonium and thus glutamine leads to an inactivation of transcription of *nit-3* [86]. The negative acting element in the *Neurospora* NR negative feedback loop has been identified as the *nitrogen metabolite repression* (*nmr*) gene. In a *Neurospora* wt strain, mutations in the *nmr* gene lead to the loss of nitrogen repression, even in the presence of sufficient amounts of glutamine [103,104]. The *nmr* gene is expressed constitutively at very low levels, and the NMR

protein does not appear to possess any DNA-binding activity [105,106]. Repression has been reported to be a result of direct binding of NMR to two α-helices of NIT-2. The first is situated in the N-terminal DNA-binding domain, and the second in the 12 amino acid C-terminal tail [105]. Thus, NMR binds to the DNA-binding motif of NIT-2, thereby hindering its binding to the *nit-3* promoter, resulting in the inhibition of *nit-3* transcription.

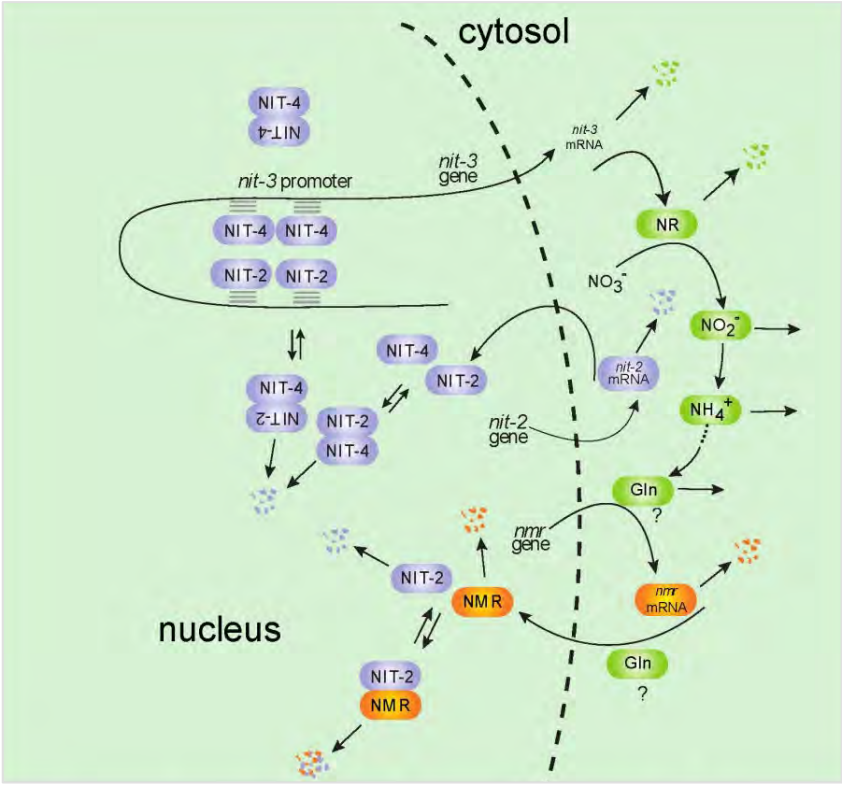

Figure 1.9. A model for the NR negative feedback loop. NIT-2 and NIT-4 form a heterodimer that binds to the *nit-3* promoter. The *nit-3* gene product, NR, reduces nitrate to nitrite in the first step of the pathway leading to accumulation of glutamine. Sufficient levels of glutamine trigger binding of NMR to NIT-2, thus inhibiting the transcription of *nit-3*, resulting in a transcriptional/translational negative feedback loop.

Figure 1.9 overviews the NR negative feedback loop. In the nucleus the NIT-2/NIT-4 complex binds to the *nit-3* promoter, activating the

transcription of NR. Nitrate is reduced to nitrite and the subsequent steps result in the production of glutamine. The internal pool of glutamine is sensed by a yet unknown element, resulting in a binding of the NMR protein to NIT-2. This results in the inhibition of the transcription of *nit-3*, closing the transcriptional/translational negative feedback loop.

1.4.2 Nitrogen metabolism and the circadian clock

Genes involved in assimilation of nitrogen in *Arabidopsis* have been shown to be circadian regulated. These genes include glutamate dehydrogenase, and both an ammonium transporter and a nitrate transporter [107]. In *Neurospora* the role of FLOs involved in conidiation rhythm as well as metabolism is of current debate (section 1.3.3). A possible role for the WC proteins in the regulation of the NR negative feedback loop has been suggested. On one hand, a WC-1 probe has been shown to bind to *nit-3* promoter [100], and putative GATA-sites have located upstream from NIT-2 and NIT-4 binding sites [83]. On the other hand, the oscillations in NR activity have also been found in a *wc-1* mutant, albeit with a lower amplitude [83,84]. The influence of the FRQ/WCC oscillator on the NR negative feedback loop remains to be elucidated.

1.5 Sulphur metabolism in Neurospora crassa

Various sulphur compounds, especially cysteine, methionine and S-adenyosylmethionine are essential for the growth and activity of all cells. Methionine initiates the synthesis of nearly all proteins in an organism, and cysteine plays a critical role in the structure, stability and function of many proteins. In addition, sulphur is an essential component of many other biologically important molecules [109]. Many organisms therefore possess a complex regulatory circuit that

controls the expression of a diverse set of enzymes that function in the acquisition and assimilation, providing a steady supply of sulphur.

1.5.1 The Neurospora crassa sulphur assimilatory pathways

For *Neurospora*, *Aspergillus*, yeast, and other fungi, as well as for plants, inorganic sulphur in form of sulphate is an important sulphur source. In *Neurospora*, sulphate is utilised by a well-defined assimilatory pathway (Figure 1.10), supported by both biochemical evidence [108], and recent genomic data [88]. ATP-sulphurylase (encoded by *cys-11*) produces adenosine-5'-phosphosulphate (APS), which is followed by the production of 3'-phosphoadenosine-5' phosphosulphate (PAPS) by adenylyl sulphate kinase. PAPS is further reduced to sulphite by PAPS reductase, which is encoded by the gene *cys-5*. Sulphite reductase (encoded by *cys-2* and *cys-4*) coverts the sulphite into sulphide, which is then condensed with *O*-acetyl serine by cysteine synthase to generate cysteine [88]. Cysteine is used as an intermediate to form methionine.

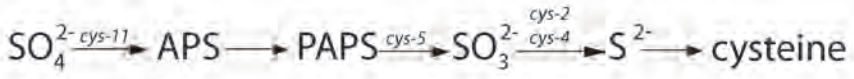

Figure 1.10. The *Neurospora crassa* sulphate assimilatory pathway. Sulphate is converted to APS, which is further converted to PAPS. PAPS is then reduced to sulphite. Sulphite is converted into sulphide, which is used to generated cysteine. The genes encoding some of the enzymes involved are indicated.

The *Neurospora* sulphur regulatory circuit (described in detail in section 1.5.4) operates to ensure that the cells maintain an adequate source of sulphur by repressing the synthesis of various sulphur catabolic enzymes when the cells possess an adequate internal sulphur supply. Sulphur metabolism in *Neurospora* is regulated in a fashion similar to that of nitrate, and the expression of the sulphur assimilatory genes is presumably controlled by transcriptional/translational feedback

loops. When faced with sulphur limiting conditions, a set of assimilatory genes is switched on, ensuring the uptake of inorganic sulphur into the cell. In the case of *Neurospora*, there is strong evidence that cysteine or a closely related compound acts as the metabolite for sulphur repression [109]. When sulphur is limited, the expression of two high-affinity sulphate transporters (permeases) is induced. The structural genes for sulphate permease I and II are *cysteine* (*cys*)-*13* and *cys-14*, respectively. *cys-13* occurs primarily in conidia, while *cys-14* is expressed in the mycelium [110-112]. *cys-14* has been shown to have a slightly lower affinity for sulphate than *cys-13* [27]. Both permeases are subject to sulphur repression and are controlled by the *cys-3* and *sulphur controller* (*scon*) regulatory genes [113] (described in detail in sections 1.5.2 and 1.5.3).

Aromatic sulphate compounds are taken into the cells by sulphate permease I and II, and sulphate is released by arylsulfatase (ARS) [113]. As is the case for the sulphate permeases, the expression of *ars-1* is also dependent on a functional *cys-3* gene. Recent genomic data have also revealed the presence of two additional permeases that presumably have specialized functional roles during other phases of the *Neurospora* life cycle [88]. In addition to the preferred sulphur sources (sulphur, cysteine, homocysteine and methionine), *Neurospora* can also utilise a number of other compounds as secondary sulphur sources. For *Neurospora* as well as other fungi, Choline-*O*-sulphate is an excellent secondary sulphur source, as well as an osmoprotectant [109]. Choline-*O*-sulphate is a storage form of sulphur in *Neurospora*, and is used during germination for the production of sulphate [27]. Upon sulphur limitation, exogenous choline-*O*-sulphate is taken into the cells via a specific permease, and is then hydrolysed by choline sulphatase (CSA) to yield an internal pool of sulphate.

1.5.2 The cysteine-3 positive regulator gene

The *cys-3* gene encodes a 236 amino acid, positive acting regulatory protein that turns on the expression of the sulphur regulatory circuit structural genes (*cys-13*, *cys-14*, *ars-1*, *csa*), as well as the negative regulator gene *scon-2* [27,113-116]. The CYS-3 protein is a sequence-specific bZIP DNA-binding protein [114,117]. Its DNA-binding domain is bipartite, consisting of a leucine zipper responsible for dimerization, and an immediate adjacent basic region (bZIP) that makes direct contact with DNA [118]. Studies show that dimerization of CYS-3 monomers is required for DNA binding. CYS-3 functions only as a homodimer, and does not associate with other bZIP proteins [119]. The CYS-3 protein binds *in vitro* to multiple sites upstream of the *cys-14*, *ars-1* and *scon-2* genes, as well as to three sites in the 5' promoter region of the *cys-3* gene itself [117,120-122]. The consensus CYS-3 DNA-binding site is the sequence ATGRYRYCAT (R = purine, Y = pyrimidine), a 10 bp palindrome representing two abutting 5 bp half-sites. Individual native binding sites differ in their affinity for CYS-3 and deviate slightly from the consensus sequence. The sequence 5'-ATGACGTCAT-3' acts as a strong binding site, and all single nucleotide changes within this sequence resulted in a reduction or even complete loss of CYS-3 DNA binding [123]. Analysis of the three CYS-3 binding sites in the *cys-14* promoter shows that the most distal site (located 1.4 kb upstream of the transcription initiation point) is necessary and sufficient to mediate full-level expression of transcriptional activation [124].

The CYS-3 protein possesses an N-terminal serine/threonine-rich segment, followed by a proline-rich domain, a short acidic region, then the bZIP DNA-binding domain, an alanine-rich segment and a C-terminal serine/threonine-rich region. The N-terminal serine/threonine-rich region may represent the activation domain that function in gene expression in *Neurospora*. It has been hypothesized that phosphorylation and de-phosphorylation of threonine and/or serine

residues in this N-terminal region, may modulate its activation function [120].

cys-3 is expressed at elevated levels when cells are subject to sulphur limiting conditions. The CYS-3 protein autogenously regulates its own expression by binding to elements in the promoter of its own structural gene, strongly enhancing its expression [114,117,125,126]. The *cys-3* promoter contains three binding sites for the CYS-3 protein [120]. The expression and degradation of the CYS-3 protein is regulated in sulphur dependent manner. Both *cys-3* mRNA and CYS-3 protein are present at high levels only in conditions of sulphur starvation. During sulphur limitation, CYS-3 is stable with a half-life greater than 4 h. The protein is however degraded relatively quickly when methionine or inorganic sulphate become available, with a half-life of 10-30 min. The amino acid residue Lys-105 has been shown to be important for CYS-3 instability. If changed to glutamine, the result was a prolonged half-life and impaired responsiveness of CYS-3 degradation to sulphur level changes [127].

1.5.3 The sulphur controller negative regulator genes

The *scon-1*, *scon-2* and *scon-3* genes are the negative regulator elements in the *Neurospora crassa* sulphur circuit. Constitutive expression of sulphur-related genes (e.g., *cys-3*, *ars-1*, *cys-14*), even in the presence of high levels of sulphur, is the typical phenotype of mutants given the *sulphur controller* designation [128]. The *scon-2* gene is reported to encode a 650 amino acid protein with a C-terminal consisting of six β-transducin (WD) repeats. Each WD-repeat consists of approximately 40 amino acid residues, and the repeats appear to mediate protein-protein interactions [122]. In addition, the *scon-2* gene has an N-terminal F-box motif, located roughly 180 residues N-terminal to the WD-repeats. This motif is required for proper function

of the SCON-2 protein. F-boxes have been found within a number of cell cycle regulatory proteins where they mediate ubiquitin-driven proteolytic events required for major cell cycle transitions. Mutational analysis has identified a role for the F-box in regulating CYS-3 expression [129].

F-box proteins have been shown to assemble with other proteins to form the SCF complex. SCF complexes act as E3 ubiquitin ligases to target proteins for ubiquitin-mediated proteolysis, the F-box providing the SCF complex with its target specificity. *scon-3* encodes a 171 amino acid polypeptide which is a Skp1 family homolog. SCON-2 is thought to interact with SCON-3 through its F-box domain. A role for an SCF complex partially comprised of SCON-2 and SCON-3 in sulphur regulation, with CYS-3 as the most likely target, has been hypothesized [128].

Full *scon-2* expression requires a functional CYS-3 protein, and the *scon-2* promoter has four putative CYS-3 binding sites [129]. The presence of CYS-3 is not however sufficient to switch on *scon-2* expression [116]. In a *scon-1* mutant, the levels of *scon-2* mRNA were found to be constitutive [116]. SCON-1 is a nuclear protein, and is postulated to sense the sulphur metabolic repressor molecule cysteine, thus functioning as a sulphur sensor catabolite [27,109].

1.5.4 The Neurospora crassa sulphur regulatory circuit

Figure 1.11 outlines a speculative model for the operation of the *Neurospora* sulphur regulatory circuit, incorporating the information currently available [27,109,120,127-129]. The positive acting *cys-3* gene is expressed when cells become limited for sulphur, and CYS-3 ensures the expression of the unlinked sulphur controlled structural genes (*cys-13*, *cys-14*, *ars-1*, *csa*). In addition, the CYS-3 protein will further increase its own expression and promote the transcription of

scon-2. When sulphur is restored, SCON-2 inhibits the expression of CYS-3. SCON-1 is presumed to convert SCON-2 into an active form by modifying or binding to it. SCON-2 or a SCON-1/SCON-2 complex, may then bind directly to the CYS-3 protein (via its WD-repeats), preventing further *cys-3* expression by inhibiting its positive autogenous control. Alternatively, SCON-2 or a SCON-1/SCON-2 complex, may bind an element in the *cys-3* promoter to directly inhibit transcription. The cellular content of CYS-3 and *cys-3* mRNA will decrease because both are subject to turnover [127]. The turnover rate is presumably increased by SCON-3, in complex with SCON-2 [128]. Thus, the sulphur structural genes requiring *cys-3* expression will be silenced [27,109,113,115,116].

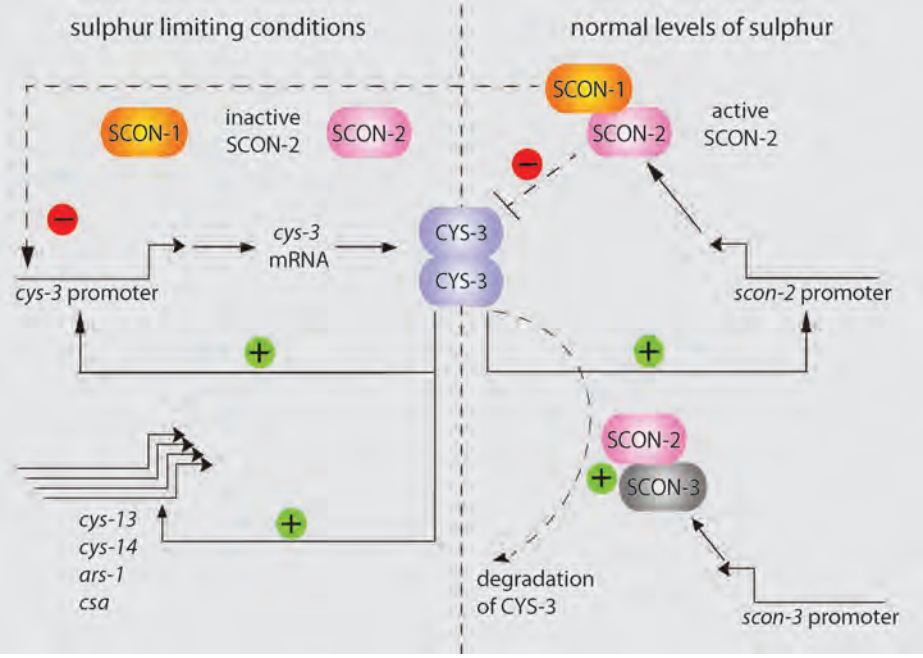

Figure 1.11. Model of the *Neurospora crassa* sulphur regulatory circuit. Under sulphur limiting conditions, CYS-3 is expressed, ensuring the transcription of the sulphur regulatory circuit structural genes. In addition, CYS-3 enhances its own expression, and promotes the transcription of SCON-2. When sulphur is no longer limited, SCON-2 inhibits the expression of CYS-3, by binding (possibly in complex with SCON-1) to the *cys-3* promoter or CYS-3 protein. Furthermore, the degradation rate of CYS-3 is increased by SCON-3 in complex with SCON-2 [27,109,120,127-129].

1.5.5 Sulphur metabolism and the circadian clock

Recent results suggest that some aspect of sulphate reduction might interact with the circadian clock in *Neurospora*. Onai and Nakashima have cloned the structural gene for a *Neurospora crassa* NADPH-dependent thioredoxin reductase, *cys-9* [130]. NTR reduces thioredoxin (THX), and THX reduced by NTR is used to reduce PAPS to sulphite in the sulphate assimilatory pathway. The study showed that a mutation in *cys-9* gene results in abnormal expression of the circadian conidiation rhythm in *Neurospora*. A *cys-9* mutant strain displayed a period length 5 h shorter than that of the wt, and in addition the mutant showed a partial loss of temperature compensation. The study showed that clock-related reaction(s) that require the thioredoxin system and support from the sulphur metabolism may exist [130]. In addition, NTR has been shown to be circadianly regulated in *Arabidopsis* [131].

Moreover in *Arabidopsis*, a cluster of five genes involved in sulphur assimilation have been found to be circadianly regulated. The genes encode enzymes catalysing the uptake and reduction of sulphate and the formation of *O*-acetyl-serine. A gene expression study by Harmer and colleagues, showed that genes encoding the sulphate as well as nitrate transporters peak coordinately towards the end of the night [107]. Cysteine is formed from the condensation of *O*-acetyl-serine and sulphide, representing a link among the sulphur, carbon and nitrogen assimilation pathways. Regulatory interactions between the pathways involved in nitrogen and sulphur assimilation have also been reported. Koprivova and colleagues demonstrated that sulphate reduction is regulated by nitrogen nutrition at the transcriptional level [132].

1.6 Luciferase as a reporter in circadian rhythm studies in Neurospora crassa

The application of luminescent reporting of clock-controlled promoter activities has revolutionized the field of circadian rhythms [133]. The luminescent reporter of choice has been the *luciferase (luc)* gene from the firefly beetle *Photinus pyralis*. The *luc* gene can be coupled to an endogenous promoter and used as a genetically encodable non-invasive reporter of the promoter's activity. The use of *luc* reporters has led to significant advances in circadian rhythm studies in *Arabidopsis*, *Synechococcus*, *Drosophila* and mammalian systems [133,134].

LUC is 62 kDA protein that catalyses the oxidation of the bioluminescent substrate luciferin in the presence of oxygen, ATP and Mg^{2+}. The energy released by this reaction produces an electronically excited state which emits a photon [135]. The *luc* gene does not require post-translational modification for enzyme activity and has a relatively short half-life (2-4 h), allowing its expression to dynamically reflect transcriptional activity. Additionally, *luc* does not require excitation from an external light source, thus avoiding endogenous responses to light [133].

In *Neurospora,* codon-optimized *luc* has been used in the study of the clock-controlled gene *ccg-2* [134,136], and *frq* [136], a key component of the core circadian clock. Two *Neurospora*-optimized *luc* genes were used in these studies, the reporters differing only in the presence of a *ccg-2*-derived intron [136]. The studies show *luc* to be a sensitive reporter of gene expression, for both highly expressed genes and genes expressed at much lower levels. Furthermore, *luc* has been used to assess the activity of the *nit-3* gene in liquid culture under 25 mM nitrate conditions. The *Neurospora* strain examined (designated *nit-3(2.6)-LUCI* in this thesis) was a non-banding strain expressing codon-optimized, intron-containing *luc* under the control of the *nit-3* promoter (i.e. the 2.6 kb DNA sequence upstream from the *nit-3* start codon).

These preliminary analyses showed that the reporter activity measured did not coincide with the NR activity levels measured in the wt assayed under the same experimental conditions and set-up.

1.7 The objective of this thesis

The objective of this thesis was to study the circadian organization of the nitrogen and sulphur metabolism using *Neurospora crassa* as a model organism. Endogenous oscillations in nitrate reductase (NR) activity with a period length of approximately 24 h were found both in the *band* (*bd*) strain (used as a wild-type (wt) strain), as well as in mutants in which putative key components of the *Neurospora* core circadian oscillator were knocked out [83,84]. To understand whether the oscillations in NR were truly temperature compensated, and to study the circadian organization in more detail, new mutants, including reporter strains, were needed.

A major problem encountered during the study was that time-course data showed clear limitations to observe the nature of the NR activity and *nit-3* (the gene encoding NR) mRNA oscillations. The time-course approach produced clear results for the first two days, while after 48 h large uncertainties in the amplitude and period length were observed. Thus, the construction of promoter-*luciferase* (*luc*) reporter strains would enable to follow the oscillations in *nit-3* transcript levels over a longer period of time. Analyses with an initially made *nit-3-luc* reporter kindly provided by Professor Luis F. Larrondo (Santiago, Chile), indicated that the reporter activity measured did not concur with the results obtained from quantitative real-time PCR (qPCR) experiments and by measuring NR activity. A closer inspection showed that this *luc* reporter strain had been transformed with the intron-containing *luc* gene, and did not contain the *bd* mutation. Due to this and due to the size of the *nit-3* promoter sequence inserted (2.6 kb), attempts were made to construct *Neurospora* strains displaying the *bd* phenotype, as

well as expressing both the intron-containing, and the intron-less *luc* gene under the control of shortened versions of the *nit-3* promoter. During the work done in this study, the construction of such strains was undertaken in order to examine the potential difference in expression for the two reporters, as well as to determine the potential effects of the promoter size on reporter expression. Two transformants were studied in detail in both liquid culture and on race tubes, both under nitrate and ammonium conditions. In addition, a spectrophotometric characterization of the *luc* emission signal was carried out to investigate the behaviour of the *luc* reporter system.

A possible role for *wc-1* in the NR oscillator has also been suggested [84]. Therefore, the construction of *wc-1-luc* reporter strains was attempted. In addition, attempts were made to construct strains expressing solely the *Neurospora* optimized *luc* genes, in order to investigate the background (base-line) signal emission pattern. A *luc* negative control strain was characterized both in liquid culture and on race tubes, both under nitrate and ammonium conditions.

The NMR protein has been implicated in the repression of NR activity by interacting with the transcription factor NIT-2. The oscillations in NR activity could therefore be understood as a result of this autonomous negative feedback loop. Thus, in a strain without functional FRQ and NMR proteins, the oscillations in the NR activity and *nit-3* mRNA levels were hypothesized to be abolished. To determine if this was indeed the case, *Neurospora frq* and *nmr* double knock-out (KO) mutant strains were made. NR activity was studied in a wt (*bd*) background, in a *wc-1* and an *nmr* KO, and in the *frq* and *nmr* double KO's. Surprisingly, endogenous oscillations in NR activity was observed in all strains, but as expected [137], NR activity levels were elevated in the *nmr* KO strains. In addition, *nit-3* mRNA levels were studied in both non-banding and in a banding *frq* and *nmr* double KO mutant. Again, oscillations in relative transcript levels of *nit-3* were surprisingly observed, as well as a difference in the *nit-3* expression

pattern between the banding and non-banding strains. Moreover, the existence of a visible sporulation rhythm in the banding strain was shown, and the rhythm was studied at 20°, 25°, and 30°C, both under nitrate and ammonium conditions. In parallel, the wt (*bd*) and the *frq*^{10} mutant, in which no functional FRQ is synthesized, were also studied.

Based on the similarities between the organization and regulation of nitrate and sulphur assimilation in *Neurospora*, it was hypothesized that periodic oscillations on a circadian time-scale would also be seen in CYS-3 and SCON-2. These proteins are assumed to be the key positive and negative components of the *Neurospora crassa* sulphur circuit. A mathematical model of the sulphur regulatory circuit was tested. The model was based on transcriptional/translational negative and positive feedback loops, and supported the presence of oscillations in both CYS-3 and SCON-2. To test this hypothesis further, *luc*-reporter strains were constructed for both the *cys-3* and *scon-2* promoters, and the transformants were characterized both under nitrate and ammonium conditions. Furthermore, primers for determining relative levels of *cys-3* mRNA were designed, and qPCR experiments were carried out. Results clearly showed that *cys-3* mRNA in the wt (*bd*) strain oscillated both under nitrate and ammonium conditions. Under ammonium conditions, the *cys-3* mRNA oscillations were found to be in phase with the emission intensity pattern of a *cys-3-luc* reporter!

Previous studies have indicated a link between the nitrogen and sulphur circuits in *Arabidopsis* [107,132], and therefore, relative *cys-3* mRNA levels were in addition studied in the *frq* and *nmr* double KO mutants. Oscillations in *cys-3* mRNA levels were observed. Surprisingly, as for *nit-3*, a difference in *cys-3* expression could be observed between the banding and non-banding *frq* and *nmr* double KO strains.

2 Materials and Methods

2.1 Strains, media and experimental set up

2.1.1 Strain maintenance

The *Neurospora crassa* strains were obtained from the Fungal Genetics Stock Center (FGSC)[3], with the exception of *frq*^{10} *a, his-3*, and the *luc* reporter strain *nit-3(2.6)-LUCI*. These strains were kindly provided Professor Luis F. Larrondo[4]. Table 2.1 includes a description of the strains used in this thesis along with its identifier. The *bd* strain was used as a wt in this study, and will be referred to as such.

Stocks of *Neurospora* were maintained in glass tubes on slants of Horowitz medium [139] at 4°C, or as conidial suspensions (stored at –20°C). To obtain the conidial suspensions, *Neurospora* was grown on Horowitz tubes for approximately 5 days after which conidia were harvested in 2-5 ml of sterilized tap water. The water was added to the slants, and the tubes vortexed vigorously for 1 min. The conidial suspension was filtered through sterile glass wool before distribution into 500 µl aliquots.

Table 2.1. The *Neurospora crassa* strains used in this thesis. FGSC identifiers in red and Dartmouth identifiers in blue.

Strain	Mutation	Phenotype	Identifier
bd A/a	*bd;ras-1*	Referred to as wt. Produces dense bands of conidia at 22 h intervals on race tubes. Not affected in circadian output of the clock [108].	328-4/87-3
frq^{10} *A/a*	NCU02265.5 *bd;ras-1*	A *frq*$^{-}$ strain produced by gene replacement resulting in a null allele. Produces no FRQ protein. Arrhythmic conidiation and loss of temperature	7490/358-6

[3] www.fgsc.net
[4] Universidad Católica de Chile, Santiago, Chile

		compensation [71]	
wc-1 a	NCU02356.5	A complete *wc-1* KO obtained by the gene replacement method [138]	11711
nmr-1 A/a	NCU04158.2	A complete *nmr* KO obtained by the gene replacement method [138]	14031/14030
fluffy (fl) A/a	*fl*	Aconidate, unable to produce conidia, highly fertile [108]. Used in mating type testing.	4317/4347
his-3 a	*his-3 bd;ras-1*	Requires histidine. Integration of gene constructs by homologue recombination at *his-3* locus [108].	87-74
nit-3-(2.6)LUCI A	*nit-3-luc* reporter strain	Intron-containing *luc* gene [136] expressed by 2.6 kb DNA sequence upstream from *nit-3* start codon.	D06L1

2.1.2 Liquid cultures and experimental set-up

In all time-series experiments Vogel's minimal medium [140] containing ammonium, ammonium nitrate, or nitrate as the nitrogen source was used. A 50X Vogel's ammonium-free medium was prepared by replacing the normally used ammonium nitrate (NH_4NO_3) with sodium nitrate ($NaNO_3$). A 50X Vogel's ammonium medium was prepared by replacing the NH_4NO_3 with ammonium chloride (NH_4Cl). The concentrations of nitrate, ammonium or ammonium nitrate in the 1X solutions were 25 mM. For the ammonium-free Vogel's medium, ammonium ions were also removed from the trace element solution. The normally used $(NH_4)_2Fe(SO_4)_2$ was replaced by an equimolar amount of $FeSO_4 \cdot 7H_2O$.

Inoculation of 200 µl of conidial suspension was done in 90 mm Petri dishes containing 1X Vogel's medium with 2% sucrose (high sucrose). The conidia were distributed evenly by slow rotary shaking for 5 min, and the dishes were placed under constant light (white fluorescent light (25 $\mu mol^{-1}m^{-2}sec^{-1}$) at 30°C (LL conditions). In liquid cultures in Petri dishes, *Neurospora* forms a mycelial mat on the surface of the medium,

followed by subsurface growth. For most strains, an incubation time of 36 h was adequate for the development of a sufficiently dense mycelial mat. For some slower growing strains, incubation in LL conditions lasted for as long as 48 or 60 h. After the period of continuous light exposure, mycelial discs were cut out using a 1 cm cork borer. Three mycelial discs were transferred to a new Petri dish containing 20 ml 1X Vogel's medium and 0.005% sucrose (low sucrose, to dampen growth). The Petri dishes were then transferred to constant darkness at 25°C (DD conditions) for experiments.

Two time-series with a 12 h time difference were prepared by inoculating series 1 and 2 at 8:00 a.m. and 8:00 p.m. respectively on day 1. The two time-courses were run staggered to cover a 48 h period, thus avoiding night time sampling. Harvesting of the mycelial discs started on day 3 (4 for longer LL incubation time) after initial inoculation. The sampling continued at 4 h intervals for 48 h. Harvesting was done by removing excess medium by placing the discs on filter paper. Each set of three discs was quickly wrapped in aluminium foils (prepared previously, marked with strain name, growth conditions, series number, date and number of hours), and the foils were rapidly frozen in liquid nitrogen and then stored at -70°C. Figure 2.1 outlines the experimental set-up for the time-course experiments.

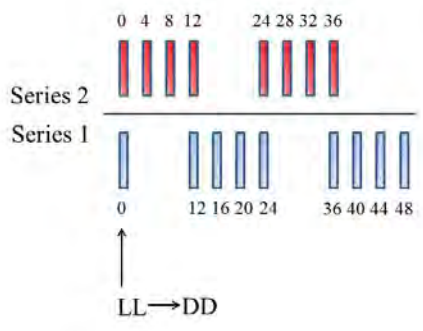

Figure 2.1. 48 h sampling time-course. Two separate time-series were run over the 48 h sampling period. Sampling was done at 4 h intervals. Each bar represents a sampling time-point.

This experimental set-up was used for both the studies of NR activity levels and qPCR experiments.

2.1.3 Shaking cultures

Prior to isolation of genomic DNA, *Neurospora* was grown in shaking cultures. A conidial suspension was used to inoculate Erlenmeyer flasks containing 25 ml of 1X Vogel's medium (high sucrose) with ammonium or ammonium nitrate as the nitrogen source. The cultures were grown in laboratory LD conditions at room temperature (RT) with vigorous shaking (200 rpm) for 24-48 h.

2.1.4 Growth rate experiments

Growth rate experiments were carried out by growing *Neurospora* on race tubes. Race tubes are hollow glass tubes, bent at the ends, partially filled with a solid growth medium (Figure 1.5). Race tube medium was made by adding 1.5% agar and 0.4% sucrose to 1X Vogel' minimal medium with either 25 mM sodium nitrate or 25 mM ammonium chloride as a nitrogen source. The race tube medium was heated until the agar dissolved, and 15 ml agar was added to each race tube. The race tubes were plugged with cotton, autoclaved, and left to solidify for 2 days before inoculation. Inoculation was performed using 5 µl of a conidial solution, or by transferring a small amount of mycelium from Horowitz tubes using an inoculating needle. The race tubes were incubated in DD conditions for the duration of the experiments. The growth of the mycelial front was marked firstly after approximately 24 h and again before the mycelial front reached the end of the tubes, also noting the date and time. At the end of the experiment, the growth rates and, (provided the strain carried the *bd* mutation), the period lengths were determined.

2.2 Neurospora crassa crosses

2.2.1 Sexual crossing

Neurospora crosses were carried out according to protocols derived from the procedures from the FGSC[5]. The crosses were done in glass tubes on slants of Synthetic Cross medium [141] solidified by agar, with 1% sucrose added as carbon source. The crosses were incubated in laboratory LD conditions at RT for approximately 3 weeks, by which time ascospores were shot to the opposite wall of the tube. Individual ascospores were picked to slants containing Horowitz medium and activated in a water bath for 40 min at 50°C[6]. The slants were then incubated in LL conditions for 2-7 days. Following germination, the strains were transferred to Horowitz tubes and conidial suspensions were obtained as described in section 2.1.1.

In an alternative procedure, ascospores were harvested from the cross tubes using a sterile q-tip, and transferred to 1 ml of sterile water in an eppendorf tube. 50 µl/100 µl of this ascospore stock solution was added to an equivalent amount of sterile water and activated at 60°C for 30 min. Following activation, 100 µl of the ascospore solution was transferred to plates containing Vogel's agar (1X Vogel's minimal medium solidified by 1.5% agar) and distributed with the help of sterile glass beads. The plates were incubated at 30°C in LL until germination, and then individual ascospores were picked and transferred to Horowitz tubes.

[5] http://www.fgsc.net/neurosporaprotocols/How%20to%20make%20a%20cross-2.pdf
[6] http://www.fgsc.net/neurosporaprotocols/How%20to%20obtain%20progeny%20as%20randomf%20inal.pdf

2.2.2 Mating type determination

Mating type determination was carried out using the highly fertile aconidiate *fluffy (fl)* strain. The *fl* strains form abundant perithecia more quickly than wt or other fertile strains, and the perithecia are more readily observed. The *mat A* and *mat a fl* strains were used as protoperithecial parents and fertilized with the strains to be scored. Parallel tests performed on both *fl A* and *fl a* provided assurance against false-negative tests, infertility, or spotting errors. Mating type determination was performed according to the protocol obtained from the FGSC[7]. Strains of known mating type were used as controls.

2.3 Molecular biology techniques

2.3.1 Working with E.coli

2.3.1.1 Growth and storage of E.coli

The bacterial strains used in this thesis are listed in Table 2.2.

Table 2.2. *E.coli* strains used in this thesis.

Strain	Genotype
DH5α	F^-, endA1, glnV44, thi-1, recA1, relA1, gyrA96, deoR, nupG, Φ80d*lacZ*ΔM15, Δ(*lacZYA-argF*)U169, hsdR17(r_K^- m_K^+), λ–
JM109	endA1, glnV44, thi-1, relA1, gyrA96, recA1, $mcrB^+$, Δ(lac-proAB), e14- [F' traD36 $proAB^+$ $lacI^q$ lacZΔM15], hsdR17($r_K^-m_K^+$)

The *E.coli* strains were cultured either in liquid Luria-Bertani (LB)-medium with shaking at 200 rpm, or on solid LB-medium in an incubator at 37°C. When applicable, ampicillin was added to the

7 http://www.fgsc.net/neurosporaprotocols/How%20to%20use%20fluffy%20testers%20for%20determining%20mating%20type%20and%20for%20other%20applications.pdf

growth medium at 60 µg/ml. For long-term storage bacterial glycerol stocks were made by mixing 800 µl of fresh overnight culture, with 200 µl sterilized 87% glycerol in a cryogenic tube. The glycerol stocks were stored at -70°C.

2.3.1.2 Transformation of E.coli

Chemically competent *E.coli* cells were prepared for all strains as follows: cells from a stock culture were streaked on an LB-agar plate (supplemented with the appropriate antibiotic) and incubated at 37°C overnight. A single, well-isolated colony was used to inoculate a starter culture (5 ml of LB-broth supplemented with the appropriate antibiotic) and incubated overnight with shaking at 200 rpm at 37°C. 2 ml of saturated overnight culture was added to a sterile 1000 ml flask containing 200 ml LB-medium (no antibiotic). The cells were incubated with shaking at 200 rpm at 37°C to an OD_{600} of 0.4-0.6, and then chilled on ice for 20 min before collection by centrifugation at 2500 rpm for 10 min at 4°C. After centrifugation, the cells were re-suspended in 5 ml of ice-cold TSS solution (85% LB-medium, 10% PEG (w/v, MW 8000), 5% DMSO (v/v), 50 mM $MgCl_2$ [pH 6.5], autoclaved or filter sterilized) before being dispensed into 100 µl aliquots.

For transformation, aliquots of chemically competent cells were thawed on ice before plasmid DNA was added. The solution was gently mixed and incubated on ice for 30 min. The cells were then subjected to heat shock at 42°C for 1 min, followed by incubation on ice for 3 min. 500 µl of LB-medium was then added to each transformation, and the cells incubated with gentle shaking for 30 min. The bacterial cells were then spread on an LB-agar plate with ampicillin added as appropriate, and set to dry for 20 min before incubation at 37°C overnight.

2.3.1.3 Screening for positive E.coli transformants

E.coli colonies were screened for the presence of plasmid DNA using the Colony Fast-Screen (Restriction Screen) Kit[8] (Epicentre), using the standard protocol according to the guidelines provided by the manufacturer.

2.3.2 Polymerase chain reaction

The polymerase chain reaction (PCR) was used to analyse *Neurospora* strains for the presence of specific genes or inserts, as well as for reporter plasmid construction. The conditions and reagent concentrations for the different PCR reactions were varied depending on the primers and the templates, the size of the expected product, and the DNA polymerase used. For analytical purposes, recombinant *Taq* DNA Polymerase and corresponding buffer (Invitrogen) was used. The total volume of the reaction was, either 25 or 50 µl containing 10 mM dNTP mix, 5 or 10 µM of each primer, 2 mM MgCl, approximately 100 ng of genomic template DNA and 1 µl (5 U/µl) of recombinant *Taq* Polymerase. For cloning and sequencing applications, the high fidelity proofreading polymerase Advantage 2 Polymerase Mix (Clontech) was used in accordance to manufacturer's instructions. The total volume of the of the reaction was 50 µl, containing 10 mM dNTP mix, 10 µM of each primer, approximately 100 or 5 ng of genomic and plasmid template DNA respectively, and 1 µl 50X Advantage 2 Polymerase Mix. For all PCR amplifications, the thermal cycling profile was preceded by a denaturation step at 94°C for 5 min. The reactions were carried out for 30-35 cycles as follows: i) denaturation for 1 min at 94°C, ii) primer annealing for 1 min between 60-67°C, iii) elongation for 1min/1 kb at 68/72°C. After the final cycle, the tubes were held at 68/72°C for 5-10 min to promote completion of partial

[8] http://www.epibio.com/pdftechlit/213pl035.pdf

extended products and annealing of single stranded complementary product. For an overview of the primers and conditions used, refer to Table 7.3 in Appendix I.

2.3.3 Nucleic acid preparation

2.3.3.1 DNA extraction

Cellular DNA extraction was carried out using the DNeasy Plant Mini Kit from Qiagen. Plasmid preparations from 5 or 50 ml bacterial overnight cultures were prepared using the QIAprep Spin Miniprep and HiSpeed Plasmid Midi kits, also from Qiagen. Extractions were carried out according to the guidelines provided by the manufacturer[9].

2.3.3.2 Purification of nucleic acids

DNA amplified by PCR was purified using the QIAquick PCR Purification Kit[10] or the QIAquick Gel Extraction Kit[11] (both from Qiagen), according to the guidelines provided by the manufacturer. For the separation of DNA on an agarose gel, gels were made at 0.8% and 5 µl of GelRed solution (1:10 000 dilution of the reagent in water) from VWR, was added to visualize the DNA.

2.3.3.3 Quantification of nucleic acids

The concentration and purity of double-stranded DNA and RNA solutions were determined using several methods. Determinations were made spectrophotometrically, using the Nanodrop 2000 (Thermo Fisher), or using the Qubit Fluorometer (Invitrogen). For

9 http://www.qiagen.com/products/genomicdnastabilizationpurification/dneasyplantsystem/dneasyplantminikit.aspx

10 http://www.qiagen.com/products/dnacleanup/gelpcrsicleanupsystems/qiaquickpcrpurificationkit.aspx

11 http://www.qiagen.com/products/dnacleanup/gelpcrsicleanupsystems/qiaquickgelextractionkit.aspx

spectrophotometric measurements, a dilution of 1:100 was made in molecular biology grade water. Concentrations were calculated using the equations:

Concentration (µg/ml) = A_{260} · dilution · 50 µg/ml DNA

Concentration (µg/ml) = A_{260} · dilution · 40 µg/ml RNA

DNA is considered pure when the ratio between A_{260}/A_{280} is approximately 1.8, whereas pure RNA should have a ratio of 2.0

When using the Nanodrop 2000, 1 µl of the DNA or RNA solution was pipetted onto the pedestal, and the concentration and purity of the sample obtained directly after each measurement.

When using the Qubit Fluorometer and corresponding Qubit DNA/RNA Assay Kit[12], the Qubit DNA/RNA reagent was diluted 1:200 in the corresponding buffer, and the standards were prepared according to the protocol provided by the manufacturer. 1 µl of DNA/RNA solution was added to the working solution, and the total amount of DNA/RNA measured with the Qubit Fluorometer after incubation at room temperature (RT) for 5 min.

2.3.3.4 DNA sequencing

DNA sequencing of both PCR products and plasmid DNA was done at the Genome Analysis Centre (Genome Enterprise Limited, Norwich, UK)[13]

[12] http://probes.invitrogen.com/media/pis/mp33211.pdf
[13] http://orders2.genome-enterprise.com/

2.3.4 Enzymatic manipulation of nucleic acids

2.3.4.1 Restriction enzyme analysis

All restriction digestions were carried out with enzymes obtained from New England Biolabs (NEB)[14]. The enzymes were used according to the manufacturer's guidelines. Reactions volumes were typically 20-50 µl (PCR products, plasmid DNA for ligations, sequencing and transformation of *E.coli*) or 100 µl (plasmid DNA to be used for transformation of *Neurospora*). Incubations were carried out at 37°C for approximately 1-2 h. For an overview of the restriction enzymes and their buffers and restriction sites used in this study, refer to Table 7.4, Appendix I.

2.3.4.2 DNA ligations

T4 DNA ligase from NEB was used in all ligation reactions. PCR products were ligated into either the pBM61, pLUCI or the pRMP62 vector using the following set-up: 0.2 µl of restriction cut and purified plasmid, 20 µl of purified PCR product, 2 µl of T4 NDA ligase buffer (10X), and 1 µl of T4 DNA ligase. The ligations were incubated at 16°C overnight followed by transformation into chemically competent *E.coli* as described in section 2.3.1.2.

2.4 Transformation of Neurospora crassa

Prior to transformation, *Neurospora* was grown on either Horowitz medium [139] or Vogel's agar (1X Vogel's minimal medium solidified by 1.5% agar with 0.2 mg/ml histidine added). Plasmids were transformed into *Neurospora* by electroporation of conidia. The strain *his-3 a* (Table 2.1) was used. The procedure was carried out according

[14] http://www.neb.com

to the protocol from the FGSC[15], using DNA concentrations varying from 500 to 4500 ng. Prior to electroporation, the pLUCI plasmids were linearized with AseI, and the p*cys-3*-NcLUC and pNcLUC plasmids were linearized with SpeI and NdeI respectively. The reaction set-up is described in section 2.3.4.1, and the reaction conditions are listed in Table 7.4 in Appendix I.

2.5 Protein activity studies

The NR activity assay was used to assess the NR activity in various *Neurospora* mutants over a 48 h time-course.

2.5.1 Nitrate reductase activity assay

NR activity is determined as the relationship between the specific activities measured using the following assay, and the total amount of protein measured (section 2.5.2). NR activity levels are given as µmol formed nitrite (NO_2^-) per mg protein per hour.

A slightly modified NR activity assay [142] was performed as follows:

1. 650 µl of assay buffer (50 mM HEPES-KOH [pH 7.5], 2 mM KNO_3, 200 µM NADPH) was pipetted into a 1.5 ml eppendorf tube and heated to 30°C. The assay buffer was prepared in advance and stored at -20°C.
2. 1 ml ice-cold extraction buffer (prepared fresh – 0.1 M HEPES, 1 mM EDTA, 3% (w/v) polyvinylpolypyrrolidone (PVPP), 7 mM cysteine) was added to a pre-cooled 3 ml glass homogenizer. Three mycelial discs were added and immediately homogenized on ice. The homogenate was then transferred to an eppendorf tube. Alternatively, homogenization was carried

15 http://www.fgsc.net/neurosporaprotocols/How%20to%20transform%20Nc%20by%20electroporation.pdf

out using the TissueLyser LT (Qiagen) processing 12 samples at a time: three mycelial discs were added to a 2 ml tube containing a steel bead placed in liquid nitrogen. The tubes were transferred to the adapter, and 1 ml extraction buffer was added. The adaptor was connected to the TissueLyser LT, the lid fastened, and the TissueLyser LT was run successively two times at 50 Hz for 1 min.

3. The samples were centrifuged for 10 min at 4°C and the supernatant transferred to new tubes.
4. 200 µl of the homogenized mycelial discs extraction buffer solution was added to the assay buffer, vortexing well, and incubated at 30°C for 10 min. This was done in triplicate for each sample.
5. 700 µl of colour developing and terminating solution (1% (w/v) sulphanilamide and 0.02% (w/v) N-(1-naphtyl)-ethylenediamine dihydrochloride in 1/10 diluted HCl) was added and the tubes vortexed.
6. The tubes were centrifuged for 30 min at 13000 rpm and the amount of nitrite formed was measured as the absorbance at 540 nm.

2.5.2 Total protein concentration

The amounts of total protein in each extract sample were measured using either the BioRad Protein Assay with IgG as a standard, or the Qubit Fluorometer and corresponding Qubit Protein Assay Kit[16] from Invitrogen. For both methods, the total protein assay was done in triplicates.

[16] http://probes.invitrogen.com/media/pis/mp33211.pdf

2.5.2.1 BioRad Protein Assay

4 µl of protein extract was added to 200 µl of a 1:5 dilution of BioRad Protein Assay concentrate in an eppendorf tube. The total protein amounts were measured after 5-20 min using the Nanodrop 2000 (Bradford Assay).

2.5.2.2 Qubit Protein Assay

The Qubit protein reagent was diluted 1:200 in the Qubit protein buffer. The standards were prepared according to the protocol provided by the manufacturer. 2 µl of protein extract was added to the working solution, and the total amount of protein measured with the Qubit Fluorometer after incubation at RT for 15 min.

2.6 mRNA levels studies

Quantitative real-time polymerase chain reaction (qPCR) studies were performed for the *nit-3* and *cys-3* genes.

2.6.1 RNA extraction

Prior to RNA extraction, samples were harvested and stored as described in section 2.1.2. RNA extraction was done using the Trizol method for RNA extraction with the TissueLyser LT.

Protocol for the Trizol method for RNA extraction

1. The TissueLyser LT adapter was pre-cooled at -20°C. Two mycelial discs were added to a 2 ml tube containing a steel bead placed in liquid nitrogen. The tubes were transferred to the adapter, and 1 ml Trizol was added. The adaptor was connected to the TissueLyser LT, the lid fastened, and the TissueLyser LT was run successively two times at 30 Hz for 1 min.

2. The tubes were incubated at RT for 5 min before centrifugation at 12000 rpm and 4°C for 10 min. The supernatant was transferred to a new tube, and 0.2 ml of chloroform per 1 ml of Trizol was added. The samples were mixed by hand and left at RT for 3 min before centrifugation at 12000 rpm and 4°C for 10 min. The supernatant was transferred to a new tube.
3. 0.5 ml of isopropanol (2-propanol) was added to each tube. The tubes were vortexed for 3 sec before centrifugation at 12000 rpm and 4°C for 10 min.
4. The supernatant was discarded and the RNA pellet was washed by adding 0.5 ml of 75% ethanol before centrifugation at 12000 rpm and 4°C for 5 min.
5. The ethanol was discarded and the pellets air-dried for 15 min.
6. The RNA was dissolved in 45-60 µl of RNase-free water with shaking at 60°C and 1000 rpm for 30 min.

The concentration and purity of the RNA was determined as described in section 2.3.3.3. The RNA was used immediately for cDNA synthesis.

2.6.2 cDNA synthesis

For cDNA synthesis, the High Capacity cDNA Reverse Transcription Kit from Applied Biosystems was used according to the manufacturer's protocol[17]. Equal amounts of RNA adjusted to 50 or 100 ng/20 µl and 2X RT master mix were combined into a reaction volume of 40 µl, and incubated using the following temperature profile: 10 min at 25°C followed by 2 h at 37°C.

17 http://www3.appliedbiosystems.com/cms/groups/mcb_support/documents/generaldocuments/cms_042557.pdf

2.6.3 Primers for quantitative real-time polymerase chain reaction

Forward and reverse primers for the target gene *nit-3* as well as the endogenous control gene *L6* (NCU02707.5, [61]) had previously been designed using the primer design program PRIMER3 [83]. The *cys-3* gene sequence (NCU03536.5) was obtained from the Broad Institute database, and the *cys-3* primers were designed using the Applied Biosystems software, Primer Express. Table 2.3 lists the primers used for qPCR in this thesis. Experiments to determine the amplification efficiency of the *cys-3* target primers were performed (Appendix III).

Table 2.3. Primers used in the qPCR reactions for the target transcripts *nit-3*, and *cys-3*, and endogenous control *L6*.

Gene	Forward primer (5'→3')	Reverse primer (5'→3')	Product size
L6	GCATCGACGAGGCCAAGAT	TCACCAGCCTTCTCCTTGGA	79
nit-3	GCCCAAGGAGATGTATTGGA	GAGTAGGATGCTCGAAACGC	104
cys-3	AAGGAGAGTTGGCGGCAGTA	GGGATTACCGCTGAGCAGAA	90

2.6.4 Quantitative real-time polymerase chain reaction

qPCR was performed using the Applied Biosystems 7300 Real-time PCR System with SYBR Green based detection (*Precision* qPCR MasterMix from Primerdesign). Equal amounts of 2X real-time PCR MasterMix and a mix of primers and template were combined into a reaction volume of 20 µl. The concentration of primers in the final reaction volume was 300 nM, and the cDNA template concentration used was 3 ng/µl. All samples were assayed in triplicates. qPCR was performed using the following temperature profile: 2 min at 50°C, 10 min at 95°C followed by 15 sec at 95°C, and 1 min at 60°C. The number of cycles was set to 40, and a dissociation step was included for each run.

The comparative C_t method was used for the analysis of the amplification results. Upon analysis, the 0 h samples taken prior to transfer to DD for each series (see section 2.1.2) were set as calibrators. The analysis was done using the 7300 System Software (version 1.4.0), and results were manually checked for accuracy.

2.7 Real-time charge-coupled device recordings

To follow the luminescence from the *Neurospora crassa* promoter-*luc* reporter strains in real-time, a liquid nitrogen cooled charge-coupled device (CCD) camera (Roper Scientific) was used. The strains were monitored in an incubator accommodated to the camera, and all experiments were carried out in DD at 25°C.

2.7.1 Experimental set-up

Experiments in both liquid culture (static conditions) and experiments on race tubes were performed. The CCD camera was in addition used to screen for positive transformants following electroporation with the promoter-*luc* plasmid constructs (see section 2.4).

2.7.1.1 Screening for positive transformants

The screening for positive *Neurospora* transformants was performed using a microtitration plate. Three parallel wells were set up for each strain to be screened, and 300 µl of 1X low sucrose Vogel's nitrate medium containing 25 µM of luciferin was added. Filter sterilized luciferin was added to the medium following autoclaving. 5 µl of a conidial suspension from the transformants was added to the wells, and the *luc* activity was monitored for approximately 24 h.

2.7.1.2 Liquid culture experiments

The experiments in liquid culture (static conditions) were performed using several set-ups. For some experiments, the strains were inoculated in 1X high sucrose Vogel's medium as described in section 2.1.2. Following incubation in LL conditions for 36 h, one or more mycelial discs were transferred to a 90 mm Petri dish containing 20 ml low sucrose Vogel's medium, with 25 μM luciferin added (filter sterilized luciferin was added to the medium after autoclaving). The cultures were placed in the incubator and the luminescence monitored for 4-10 days depending on the experiment. In a slightly different set-up, the strains were inoculated as described and, following incubation in LL conditions, one disc was transferred to low sucrose Vogel's medium with 25 μM luciferin added. The cultures were then placed back in LL for 36, 24 12 and 0 h before transfer to DD. In the final set-up, inoculation was done directly in low sucrose Vogel's medium containing 25 μM luciferin, and the cultures were immediately transferred DD conditions.

2.7.1.3 Race tube experiments

Race tube medium was made as described in section 2.1.4. Filter sterilized luciferin from a 2.5 mM stock solution was added to the medium after autoclaving, to a final luciferin concentration of 25 μM. 15 ml race-tube medium containing luciferin was then added to a sterile race tube. The race tubes were plugged with sterile cotton and left to solidify overnight. Similarly, if histidine was added to the race tube medium, 200 mg/ml sterile filtered histidine was added following autoclaving. Inoculation was performed using 5 μl of a conidial solution. The tubes were then transferred to DD conditions for monitoring of luminescence. For some experiments, recordings were started immediately following transfer to DD, and for others, recordings were started approximately 24 h after transfer.

2.7.2 Charged-coupled device recording and signal quantification

The liquid nitrogen cooled CCD camera was set to record 250 frames. Prior to each experiment, the camera was focused to ensure precise recordings. Luminescent signals were accumulated for 10 min every 1 h in DD. Following recording, *luc* emission signals from regions of interest (ROIs) from the cameras field of view were analyzed using the WinView/32 software. Cross sections quantifying the average amount of photons per pixel in the ROI per time frame were taken. For the liquid culture experiments, quantification was performed on the whole Petri dish, on the mycelial disc(s) only, and on smaller regions outside of the discs. For the race tube experiments, quantification was performed on the individual race tube. The cross section data was processed in Microsoft Excel and KaleidaGraph (version 4.0). In pictures of individual frames from the experiments, false-colour luminescence was added. The colours represent luminescence intensity, white to red being brightest and blue dimmest.

2.8 Spectrophotometric studies of the LUCIFERASE-luciferin interaction

Neurospora crassa strains expressing *nit-3-luc* reporter constructs were used for spectrophotometric studies of the interaction between the LUC protein and its substrate luciferin.

2.8.1 Experimental set-up

The strains were inoculated in high sucrose Vogel's as described in section 2.1.2. The strains were incubated in LL for approximately 40 h. 4-8 mycelial discs were cut out and transferred to a 2 ml disposable fluorescence cuvette. 1/1.5 ml of high/low sucrose Vogel's medium or water (depending on the experiment) was added to the cuvette.

Immediately prior to each measurement, 10 µl/15 µl of a 2.5 mM luciferin stock was added to the cuvette. Emitted luminescence was measured using an F-7000 fluorescence spectrophotometer from Hitachi.

2.8.2 Fluorescent spectrophotometer settings

Luminescence was measured at RT in the dark. The Xenon lamp was switched off, and the spectrophotometer was adjusted to the following settings: the shutter was closed and the spectrophotometer set to wavelength scan. The emission start and end wavelengths were set to 450 nm and 700 nm respectively. The scan speed was set to either 1200 nm/min or 2400 nm/min depending on the experiment. The emission slit was set to 20 nm and the response time to 0.5 sec. 5 replicates with a cycle time of 30 sec were measured.

2.9 Computational methods

The programs describing the reaction kinetic models were written using the programming language FORTRAN 77. The subroutine Livermore Solver of Ordinary Differential Equations (LSODE)[18] with double precision was used for solving the differential equations. The compiler Absoft Pro FORTRAN 8.0 was used for compiling and running the programs. Plots were generated by gnuplot[19], and a combined command and Perl[20] script allowed the automated generation of the numerical and graphical output. Gnuplot and Perl are free software.

[18] https://computation.llnl.gov/casc/odepack/download/lsode_agree.html
[19] http://www.gnuplot.info
[20] http://www.perl.org

3 Results

This chapter presents the results achieved during work with this thesis. Firstly, section 3.1 describes the cloning of the *Neurospora* promoter-*luc* reporter strains, and section 3.2 and 3.3 describes their use in the study of nitrate metabolism. Sections 3.4 through 3.7 overview the construction and characterization of Δ*frq*Δ*nmr* double KO strains. Lastly, section 3.8 describes the study of sulphur metabolism in *Neurospora*.

3.1 Cloning of Neurospora crassa promoter-luciferase reporter strains

In a *luc*-based transcriptional reporter the activity of a gene in question is measured by inserting its promoter sequence in front of the *luc* gene, and expressing the reporter construct in the organism of choice. When provided with its substrate luciferin, LUC catalyses the ATP-dependent reaction of luciferin and oxygen, resulting in the emission of chemoluminescence. With an increase of the transcriptional activity of the promoter, the amount of expressed *luc* is also increased, leading to augmented levels of emitted light.

Optimizing the *luc* gene for the codon usage in *Neurospora* has made it possible to monitor the activity of the *frq* and *ccg-2* genes *in vivo*, allowing to follow the clock in real time, even in strains or under conditions in which the circadian rhythm in conidial banding is not expressed [136]. This *luc* reporter has also been used to study the activity of the *nit-3* gene. The strain, *nit-3(2.6)-LUCI* (see Table 2.1), was kindly provided by Professor Luis F. Larrondo (Santiago, Chile). The *nit-3(2.6)-LUCI* strain is a primary transformant, containing a 2.6 kb DNA sequence located upstream from the *nit-3* start codon inserted in front of an intron-containing *luc* gene. Preliminary results with this

strain suggested a phase shift in the *luc* activity measured, compared to qPCR data.

During the work presented in this thesis, two *his-3* targeting vectors containing two different *luc* genes were used in the cloning of the *Neurospora luc*-reporter strains. Both *luc* variants were fully optimized for the codon usage of *Neurospora*, but differed in the presence of an intron. The gene designated *lucI*, contained the *luc* ORF with an intron from the *ccg-2* gene inserted at the location of the first natural occurring intron of the *P.pyrialis* gene [136]. The gene designated *NcLUC* was kindly provided by Professor Deborah Bell-Pedersen[21], and contained the *luc* ORF without any introns inserted. Attempts were made to engineer *luc* reporter strains for the *nit-3*, *wc-1*, *cys-3* and *scon-2* promoter sequences. The promoters were inserted in front of both optimized *luc* genes (using slightly varying cloning strategies) in the hope of determining whether or not the presence of the *ccg-2* intron would have an effect on oscillations in the promoter activity. For the promoter sequences used, as well as for the alignment of the *lucI* and *NcLUC* gene sequences, refer to Table 7.1 and Figure 7.1 in Appendix I.

3.1.1 The sub-cloning of the Neurospora crassa promoter-LUCI reporter constructs

The sub-cloning of the *lucI* gene and the promoter-*lucI* constructs is outlined in Figure 3.1.

[21] Department of Biology, Texas A&M University, USA

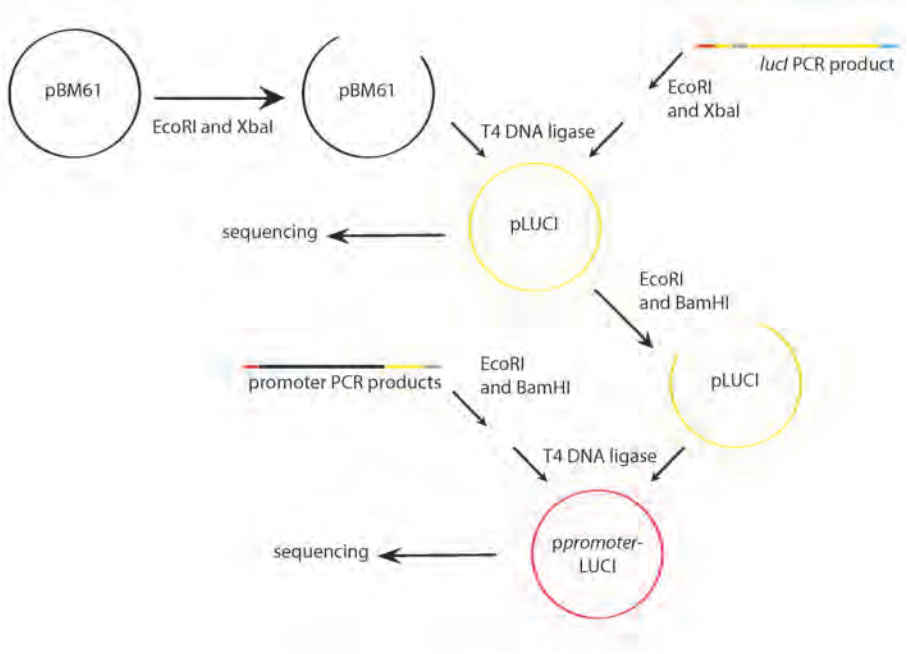

Figure 3.1. Overview of the sub-cloning of the promoter-*lucI* reporter constructs. The *lucI* sequence was amplified by PCR before digestion with the restriction enzymes EcoRI and XbaI. The restriction reaction was then ligated into pBM61 digested with the same enzymes. The resulting plasmid was designated pLUCI, and the *lucI* sequence was verified by sequencing. The promoter PCR products were constructed in the same manner using EcoRI and BamHI restriction sites inserted at the 5'- and 3'-end of the PCR product respectively. The promoter fragments were ligated into the vector pLUCI, and verified by sequencing. EcoRI sites are depicted in red, XbaI sites in blue, and BamHI sites in grey.

The *Neurospora crassa* optimized *lucI* gene containing the *luc* ORF with the *ccg-2* intron inserted, was available in the plasmid pVG110 (Figure 7.2, Appendix I), obtained from the FGSC. The *lucI* gene and the *Neurospora crassa* promoter sequences *nit-3*, *wc-1*, *cys-3*, and *scon-2*, were amplified by PCR (section 2.3.2) using the pVG110 plasmid and genomic DNA isolated from the wt strain (strain #328-4), respectively, as a template. To enable the cloning of the desired promoters, the 5'-end ApaI site in the original *lucI* sequence was removed, and a BamHI site was introduced. This resulted in an alanine to proline mutation at the fourth amino acid in the LUC protein. In

addition, EcoRI and XbaI restriction sites were introduced at the 5'- and 3'-end of the *lucI* sequence respectively. For primer sequences and details regarding the PCR conditions, refer to Table 7.3 in Appendix I. The *lucI* PCR product was analysed on a 0.8% agarose gel, isolated (section 2.3.3.2), and digested with the restriction enzymes EcoRI and XbaI as described in section 2.3.4.1. The pBM61 vector (Figure 7.3, Appendix I) was obtained from the FGSC, and is designed for targeted transformation at the *his-3* locus of *Neurospora* [143]. The restriction reaction was purified as described in section 2.3.3.2 before the *lucI* gene was ligated into linearized pBM61 (section 2.3.4.2). The resulting plasmid was designated pLUCI, and was amplified in *E.coli*, prior to plasmid DNA isolation (sections 2.3.1 and 2.3.3.1). The *lucI* sequence was verified by sequencing (section 2.3.3.4), and *E.coli* strains carrying the vector with the correct insert were preserved as glycerol stocks.

For the sub-cloning of the *nit-3*, *wc-1*, *cys-3* and *scon-2* promoter sequences, restriction sites for EcoRI and BamHI were introduced at the 5'- and 3'-end of the promoter fragments, respectively. In addition, the first part of the *lucI* sequence (from the *lucI* ATG, including the BamHI restriction site) was added to the 3'-flanking primer. This was done to accommodate the ligation of the promoter fragments in frame with the *lucI* gene. For primer sequences and details regarding the PCR conditions, refer to Table 7.3 in Appendix I. Two different *nit-3* promoter constructs were made: *nit-3* (stretching -2000 bp upstream from the *nit-3* start codon), and *nit-3*Δ (-1568 bp upstream from the *nit-3* start codon). The *nit-3*Δ construct was made in the hope to determine if the putative GATA sites in the *nit-3* promoter [83] would affect the transcriptional activity of the *luc* reporter. The sub-cloning procedure for the promoter fragments was the same as for *lucI*, differing only in the restriction enzymes and vector used. Prior to ligation, the PCR products and pLUCI vector were digested with EcoRI and BamHI. The promoter fragments were verified by sequencing, and the resulting

promoter-*luc* reporter constructs were designated p*nit-3*-LUCI, p*nit-3*Δ-LUCI, p*wc-1*-LUCI, p*cys-3*-LUCI, and p*scon-2*-LUCI.

3.1.2 The sub-cloning of the Neurospora crassa promoter-NcLUC reporter constructs

The promoter-NcLUC sub-cloning procedure is outlined in Figure 3.2. The *Neurospora crassa* optimized *NcLUC* gene contains the *luc* ORF without any introns inserted. The gene was available in the plasmid pRMP62 (Figure 7.4, Appendix I), kindly provided by Professor Deborah Bell-Pedersen (Texas A&M University, USA). The pRMP62 is a *Neurospora* expression vector engineered for *his-3* targeting and promoter-*luc* expression. The vector contains the *NcLUC* gene as well as unique restriction sites upstream of the gene, designed to facilitate cloning. The sub-cloning procedure for the *Neurospora nit-3*, *wc-1*, *cys-3*, and *scon-2* promoter fragments was similar to the procedure used for the cloning of the p*promoter*-LUCI constructs described in section 3.1.1. The promoter fragments were amplified by PCR using the genomic DNA isolated from the wt strain (strain #328-4) as a template. For the *nit-3*, *nit-3Δ*, *wc-1*, and *scon-2* promoter fragments restriction sites for NotI and AscI were introduced at the 5'- and 3'-end respectively. For the *cys-3* promoter fragment, a 5'-XbaI and a 3'-NotI restriction site was introduced. For primer sequences and details concerning PCR conditions and the sizes of the PCR products, refer to Table 7.3 in Appendix I. The promoter fragments, as well as the pRMP62 vector were digested with either, NotI and AscI, or with XbaI and NotI. The digested promoter fragments and vectors were then ligated together before proliferation in *E.coli*, identification of positive transformants and plasmid DNA isolation. The promoter fragments were verified by sequencing, and *E.coli* strains carrying the vector with the correct insert were preserved as glycerol stocks. The resulting promoter-NcLUC reporter constructs were designated p*nit-3*-NcLUC,

p*nit-3*Δ-NcLUC, p*cys-3*-NcLUC, and p*wc-1*-NcLUC. The attempts to sub-clone a p*scon-2*-NcLUC construct were unsuccessful.

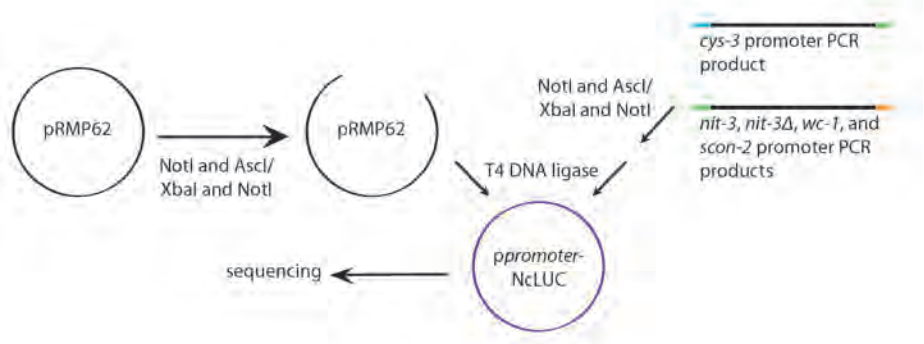

Figure 3.2. Overview of the sub-cloning of the promoter-NcLUC reporter constructs. The promoter sequences were amplified by PCR before digestion with the restriction enzymes NotI and AscI, or XbaI and NotI. The restriction reaction was then ligated into the vector pRMP62 containing the *Neurospora* optimized *NcLUC* gene, digested with the same enzymes. The promoter sequences were verified by sequencing. NotI sites are depicted in green, AscI sites in orange, and XbaI sites in blue.

3.1.3 Transformation of the promoter-luciferase reporter constructs into Neurospora crassa

To express the promoter-*luc* reporter constructs in *Neurospora*, conidia harvested from the *his-3* strain (strain #87-74) were transformed by electroporation. The *his-3* strain contains a mutation in the *his-3* gene, rendering it unable to grow without the addition of histidine in the medium. The expression vectors pBM61 and pRMP62 used in the sub-cloning of the promoter-*luc* reporter constructs are both designed for homologues recombination at the *his-3* locus in *Neurospora*. They contain a wt *his-3* gene fragment followed by a *his-3* 3'-downstream sequence into which the multiple cloning site is inserted. Portions of the plasmids can thus be integrated at *his-3* by a double crossover event. The first crossover regenerates a functional copy of *his-3*, conferring histidine prototrophy on the transformant, and the second

completes the integration of the *his-3* sequence and the DNA insert. This results in the stable incorporation of the DNA fragments into the genome [143,144].

Plasmid DNA was isolated as described in section 2.3.3.1, and electroporation was carried out as described in section 2.4. Prior to electroporation, the pLUCI and p*promoter*-LUCI plasmids were linearized with AseI, and the p*cys-3*-NcLUC and pRMP62 plasmids were linearized with SpeI and NdeI respectively. The additional p*promoter*-NcLUC plasmids could not be linearized as restriction sites for both SpeI and NdeI were present in the promoter sequences. The reaction set-up is described in section 2.3.4.1, and the reaction conditions are listed in Table 7.4, Appendix I. Screening for potential positive transformants were performed as described in section 2.7.1.1.

The promoter-*luc* reporter strains that resulted from the transformation attempts are overviewed in Table 3.1.

Table 3.1. The *Neurospora crassa luc* reporter strains that resulted from the transformation attempts.

Plasmid construct	Transformation	Strain names	Description
pLUCI	Resulted in four transformants with varying signal intensities	*LUCI#4* *LUCI#13* *LUCI#15* *LUCI#16*	Negative control. No promoter inserted. Intron-containing *luc* gene
p*nit-3*-LUCI	Unsuccessful	-	2000 bp upstream from the *nit-3* start codon. Intron-containing *luc*
p*nit-3*Δ-LUCI	Resulted in two transformants with varying signal intensities	*nit-3*Δ*-LUCI#1* *nit-3*Δ*-LUCI#3*	1568 bp upstream from the *nit-3* start codon. Intron-containing *luc*
p*wc-1*-LUCI	Unsuccessful	-	2223 bp upstream from *wc-1* start codon followed by the first 200 bp of the *wc-1* ORF.

			Intron-containing *luc*
p*cys-3*-LUCI	Resulted in four transformants with varying signal intensities	*cys-3-LUCI#1* *cys-3-LUCI#2* *cys-3-LUCI#3* *cys-3-LUCI#5*	1885 bp upstream from the *cys-3* start codon. Intron-containing *luc*
p*scon-2*-LUCI	Resulted in six transformants with varying signal intensities	*scon-2-LUCI#1* *scon-2-LUCI#2* *scon-2-LUCI#3* *scon-2-LUCI#4* *scon-2-LUCI#5* *scon-2-LUCI#6*	2106 bp upstream from the *scon-2* start codon. Intron-containing *luc*
pRMP62	Unsuccessful	-	Negative control. No promoter inserted. Intron-less *luc*
p*nit-3*-NcLUC	Resulted in one positive transformant	*nit-3-NcLUC*	2000 bp upstream from the *nit-3* start codon. Intron-less *luc*
p*nit-3*Δ-NcLUC	Unsuccessful	-	1568 bp upstream from the *nit-3* start codon. Intron-less *luc*
p*wc-1*-NcLUC	Unsuccessful	-	Promoter sequence: 2223 bp upstream from *wc-1* start codon followed by the first 200 bp of the *wc-1* ORF. Intron-less *luc*
p*cys-3*-NcLUC	Unsuccessful	-	1885 bp upstream from the *cys-3* start codon. Intron-less *luc*

The pLUCI and pRMP62 plasmids containing solely the *Neurospora* optimized *luc* genes without a promoter inserted were transformed as negative controls. Transformation of *Neurospora* conidia with pLUCI resulted in four positive transformants. Transformations with both linearized and non-linearized pRMP62 were unsuccessful, as was the case for the *wc-1-luc* reporter constructs, as well as for p*nit-3*-LUCI, p*nit-3*Δ-NcLUC, and p*cys-3*-NcLUC. Attempts were made to optimize the electroporation procedure by varying the amount of both linearized

and non-linearized plasmid DNA, as well as the voltage gradient and the number of pulses.

The *luc* reporter strains selected for further studies were chosen on the basis of their signal intensity levels and oscillatory pattern in liquid culture experiments. The strains selected were *nit-3Δ-LUCI#3*, *LUCI#16*, *cys-3-LUCI#1* and *cys-3-LUCI#5*, and *scon-2-LUCI#4* and *scon-2-LUCI#5*. Being the sole positive transformant carrying a promoter-NcLUC construct, the strain *nit-3-NcLUC* was assayed, although it displayed very low signal emission levels and poor growth. For the characterization of all of the promoter-*luc* primary transformants, refer to Appendix II.

3.2 *Nitrogen metabolism - real-time monitoring of the transcriptional activity of the Neurospora crassa nit-3-luciferase reporter strains*

The promoter activity of the *nit-3-luc* reporter strains was assayed under various experimental set-ups and nutritional conditions as described in section 2.7.1. A liquid-nitrogen cooled CCD camera was used to record the levels of emitted light, and the results were analysed as described in section 2.7.2.

3.2.1 nit-3 promoter activity in liquid culture under nitrate conditions

Experiments in liquid culture (static conditions) were carried out as described in section 2.7.1.2. The promoter activities of the *nit-3Δ-LUCI#3*, *nit-3-NcLUC* and *nit-3(2.6)-LUCI* strains were assayed under 25 mM nitrate conditions.

3.2.1.1 The nit-3Δ-LUCI#3 strain

The *nit-3Δ-LUCI#3* strain was inoculated in high sucrose Vogel's medium and incubated in LL at 30°C for 60 h. Following incubation, one mycelial disc was punched out and transferred to 20 ml low sucrose Vogel's medium with 25 μM of luciferin added. The dishes were placed back in LL conditions for 36, 24, 12 and 0 h before transfer to DD conditions. Two parallels were set up for each time-point, and the dishes were monitored for approximately 3 ½ days (84 h). The results are shown in Figure 3.3.

For the parallels incubated for 36 and 24 h in LL prior to transfer to DD, the emission intensity peaked at approximately 6 h in both the mycelial discs and the whole Petri dishes. This was followed by a decline in the signal intensity and the development of oscillations, which period lengths varied between 12 and 24 h. For the parallels incubated for 12 h in LL, oscillations with period lengths between 8 and 24 h developed. For the parallels transferred directly to DD conditions, oscillations with period lengths between 12 and 22 h were observed. In general, the highest peak in the signal emission intensity appeared first for the discs incubated for 36 and 24 h in LL; second, for the parallels incubated for 12 h in LL; and third, for the parallels transferred directly to DD.

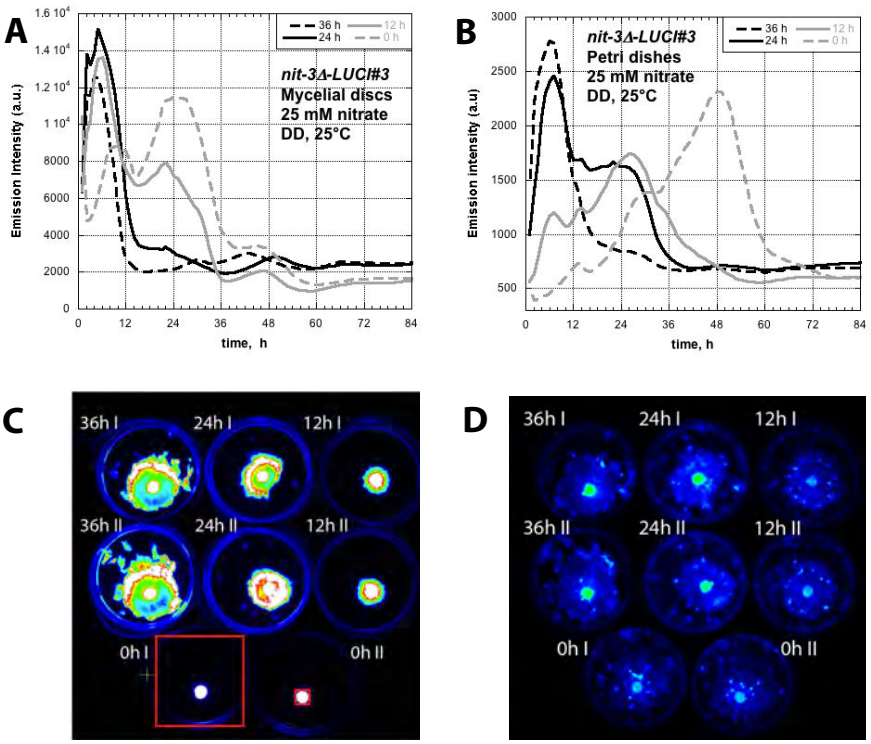

Figure 3.3. Liquid culture experiments performed with the *nit-3Δ-LUCI#3* strain in 25 mM nitrate. The average emitted intensities of the two parallels are shown for the mycelial discs (panel A) and whole Petri dishes (panel B). Panel C shows a picture of the first frame taken after transfer to DD. Typical cross sections of a mycelial disc and a Petri dish used for the emission intensity measurements are shown as red squares, and hours of incubation in LL are indicated. Panel D shows a picture of the last frame taken at the end of the experiment. Colours represent luminescence intensity, white to red being brightest, and blue dimmest.

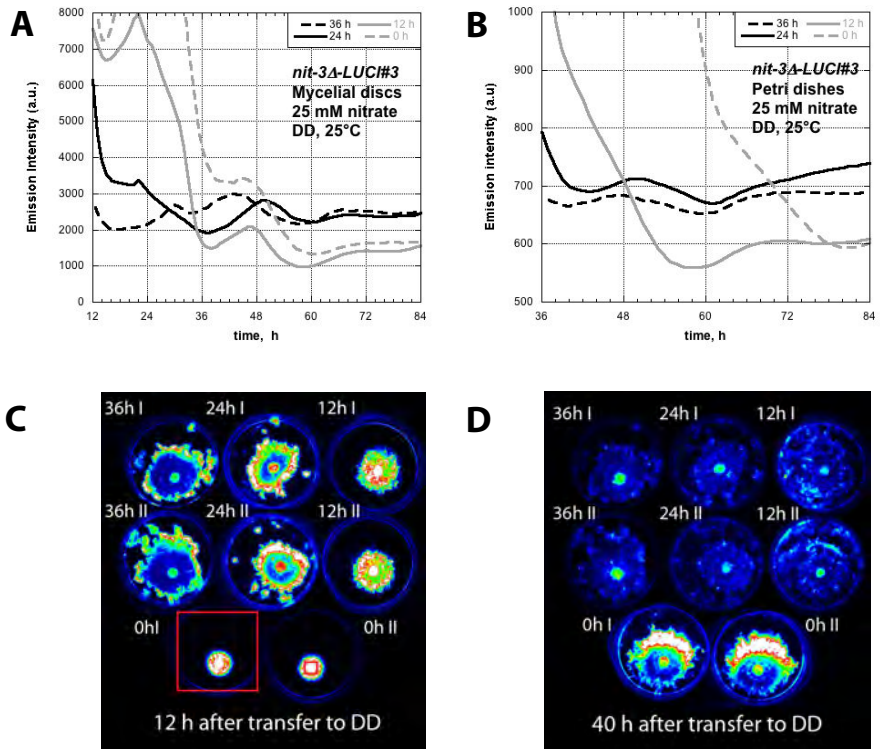

Figure 3.4. Time-sections of the two graphs presented in Figure 3.3. Panel A: the average emission intensity from the *nit-3Δ-LUCI#3* mycelial discs from 12-84 h after transfer to DD. Panel B: the average emission signal from the whole Petri dishes from 40-84 h after transfer to DD. Panel C shows a picture of the frame taken 12 h after transfer to DD. Typical cross sections of a mycelial disc and a Petri dish used for the emission intensity measurements are shown as red squares, and hours of incubation in LL are indicated. Panel D shows a picture of the frame taken 40 h after transfer to DD. Colours represent luminescence intensity, white to red being brightest, and blue dimmest.

Figure 3.4, panels A and B show time-sections of the two graphs presented in Figure 3.3. Panel A shows the oscillations in the *luc* emission signal from the mycelial discs from 12-84 h after transfer to DD. Panel B shows the oscillations in the *luc* emission signal from the whole Petri from 36-84 h after transfer to DD.

3.2.1.2 The nit-3-NcLUC strain

The *nit-3-NcLUC* strain was assayed in the same manner and under the same conditions as described for *nit-3Δ-LUCI#3* in order to determine if the absence of the *ccg-2* intron in the *luc* sequence could account for any differences in reporter expression. Due to the very low signal intensity of the strain, high backgrounds were common. Nevertheless, as for the *nit-3Δ-LUCI#3* strain, results showed an initial rise in emission intensity followed by the development of oscillations with a period of approximately 20 h. Moreover, the oscillations were more distinct with a higher amplitude than for the *nit-3Δ-LUCI#3* strain. The data from this experiment can be found in Appendix II, Figure 8.7.

3.2.1.3 The nit-3(2.6)-LUCI strain – addition of histidine

The emission pattern for the *nit-3(2.6)-LUCI* strain had previously been characterized under static conditions, and it was shown to display a similar emission pattern as that of the *nit-3Δ-LUCI#3* and *nit-3-NcLUC* strains (refer to Figure 8.6, Appendix II). Histidine is a growth-promoting amino acid and has been shown to repress NR activity [145]. An experiment to assess the expression of the *luc* reporter signal with the addition of histidine was performed. The *nit-3(2.6)-LUCI* strain was inoculated in low sucrose Vogel's medium containing 25 mM nitrate and 25 μM of luciferin. A total of six dishes were set up; half with 0.2 mg/ml histidine added to the growth medium. Following inoculation, the dishes were immediately transferred to DD monitored for approximately 8 days (192 h). Figure 3.5 displays the results.

An initial rise and decline in the emission intensity was observed, both with and without histidine added. Following the decline, oscillations with a period of approximately 20 h could be seen for both conditions. The oscillations were more distinct with a higher amplitude when histidine was added. Without the addition of histidine, the emission intensity the signal showed a steady rise in intensity. The signal

reached a second maximum around 96 h when histidine was added (Figure 3.5, panel B). A phase shift between the two conditions was also observed. Emission signals without histidine added showed a 6 h phase advance in the oscillations compared to the signal when histidine was added.

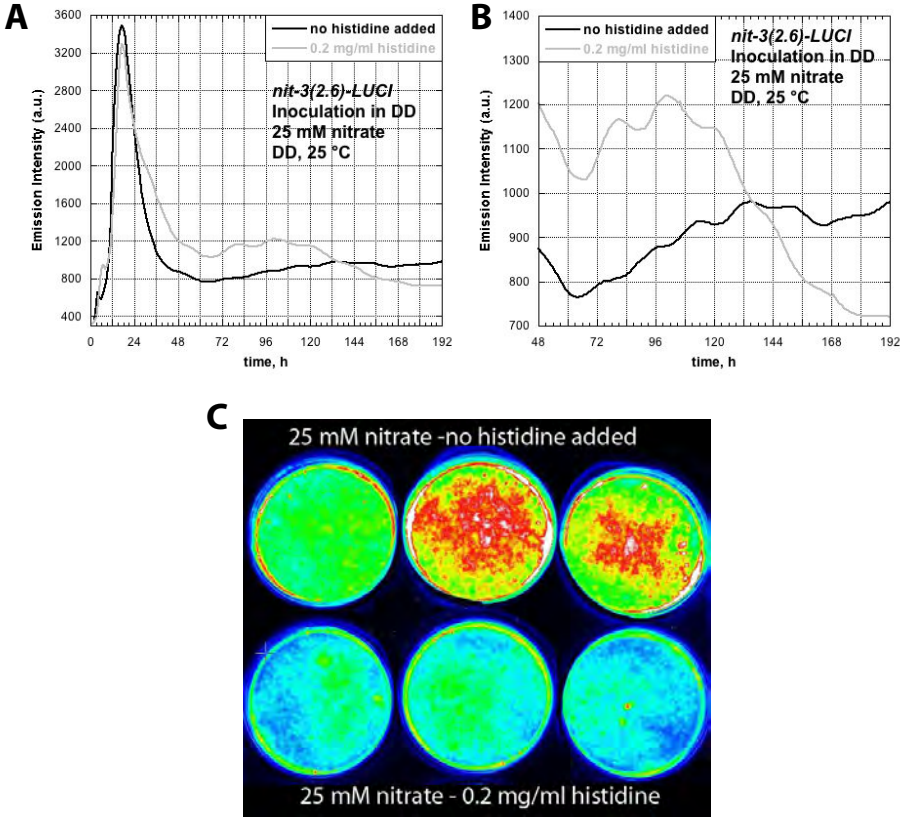

Figure 3.5. Liquid culture experiments performed with the *nit-3(2.6)-LUCI* strain in 25 mM nitrate with and without histidine added. Panel A shows the average emission intensity of the three parallel Petri dishes with and without histidine added. Panel B shows a section of the graph presented in panel A where the average emission intensity from 48 to 192 h with and without histidine added is shown. Panel C shows a picture of the last frame taken at the end of the experiment. Colours represent luminescence intensity, white to red being brightest, and blue dimmest.

3.2.2 nit-3 promoter activity on race tubes under nitrate and ammonium conditions

3.2.2.1 The nit-3Δ-LUCI#3 strain

Race tube experiments were also carried out with the *nit-3Δ-LUCI#3* strain. In total 12 race tubes were made as described in section 2.1.4. One half contained 25 mM nitrate, and in the other half 25 mM ammonium chloride was used as the nitrogen source. Immediately following inoculation, the strains were transferred to DD conditions where the emission intensity was monitored for approximately 10 days (250 h). Figure 3.6 shows the results.

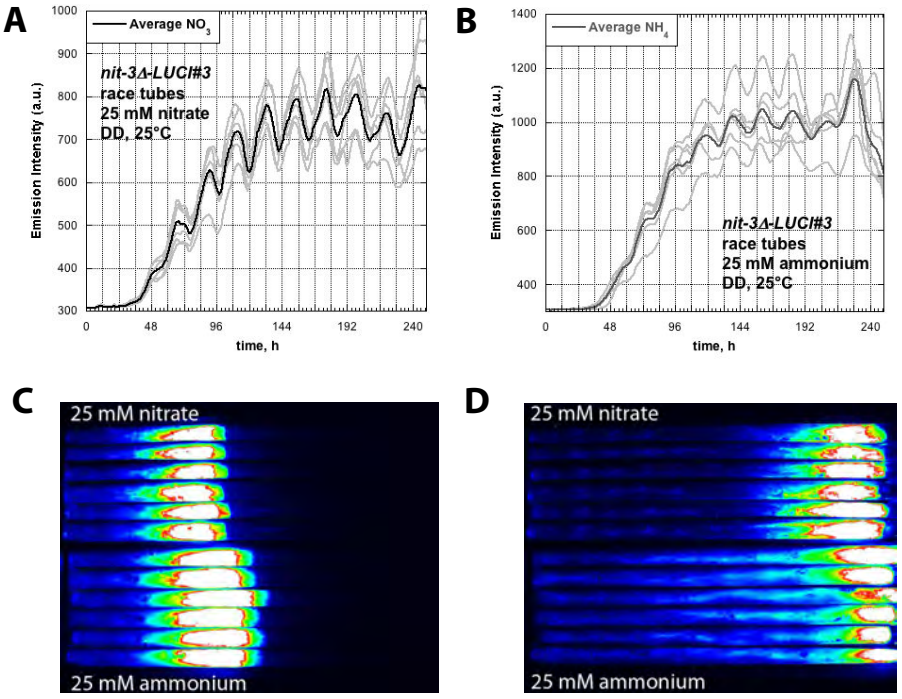

Figure 3.6. Race tube experiments performed with the *nit-3Δ-LUCI#3* strain under 25 mM nitrate and 25 mM ammonium conditions. The average emitted intensities of the six parallel race tubes are shown for both nitrate (panel A) and ammonium conditions (panel B). Panel C shows a picture of the frame taken 125 h after transfer to DD. Panel Dshows a

picture of the last frame of the experiment taken 250 h after transfer to DD. Colours represent luminescence intensity, white to red being brightest, and blue dimmest.

Clear oscillations in the emission intensity with a period of approximately 21 h could be seen when the strain was grown under both nitrate and ammonium conditions. The oscillations were dampened in ammonium compared to nitrate, however the overall emission intensity was higher. Interestingly, a phase shift between the two conditions was observed, and the emission intensity in nitrate peaked 6 h in advance of ammonium conditions.

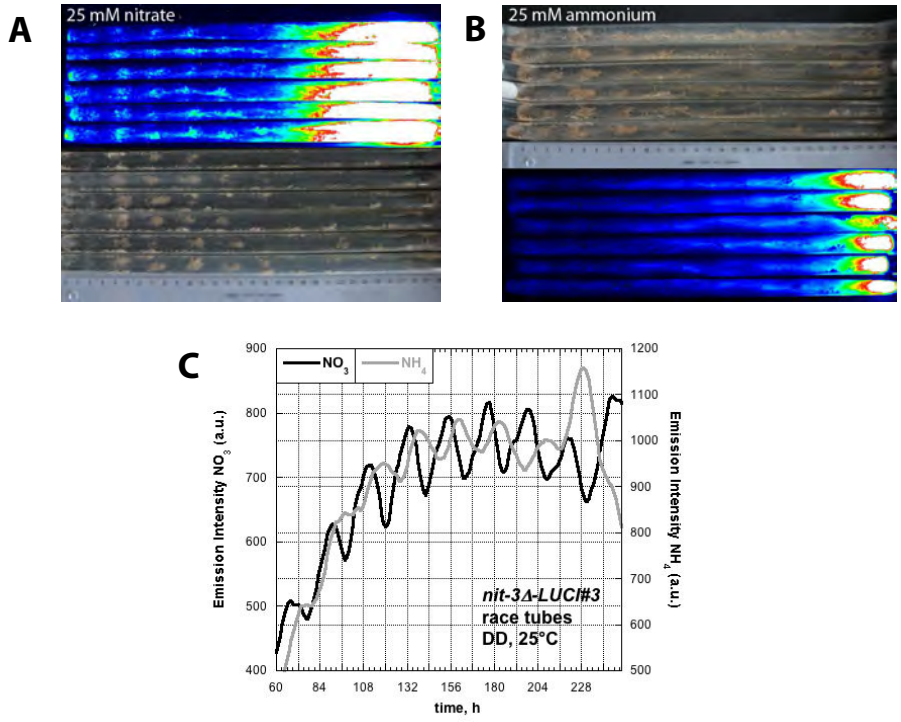

Figure 3.7. The sporulation rhythm of the *nit-3Δ-LUCI#3* strain. Panels A and B show the sporulation rhythm of the *nit-3Δ-LUCI#3* together with a picture of the last frame taken in DD conditions under 25 mM nitrate and 25 mM ammonium conditions, respectively. Colours represent luminescence intensity, white to red being brightest, and blue dimmest. Panel C shows a comparison of the average emission intensity for the strain under nitrate and ammonium conditions, from 60-250 h.

The average emission intensities under nitrate and ammonium conditions are compared in Figure 3.7, panel C. On average, the emission intensity peaked 6 ½ to 7 ½ h before conidiation, and banding was generally less distinct in ammonium than under nitrate conditions. Representative photographs of the sporulation rhythm are shown together with the picture of the last frame of the experiment in Figure 3.7, panels A (nitrate) and B (ammonium). In the growth rate experiments performed under nitrate conditions without luciferin, the period of the sporulation rhythm of the *nit-3Δ-LUCI#3* strain was determined to be 23.11±0.97 h. Representative photographs from this experiment are shown Figure 8.5, Appendix II.

3.2.2.2 The nit-3-NcLUC strain

The *nit-3-NcLUC* strain was also assayed on race tubes using an experimental set-up identical to that of the *nit-3Δ-LUCI#3* strain. The *nit-3-NcLUC* strain expressed the intron-less version of *luc* under the control of a 2 kb sequence upstream from the *nit-3* start codon. Emission intensities were monitored for the duration of 10 days (250 h).

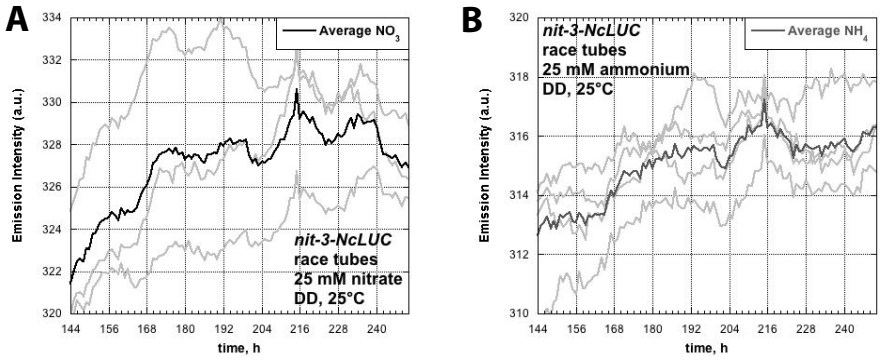

Figure 3.8. Race tube experiments performed with the *nit-3-NcLUC* strain under nitrate and ammonium conditions. Panels A and B show the emission intensity from days 6-10 (144-250 h) in nitrate and ammonium medium, respectively.

Figure 3.8 shows the emission intensity from day 6 until day 10 (144-250 h) for the strain grown under nitrate and ammonium conditions. For the emission intensities for both conditions covering the full duration of the experiments, refer to Figure 8.8, Appendix II.

The *nit-3-NcLUC* mutant had previously been assayed on race tubes (as described in section 2.1.4) in order to determine its growth rate and phenotype (results not shown). The strain was found to be a non-banding and very slow growing strain, with a growth rate of 2.02±0.20 and 1.59±0.70 cm/day under nitrate and ammonium conditions respectively. In addition, as noted in section 3.1.3, the emission intensity levels were very low with a high background. No clear oscillations could be observed during the first 5 days. On day 6, oscillations with a period of approximately 22 h began in half of the parallel race tubes for both nitrate and ammonium conditions. The oscillations were somewhat more distinct in nitrate. No phase shift between the two nutritional conditions could be observed.

3.2.2.3 The nit-3(2.6)-LUCI strain – addition of histidine

Race tube experiments were also carried out with the *nit-3(2.6)-LUCI* strain. The *nit-3(2.6)-LUCI* expressed the intron-containing version of *luc* under the control of a 2.6 kb sequence upstream from the *nit-3* start codon. 0.2 mg/ml of histidine was added to half of 10 race tubes containing 25 mM nitrate and 25 μM luciferin. Following inoculation, the strains were immediately transferred to DD conditions where the emission intensity was monitored for approximately 6 days (139 h). Figure 3.9 shows the results from the experiment.

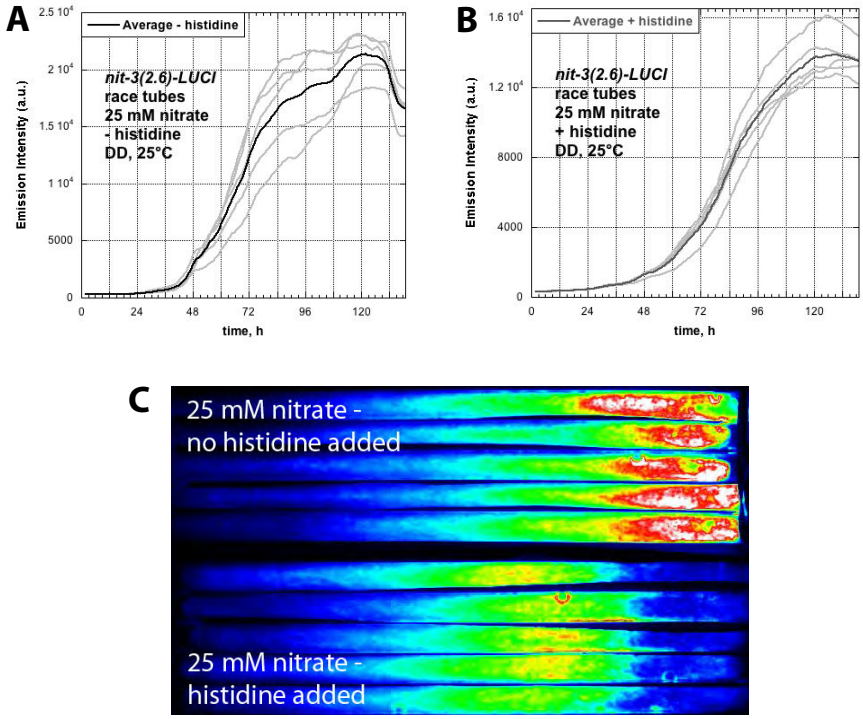

Figure 3.9. Race tube experiments performed with the *nit-3(2.6)-LUCI* strain under 25 mM nitrate conditions with and without the addition of histidine. The average emitted intensities of the five parallel race tubes are shown: Panel A: no histidine added, panel B: 0.2 mg/ml histidine added. Panel C shows a picture of the last frame taken at the end of the experiment 139 h after transfer to DD. Colours represent luminescence intensity, white to red being brightest, and blue dimmest.

Contrary to the experiment performed in liquid culture (section 3.2.1.3), no clear oscillations could be observed with the addition of histidine to the race tube medium. In the race tubes without histidine added, oscillations in some of the parallels could be seen. It was however not possible to determine the period length with any accuracy. Moreover, the emission intensity was higher, and the growth more rapid without the addition of histidine. In this case, increased sporulation was in addition observed.

3.3 The LUCI negative control strain and spectrophotometric measurements of the luciferase system

3.3.1 Luciferase emission pattern in the LUCI negative control strain

The negative control strain *LUCI#16* contained solely the intron-containing *lucI* sequence without a promoter inserted. The strain was assayed in both liquid culture and on race tubes, and under both 25 mM nitrate and 25 mM ammonium conditions to determine if oscillations in reporter activity could be seen. The experimental set-up used was the same as described for the *nit-3Δ-LUCI#3* strain (section 3.2.1.1 and 3.2.2.1).

3.3.1.1 Growth in liquid medium

Figure 3.10 shows the results from experiments performed with the *LUCI#16* strain under 25 mM nitrate and 25 mM ammonium conditions. Mycelial discs were incubated in LL for 36, 24, 12 and 0 h before transfer to DD conditions. Two parallels were set up for each time-point, and the dishes were monitored for approximately 6 and 5 ½ days (153 and 134 h) for nitrate and ammonium conditions, respectively.

Figure 3.10, panels A and C show the average emission intensities for the *LUCI#16* mycelial discs in nitrate and ammonium conditions, respectively. Results from the whole Petri dishes are not included due to high background signals. In both nitrate and ammonium conditions, emission intensities followed a similar pattern: a rise in intensity was followed by a decrease and the development of oscillations. The emission signal from the mycelial discs that had a longer light exposure (36 and 24 h) peaked earlier than the signal from the discs with shorter

exposure (12 and 0 h). The most distinct oscillations could be seen in the discs with a 36 h exposure, and had a period of 18 h in nitrate, and 21 h in ammonium. Moreover, the signal emission intensities were surprisingly higher when the strain was grown under ammonium compared to nitrate conditions.

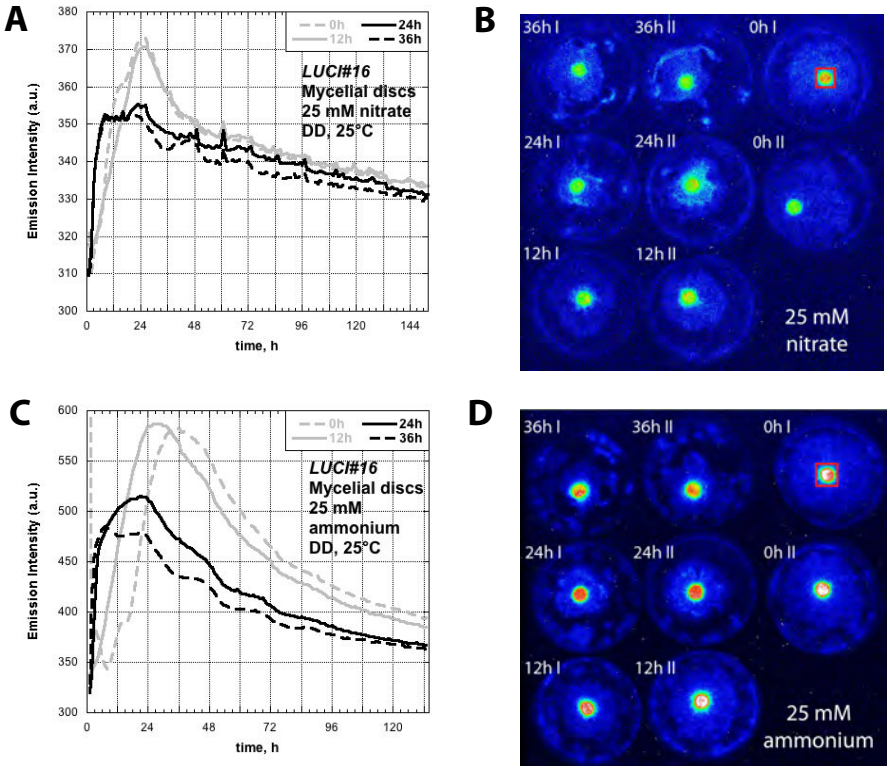

Figure 3.10. Liquid culture experiments performed with the *LUCI#16* negative control strain in 25 mM nitrate and 25 mM ammonium conditions. Panels A and C: the average emitted intensities of the two parallels are shown for the mycelial discs in nitrate and ammonium, respectively. Panel B shows a picture of the last frame taken at the end of the experiment in nitrate conditions. Panel D shows a picture of the last frame taken at the end of the experiment in ammonium conditions. Colours represent luminescence intensity, white to red being brightest, and blue dimmest. A typical cross section of a mycelial disc used for the emission intensity measurements is shown as a red square, and hours of incubation in LL are indicated.

3.3.1.2 Race tube experiments

The *LUCI#16* strain was assayed on race tubes containing 25 mM of nitrate, or 25 mM of ammonium as the sole nitrogen source. Six parallel race tubes were set up for each condition. Following inoculation, the tubes were immediately transferred to DD and monitored for approximately 8 days (200 h). Figure 3.11 shows the results.

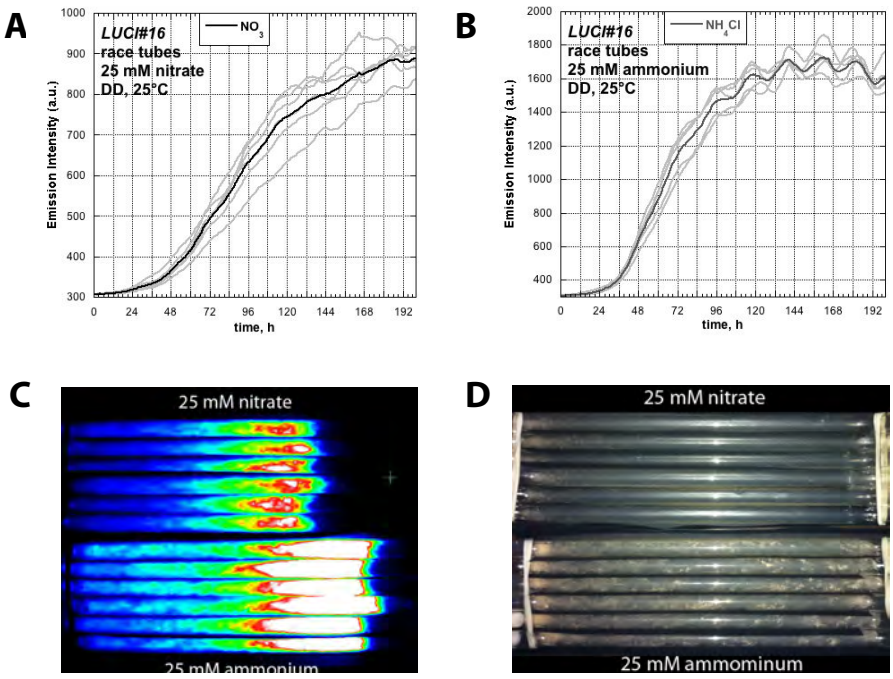

Figure 3.11. Race tube experiments performed with the *LUCI#16* strain under 25 mM nitrate and 25 mM ammonium conditions. The average emitted intensities of six parallel race tubes are shown for both nitrate (panel A) and ammonium conditions (panel B). Parallel race tubes are depicted in grey. Panel C shows a picture of the last frame taken at the end of the experiment at 200 h. Colours represent luminescence intensity, white to red being brightest, and blue dimmest. Panel D shows a photograph of the *LUCI#16* sporulation pattern in nitrate and ammonium conditions.

The *LUCI#16* mutant was found to be a non-banding strain with a growth rate of 3.07±0.03 cm/day when grown on nitrate and 3.50±0.10

cm/day when grown on ammonium (determined in a separate experiment). The strain displayed overall better growth and more sporulation when grown on ammonium as opposed to nitrate (Figure 3.11, panel D). Surprisingly, oscillations in the signal intensities for most parallels could be observed under both nitrate and ammonium conditions (Figure 3.11, panels A and B). When the strain was grown under ammonium conditions (Figure 3.11, panel B), oscillations with a period of 22 h appeared after approximately 4 days (96 h). The overall emission intensity under ammonium conditions was, in addition, twice as high compared to nitrate conditions. The oscillations observed under nitrate conditions (Figure 3.11, panel C) were less distinct, and the period length could therefore not be determined.

3.3.2 The interaction between LUCIFERASE and luciferin monitored by spectrophotometry

Spectrophotometric measurements of luminescence were used to study the behaviour of the LUC-luciferin interaction in liquid samples. Experiments were performed as described in section 2.8. Mycelial discs from the *nit-3Δ-LUCI#3* strain were added to a cuvette containing high sucrose Vogel's medium. 25 μM of luciferin stock solution was added immediately prior to each measurement. Two additions of luciferin were performed, and for each addition, five sequential measurements with a 30 sec time difference were performed. Figure 3.12 gives an overview of the results.

The luminescence resulting from the LUC-luciferin reaction was registered as at approximately 570 nm. Measurements of the emission intensity were performed under both nitrate (Figure 3.12, panels A and B) and ammonium conditions (Figure 3.12, panels C and D). The emission pattern was found to be the same for both conditions! Upon the first addition of luciferin (panels A and B), the emission intensities for R2 and R3 rose past the levels registered for measurement R1. In

measurement R4 and R5, the intensity was found to decrease to the levels observed for R1. Upon the second addition of luciferin (panels C and D), the emission intensity R1 significantly exceeded the levels observed for the first luciferin addition. Then, the intensity declined until reaching the levels previously measured by R4 and R5 when the first addition of luciferin took place. Such behaviour was also observed for the *nit-3Δ-LUCI#1* and *nit-3(2.6)-LUCI* strains, in both high and low sucrose Vogel's medium.

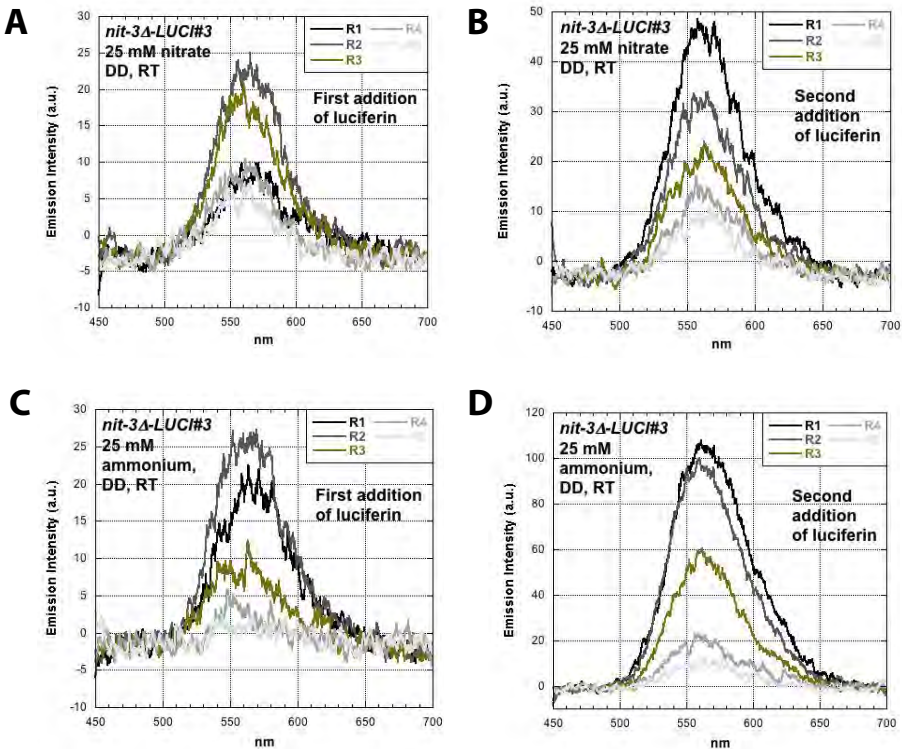

Figure 3.12. Measurements of the bioluminescent emission intensities upon addition of luciferin to the *nit-3Δ-LUCI#3* strain in nitrate (panels A and B), and ammonium medium (panels C and D). R1-R5 indicate five sequential measurements. The experiments were carried out at RT.

3.4 The construction and characterization of *Neurospora crassa* Δ*frq*Δ*nmr* double knock-out mutant strains

Circadian rhythmicity in light-induced NR activity has been observed in a number of higher plants [146-148] as well as in the algae, *Gonyaulax polyedra* [149]. In these organisms, the rhythmicity can be understood as a result of an autonomous negative feedback loop. The existence of endogenous oscillations in NR activity in *Neurospora* has also been shown, and the oscillations were found to be independent of FRQ [84]. When nitrate is present as the only nitrogen source, expression of *nit-3* is induced, resulting in the production of NR. The NMR protein is involved in repressing transcription of the *nit-3* gene, forming a negative feedback loop regulating NR activity. *nmr* mutant strains therefore display a loss of nitrogen repression. Previous NR activity experiments performed with an *nmr* KO mutant, gave no indications of oscillations in the enzyme activity, however *nit-3* mRNA expression experiments using qPCR, showed oscillations in *nit-3* mRNA levels [83]. It was therefore of interest to see whether or not oscillations in both NR activity and *nit-3* mRNA levels would persist in a *Neurospora* Δ*frq*Δ*nmr* double KO mutant strain.

The *Neurospora crassa frq*^{10} *A* (FGSC #7490) and *nmr-1 a* (FGSC #14030) strains, (Table 2.1), were crossed in order to obtain Δ*frq*Δ*nmr* double KO mutant. The cross was carried out as described in section 2.2. The resulting progenies of the approximately 90 individual ascospores picked were sequentially numbered progeny 1, progeny 2, progeny 3 etc. (abbreviated p_1, p_2, p_3 etc.). Close to half of the picked ascospores germinated following heat shock, and conidia were harvested as described in section 2.1.1.

3.4.1 Screening for Δ*frq*Δ*nmr* double knock-out mutants

The germinated progenies were grown in shaking cultures (section 2.1.3) prior to the isolation of genomic DNA from 39 of the strains (section 2.3.3.1). The strains were then screened by PCR for the presence of the *frq* and *nmr* genes. The screens were repeated two times for all strains assayed, and the wt (*bd*), *frq*^{10} and *nmr-1* strains were included as positive controls in each PCR set-up. The expected sizes of the *frq* and *nmr* PCR products were 747 bp and 545 bp respectively. Figure 3.13 shows the results from the first screening of the strains p_1, p_2, p_3, p_7, p_8 and p_{12}. For primer sequences and PCR conditions, refer to Table 7.2 in Appendix I.

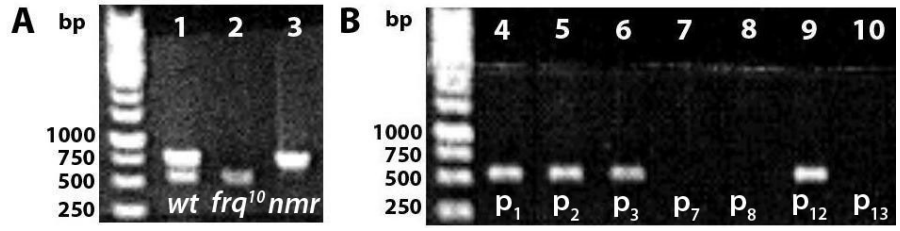

Figure 3.13. Representative results from the PCR screening of the germinated progenies with the *frq* and *nmr* gene-specific primers. The screens were repeated two times for each strain. The positive controls are shown in panel A, wells 1-3. The strains shown in panel B, wells 4-6 as well as 9 are single *frq* KO stains, displaying only the *nmr* PCR product. The strains shown in wells 7 and 8 are assumed positive *ΔfrqΔnmr* double KO's that do not display either the *frq*, or the *nmr*-specific PCR products.

The wt (*bd*) strain displayed both the *frq* and *nmr* PCR products (Figure 3.13, panel A, well 1), and the *frq*^{10} and *nmr-1* strains in turn displayed only the *nmr* PCR product and the *frq* PCR product respectively (Figure 3.13, panel A, wells 2 and 3). Six Δ*frq*Δ*nmr* double KO mutants emerged from the screening: p_7, p_8, p_9, p_{13}, p_{16} and p_{37}, none of which displayed either the *frq*, or the *nmr*-specific PCR products. The strains were re-named Δ*frq*Δ*nmr#7*, Δ*frq*Δ*nmr#8*, Δ*frq*Δ*nmr#9*, Δ*frq*Δ*nmr#13*, Δ*frq*Δ*nmr#16* and Δ*frq*Δ*nmr#37*.

In the *frq*^{10} and *nmr-1* single KO parental strains, the gene *hygromycin B phosphotransferase* (*hph)*, which confers hygromycin resistance, has replaced the knocked out genes [71,138]. To further ensure the Δ*frq*Δ*nmr* genotype of the six double KO strains, the *hph* cassette was amplified using *hph*-specific primers[22]. The wt (*bd*) and the *frq*^{10} and *nmr-1* strains were included as controls in each PCR set-up, and the expected size of the *hph*-specific PCR product was 1435 bp. For primer sequences and PCR conditions, refer to Table 7.2 in Appendix I. The results from the PCR screen of the six Δ*frq*Δ*nmr* double KO mutants are shown in Figure 3.14. The *frq*^{10} and *nmr-1* positive control strains as well as all six Δ*frq*Δ*nmr* KO strains, displayed the *hph*-specific bands (Figure 3.14, panel A, wells 2-3, and panel B, wells 4-9), and as expected, the wt strain did not (Figure 3.14, panel A, well 1). The *hph* PCR products from all strains were furthermore verified by sequencing.

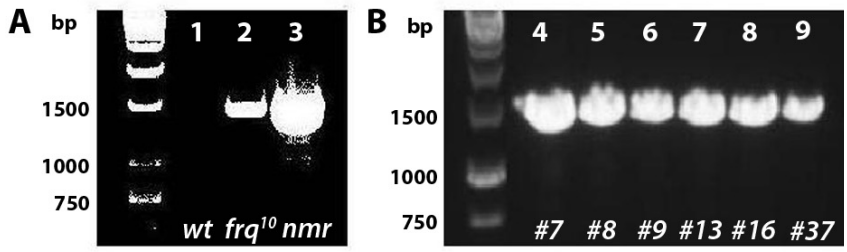

Figure 3.14. Results from the PCR screening with *hph*-specific primers. Negative control (wt) and positive single KO controls (*frq*^{10} and *nmr-1*) are shown in panel A, wells 1-3. The six Δ*frq*Δ*nmr* KO strains are shown in panel B, wells 4-9. All Δ*frq*Δ*nmr* KO strains displayed the *hph*-specific PCR product.

3.4.2 Characterization of the positive ΔfrqΔnmr double knock-out mutants

Neurospora is an ideal model organism for the study of circadian rhythms, and its development through the formation of conidia is an

[22] http://www.dartmouth.edu/~neurosporagenome/Projects_files/Project%201/KO%20Protocols.pdf

easily visible output of the circadian clock. The *bd* mutant displays all of the characteristic properties of the clock, exhibits a very clear rhythm of conidial banding under varied conditions, and has since its discovery been used in virtually all circadian clock experiments [32]. In order to rapidly determine whether or not any of the Δ*frq*Δ*nmr* double KO mutants displayed a rhythmic conidiation and thus could potentially be assayed on race tubes, the strains were examined for expression of the *bd* phenotype. This was done by inoculating the strains on 140 mm Petri dishes, containing race tube agar made with 25 mM nitrate (section 2.1.4). In addition, the strains were inoculated in liquid culture as described in section 2.1.2. This was done to determine their ability to form an adequately dense mycelial mat, making them suitable for further use in protein and mRNA level studies. Mating types were also determined as described in section 2.2.2. The main characteristics of the Δ*frq*Δ*nmr* double KO strains are shown in Table 3.2.

Table 3.2. Determination of mating type and presence of the *bd* phenotype in the Δ*frq*Δ*nmr* double KO mutant strains. Mating type results were inconclusive for the Δ*frq*Δ*nmr#13* strain. The suitability for use in further studies was assessed, and the strains selected for use in further studies are highlighted in bold.

Strain	Mating type	*bd* phenotype	Use in further studies
Δ*frq*Δ*nmr*#7	*A*	N	N
Δ*frq*Δ*nmr*#8	*a*	N	Y
Δ*frq*Δ*nmr*#9	*a*	N	Y
Δ*frq*Δ*nmr*#13	-	Y	N
Δ*frq*Δ*nmr*#16	*A*	N	Y
Δ*frq*Δ*nmr*#37	*A*	Y	Y

The two strains Δ*frq*Δ*nmr#13* and Δ*frq*Δ*nmr#37* were found to display the *bd* phenotype; the former however failed to develop an adequate mycelial mat and was in addition extremely slow growing. This was also the case for Δ*frq*Δ*nmr#7*. Thus, the strains Δ*frq*Δ*nmr#8*, Δ*frq*Δ*nmr#9*, Δ*frq*Δ*nmr#16*, and Δ*frq*Δ*nmr#37* were selected for use in further studies.

3.5 The sporulation rhythm of the wild-type, frq^{10} and ΔfrqΔnmr#37 strains

3.5.1 The sporulation rhythm of the wild-type, frq^{10} and ΔfrqΔnmr#37 strains under nitrate and ammonium conditions

The conidiation rhythm in *Neurospora crassa* wt (*bd*) strain when grown on media with normal Vogel's salts (ammonium nitrate) is well documented to be approximately 22 h [27]. The frq^{10} strain is a *frq* null mutant which displays sparse and sporadic production of conidia and only a rudimentary sporulation rhythm when grown under the same conditions [82]. Both the frq^{9} and the frq^{10} strains are arrhythmic during the first days of growth on race tubes, but cultures often produce rhythmic banding later on (5-7 days after transfer to DD). Given that the *ΔfrqΔnmr#37* double KO mutant strain was found to display the *bd* phenotype, it was therefore interesting to determine if the sporulation was indeed rhythmic, and if the period length of the *ΔfrqΔnmr#37* mutant differed from that of the wt and the frq^{10} strain. The three strains were thus assayed on race tubes containing only nitrate or only ammonium as the sole nitrogen source. The experiments were performed as described in section 2.1.4. Table 3.3 overviews the results.

Table 3.3. Growth rate and period length determined for the wt, *frq*^{10} and Δ*frq*Δ*nmr#37* strains grown under nitrate (NO_3) and ammonium (NH_4) conditions at 25°C. n is the number of experiments with six parallel race tubes. The average growth rate for all race tubes included in n, is given along with the standard deviation.

Strain	Nutritional conditions	Growth rate (cm/day)	Period length (hours)
wt	25 mM NO_3 (n=4)	4.37±0.21	22.27±0.81
	25 mM NH_4 (n=2)	4.71±0.09	19.52±0.91
frq^{10}	25 mM NO_3 (n=4)	4.29±0.17	20.50±0.97
	25 mM NH_4 (n=1)	4.38±0.04	no sporulation
ΔfrqΔnmr#37	25 mM NO_3 (n=5)	3.76±0.05	21.46±0.66
	25 mM NH_4 (n=4)	4.02±0.12	no sporulation

For the wt strain, a difference in both the growth rate and period length between the two nutritional conditions was observed. The growth rate was higher under ammonium conditions, while a longer period length was found in nitrate. The same trend was observed for the growth rates of the *frq*^{10} and *ΔfrqΔnmr#37* strains. Surprisingly, despite its earlier described phenotype, rhythmic sporulation began to occur in the *frq*^{10} strain approximately 2 days after transfer to DD under nitrate conditions. The rhythm was found to have a period of approximately 20 ½ h. Moreover, the Δ*frq*Δ*nmr#37* strain also displayed a rhythmic sporulation pattern in nitrate, with a period of around 21 ½ h. Contrary to what was the case for the wt, no sporulation rhythm could be observed for the *frq*^{10} strain grown on ammonium. For the *ΔfrqΔnmr#37* strain however, banding could be observed under ammonium only conditions, however abated after approximately one cycle for most parallels. Representative photographs of the wt, *frq*^{10} and *ΔfrqΔnmr#37* strains grown under nitrate and ammonium conditions are shown in Figure 3.15.

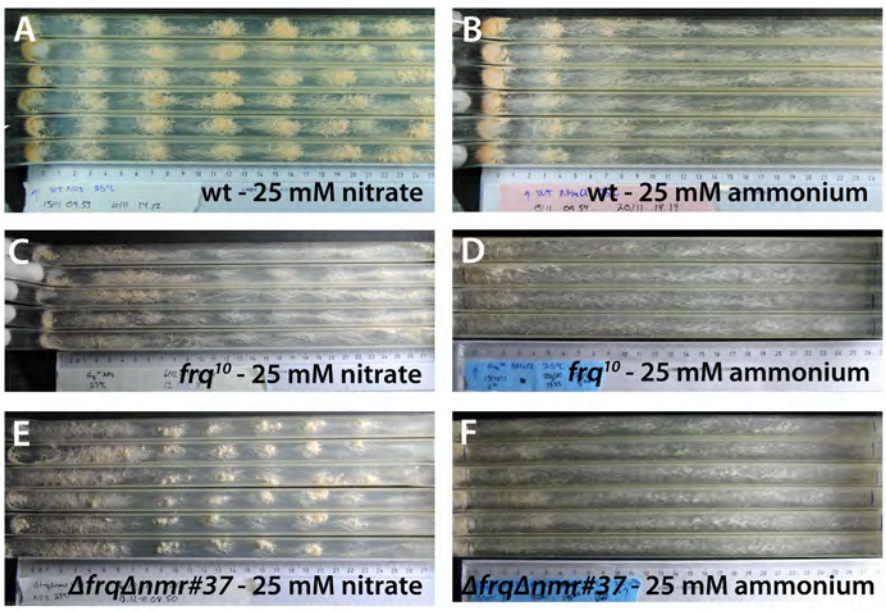

Figure 3.15. Representative photographs of the race tube experiments performed the wt, *frq*^{10}, and Δ*frq*Δ*nmr#37* strains grown under 25 mM nitrate and 25 mM ammonium conditions in DD at 25°C.

3.5.2 Temperature compensation of the sporulation rhythm in the wild-type, *frq*^{10}, and *ΔfrqΔnmr#37* strains under nitrate and ammonium conditions

The sporulation rhythm of the wt strain grown on normal Vogel's salts (ammonium nitrate) has been shown to be temperature compensated between 20° and 30°C, whilst the *frq*^{10} mutant displays a loss of temperature compensation [71,82]. Because a rhythmic sporulation rhythm was observed for the *ΔfrqΔnmr#37* strain under nitrate conditions, it was interesting to see if the rhythm would be temperature compensated. Parallel race tube experiments were performed under both nitrate and ammonium conditions at 20°, 25° and 30°C for the wt,

frq^{10} and *ΔfrqΔnmr#37* strains in order to determine the potential effect of temperature on the period lengths. Table 3.4 overviews the results.

Table 3.4. Growth rate and period length determined for the wt, *frq*^{10} and Δ*frq*Δ*nmr#37* strains grown under nitrate (NO_3) and ammonium (NH_4) conditions at 20°, 25°, and 30°C. n is the number of experiments with six parallel race tubes. The average growth rate for all race tubes included in n, is given along with the standard deviation.

Strain	Temperature	Nutritional conditions	Growth rate (cm/day)	Period length (hours)
wt	20°C	25 mM NO_3 (n=3)	2.82±0.09	27.28±1.10
		25 mM NH_4 (n=2)	3.09±0.05	21.10±1.35
	25°C	25 mM NO_3 (n=4)	4.37±0.21	22.27±0.81
		25 mM NH_4 (n=2)	4.71±0.09	19.52±0.91
	30°C	25 mM NO_3 (n=3)	5.74±0.07	20.27±0.98
		25 mM NH_4 (n=1)	5.71±0.14	20.80±0.50
frq^{10}	20°C	25 mM NO_3 (n=2)	2.74±0.07	35.50±1.94
		25 mM NH_4 (n=1)	2.98±0.04	no sporulation
	25°C	25 mM NO_3 (n=4)	4.29±0.17	20.56±0.97
		25 mM NH_4 (n=1)	4.38±0.04	no sporulation
	30°C	25 mM NO_3 (n=2)	5.41±0.05	15.16±2.01
		25 mM NH_4 (n=1)	5.71±0.07	no sporulation
ΔfrqΔnmr#37	20°C	25 mM NO_3 (n=2)	2.46±0.05	34.99±2.88
		25 mM NH_4 (n=2)	2.60±0.10	no sporulation
	25°C	25 mM NO_3 (n=5)	3.76±0.05	21.46±0.66
		25 mM NH_4 (n=4)	4.02±0.12	no sporulation
	30°C	25 mM NO_3 (n=3)	4.96±0.14	15.61±0.94
		25 mM NH_4 (n=1)	5.16±0.10	17.15±2.19

In general, the growth rates were slightly higher under ammonium than under nitrate conditions for all strains, and increased proportionally with temperature. As expected, the wt strain displayed a rhythmic sporulation for all the temperatures and nutritional conditions assayed. However, the period length varied considerably for nitrate conditions, with a high standard deviation for the race tubes grown at 20°C. The *frq*^{10} strain displayed no sporulation under ammonium conditions at any of the different temperatures. Under nitrate conditions however, rhythmic sporulation began approximately 2 days after the transfer to DD. The period lengths for the different temperatures shortened with increasing temperature, and the standard deviation was high for the

parallels grown on both 20° and 30°C. The same was found to be the case for the Δ*frq*Δ*nmr#37* mutant, which similarly to the *frq*^{10} strain, displayed no sporulation under ammonium conditions at 20° or 25°C. A steady rhythm could however be observed at 30°C in ammonium. Representative photographs of the strains grown under the two nutritional conditions at 20° and 30°C are shown in Figure 3.16 and Figure 3.17, respectively.

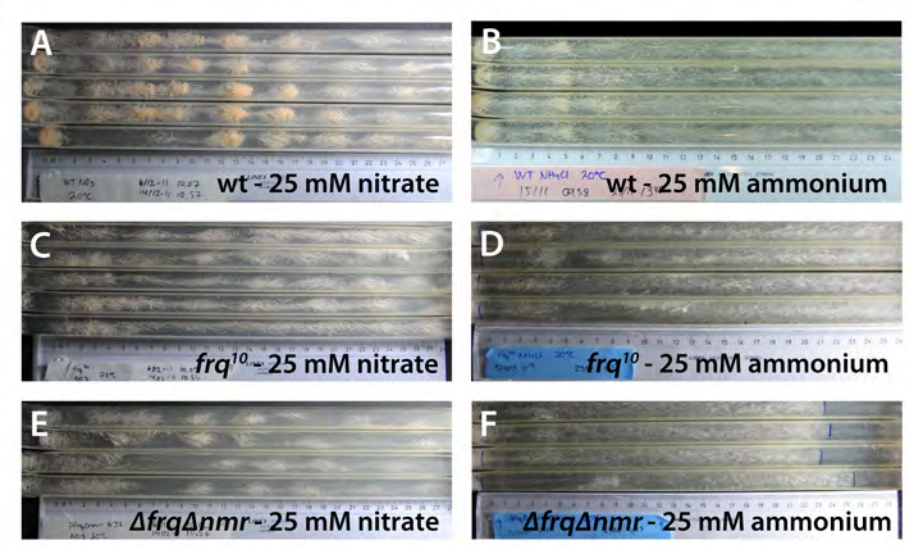

Figure 3.16. Representative photographs of the race tube experiments performed with the wt, *frq*^{10}, and Δ*frq*Δ*nmr#37* strains grown under 25 mM nitrate and 25 mM ammonium conditions in DD at 20°C.

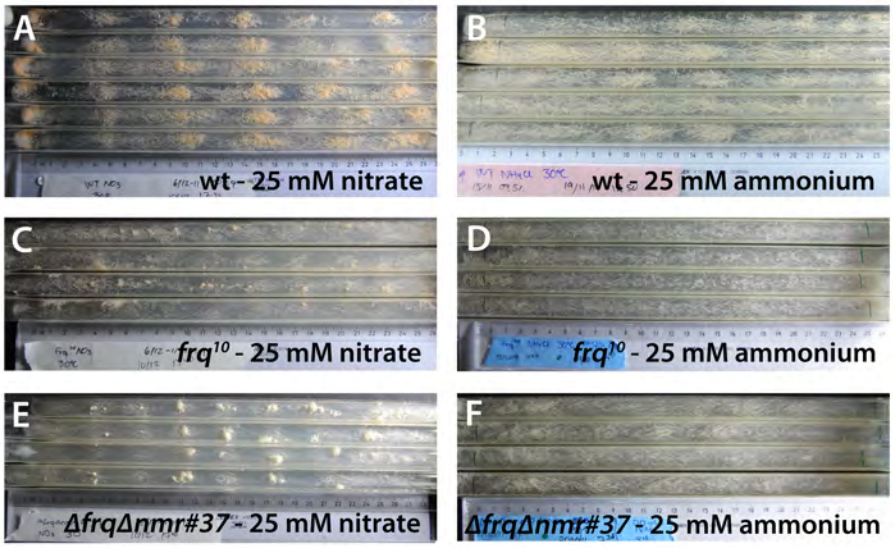

Figure 3.17. Representative photographs of the race tube experiments performed with the wt, *frq*^{10}, and Δ*frq*Δ*nmr#37* strains grown under 25 mM nitrate and 25 mM ammonium conditions in DD at 30°C.

3.6 Nitrate reductase activity studies

Endogenous oscillations in NR activity in *Neurospora* have been found in both the wt and *frq*^{9} strains in both LL and DD. This is also the case for the *frq*^{10} and *wc-1*^{KO} [23] strains in DD [84]. NR activity has in addition been assayed for an *nmr* KO strain (*nmr-1*) [83]. In this thesis, NR activity was assayed for the wt, a *wc-1* KO and the *nmr-1* strain, as well as in the Δ*frq*Δ*nmr* double KO mutants. Time-course sampling was carried out as described in section 2.1.2 and the NR activity assay performed as described in section 2.5. Some of the experiments were performed in collaboration with I. W. Jolma (Stavanger).

[23] Obtained from Kwangwon Lee, genotype *bd;his-3;wc-1*^{KO}, *wc-1* ORF including adjacent 5'- and 3'-UTR regions were replaced with the *hph* gene [61].

3.6.1 Nitrate reductase activity levels in the wild-type

Figure 3.18 shows the NR activity measured in six individual experiments performed with the *Neurospora* wt (*bd*) strain under 25 mM nitrate conditions. The results confirmed endogenous oscillations in the NR activity, with a period of approximately 24 h and peak at around 20 h.

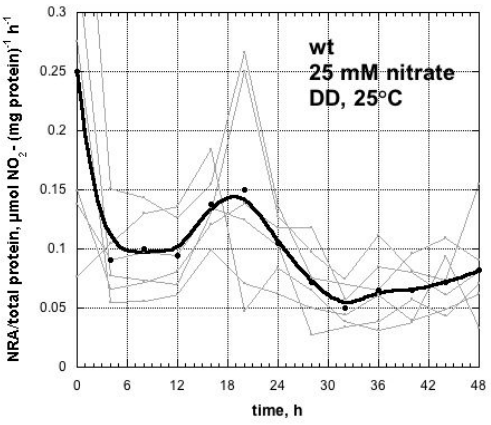

Figure 3.18. NR activity in the *Neurospora* wt *(bd)* strain in DD at 25°C. Time t=0 represents the transfer of mycelial discs from LL to DD conditions, and from high to low sucrose medium as described in section 2.1.2. Average value at t=0 is 0.25±0.16 µmol NO_2^- (mg protein)$^{-1}$ h^{-1}. Thick black line is curve fit to averaged experimental values. Results for the individual experiments (n=6) are shown in grey.

3.6.2 Nitrate reductase activity levels in a wc-1 knock-out mutant

WC-1 is considered to be the main blue-light receptor in *Neurospora*, and is also an essential part of the WCC, responsible for the transcriptional activation of the *frq* and other light induced genes [52,55]. In this thesis, the NR activity was assayed in the non-banding *wc-1* KO (FGSC#11711) in which no WC-1 protein is synthesized.

Figure 3.19 shows the results from two individual experiments with the *wc-1* KO strain grown under 25 mM nitrate conditions. Oscillations in the NR activity were observed in only two of the three experiments

performed. As found for the wt, the oscillations appeared to have a period length of 24 h, with a peak around 20 h.

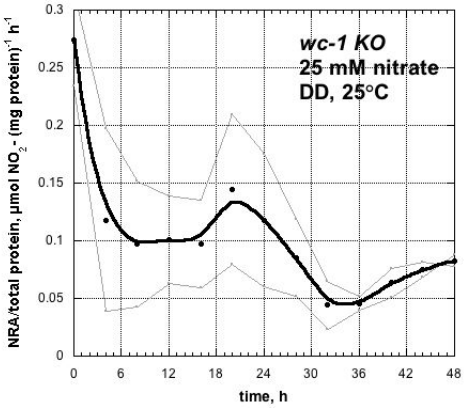

Figure 3.19. NR activity in the *Neurospora wc-1* KO strain in DD at 25°C. Time t=0 represents the transfer of mycelial discs from LL to DD conditions, and from high to low sucrose medium as described in section 2.1.2. Average value at t=0 is 0.27±0.05 µmol NO_2^- (mg protein)$^{-1}$ h^{-1}. Thick black line is curve fit to averaged experimental values. Results for the individual experiments (n=2) are shown in grey.

3.6.3 Nitrate reductase activity in a nitrogen repression defect background

In *nmr* mutant strains, NR is reported to be constitutively expressed resulting in a loss of nitrogen repression (often referred to as de-repression of activity) [103,104,106]. Thus, the *Neurospora nmr-1* mutant displays elevated levels of NR and NiR due to greater enzyme concentrations [137]. NR activity was assayed in the *nmr-1* mutant strain, in which no NMR protein is synthesized.

Figure 3.20 shows the results from three individual experiments with the *nmr-1* strain grown under 25 mM nitrate conditions. As expected, generally higher levels of NR were observed compared to the wt strain. Surprisingly, oscillations in the NR activity were also found in three out of four experiments performed. The rhythm had a period of approximately 24 h with a peak around 20 h.

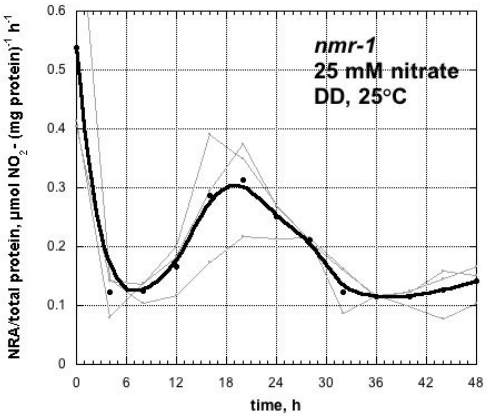

Figure 3.20. NR activity in the *Neurospora nmr-1* mutant in DD at 25°C. Time t=0 represents the transfer of mycelial discs from LL to DD conditions, and from high to low sucrose medium as described in section 2.1.2. Average value at t=0 is 0.53±0.23 µmol NO_2^- (mg protein)$^{-1}$ h^{-1}. Thick black line is curve fit to averaged experimental values. Results for the individual experiments (n=3) are shown in grey.

3.6.4 Nitrate reductase activity in the Δ*frq*Δ*nmr* mutant strains

The *frq* and *nmr* genes both encode negative regulator elements involved in the regulation of the FRQ/WCC and the NR negative feedback loops, respectively. Thus, in a Δ*frq*Δ*nmr* double KO mutant, both feedback loops are disrupted. Based on the results from experiments with the *frq*^{9} and *frq*^{10} mutants [84], as well as with the *nmr-1* mutant (section 3.6.3), it was hypothesized that oscillations in NR activity levels would be observed in the Δ*frq*Δ*nmr* double mutant.

Figure 3.21 shows the results from seven individual NR activity experiments performed with the *ΔfrqΔnmr* KO strains grown under 25 mM nitrate conditions. In general, elevated levels of NR were observed compared to the *nmr-1* mutant, and oscillations in the NR activity were found in seven out of ten experiments where the strains *ΔfrqΔnmr#8*, *#9*, *#16* and *#37* were assayed. Similar to the wt strain, the NR activity levels oscillated with a period of approximately 24 h, however with a peak around 18 h.

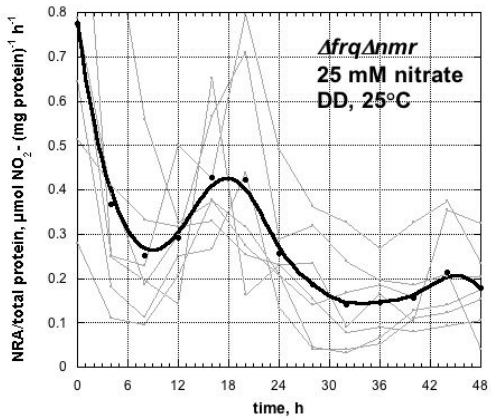

Figure 3.21. NR activity in the *Neurospora ΔfrqΔnmr* double mutants in DD at 25°C. Time t=0 represents the transfer of mycelial discs from LL to DD conditions, and from high to low sucrose medium as described in section 2.1.2. Average value at t=0 is 0.77±0.34 µmol NO_2^- (mg protein)$^{-1}$ h^{-1}. Thick black line is curve fit to averaged experimental values. Results for the individual experiments (n=7) are shown in grey.

3.6.5 Nitrate reductase activity in all strains

Figure 3.22 overviews the results from the NR activity experiments in the wt and the three KO mutants assayed.

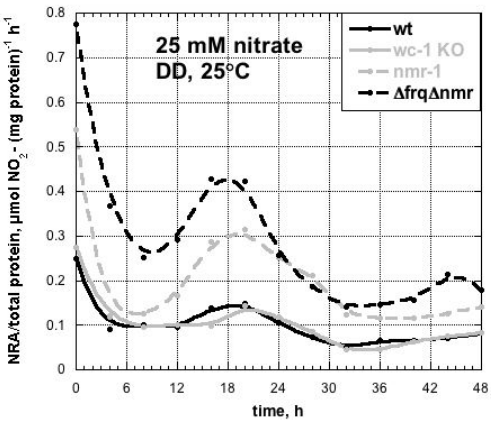

Figure 3.22. NR activity in the *Neurospora* wt (*bd*) and mutant strains in DD at 25°C. Time t=0 represents the transfer of mycelial discs from LL to DD conditions, and from high to low sucrose medium as described in section 2.1.2. Curves fit to the averaged experimental values for the wt, *wc-1* KO, *nmr-1* mutant and the *ΔfrqΔnmr* double KO strains are shown.

All strains displayed oscillations in their NR activity with a rhythm of approximately 24 h. NR activity levels were found to be similar in the wt and the *wc-1* KO mutant. NR levels were generally higher in the *nmr-1* and the *ΔfrqΔnmr* mutants, levels in the latter being the highest out of all strains assayed. Furthermore, the oscillations in NR activity

generally peaked at approximately 20 h, with the exception of the *ΔfrqΔnmr* mutants, in which the oscillations peaked at 18 h.

3.7 qPCR studies of nit-3 expression in the wild-type and the ΔfrqΔnmr knock-out strains

Results from the NR activity experiments described in section 3.6, led to the question of whether or not *nit-3* mRNA levels in the *ΔfrqΔnmr* KO strains would oscillate in the same manner under the same conditions (25 mM nitrate, DD, 25°C). qPCR experiments were therefore performed with both the wt as well as the *ΔfrqΔnmr* KO mutants. Time-course sampling was carried out as described in section 2.1.2 and the qPCR experiments performed as described in section 2.6.

3.7.1 nit-3 mRNA expression in the wild-type

In a transcriptional/translational negative feedback oscillator, it is expected that the transcript of the core element shows rhythmicity. Figure 3.23 shows the results from the qPCR experiments performed with the wt (*bd*) strain. The standard deviation between experiments was in some cases quite large, however the first peak was relatively clear. As expected, mRNA levels show oscillations with a period length of 24 h, peaking at 16 h. Compared to NR activity levels, a phase shift was observed, mRNA levels peaking approximately 4 h prior to the NR activity.

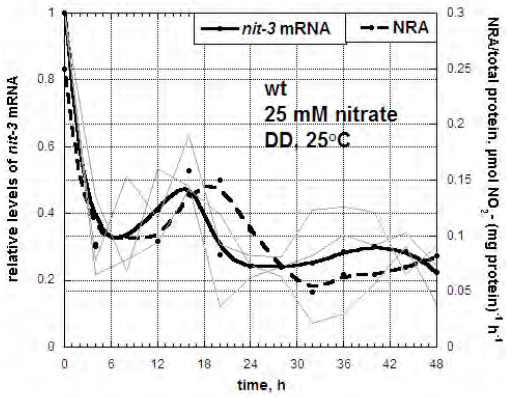

Figure 3.23. *nit-3* mRNA and NR activity levels in the *Neurospora* wt (*bd*) strain in DD at 25°C. Curve fit to averaged experimental values for mRNA levels is shown on the left Y-axis and curve fit to averaged experimental values for NR activity levels is shown on the right. Time t=0 represents the transfer of mycelial discs from LL to DD conditions, and from high to low sucrose medium as described in section 2.1.2. Results for the individual qPCR experiments (n=3) are shown in grey.

3.7.2 *nit-3* mRNA expression in the ΔfrqΔnmr knock-out mutants

Oscillations in *nit-3* mRNA levels have been reported for the *Neurospora nmr-1* mutant strain [83], and work during this thesis also showed endogenous oscillations of the NR activity in the same mutant (section 3.6.3). This led to the hypothesis that *nit-3* mRNA levels, like that of the NR activity, would oscillate in the *ΔfrqΔnmr* KO mutants. *nit-3* mRNA levels were measured for the non-banding *ΔfrqΔnmr#8* and *ΔfrqΔnmr#16* strains, as well as for the banding *ΔfrqΔnmr#37* strain. Figure 3.24 overviews the results.

As expected, qPCR results showed oscillations in the *nit-3* mRNA expression in the *ΔfrqΔnmr* mutant strains. Surprisingly, a difference in the *nit-3* expression pattern for the banding and the non-banding strains was found (Figure 3.24, panel A). For the non-banding strains, the oscillations in the *nit-3* expression had a period of 24 h and peaked at approximately 16 h. The banding strain was markedly distinct from the non-banding strains in the sense that no clear rhythm could be observed in the oscillations. After approximately 16 h, a steep rise in *nit-3* expression could be seen. No such differences in NR activity levels

between the banding and the non-banding strains were observed (Figure 3.24, panel B).

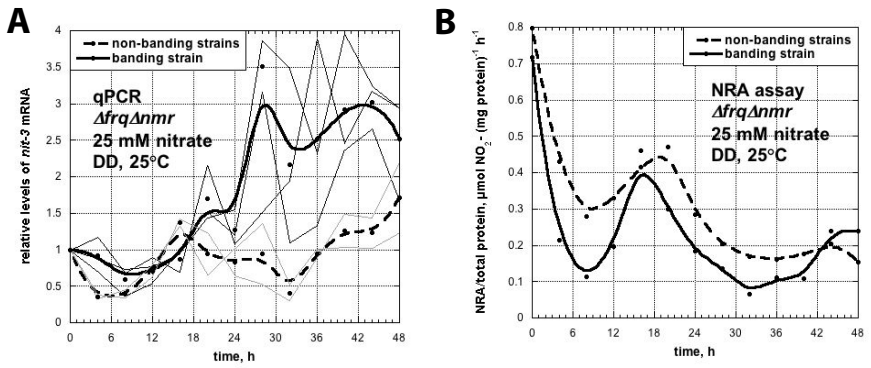

Figure 3.24. Relative levels of *nit-3* mRNA expression in the banding (n=3) and non-banding (n=2) *ΔfrqΔnmr* strains (panel A). Results for the individual qPCR experiments with the banding and non-banding strains are shown in grey and black respectively. Panel B shows the NR activity levels in the banding (n=2) and non-banding (n=5) *ΔfrqΔnmr* strains. Curve fits to averaged experimental values are shown. Time t=0 represents the transfer of mycelial discs from LL to DD conditions, and from high to low sucrose medium as described in section 2.1.2. All experiments were carried out in DD at 25°C.

3.8 Sulphur metabolism in Neurospora crassa

Sulphur is an essential component of in many biologically important molecules and is thus essential for the growth and activity of all cells. In *Neurospora*, sulphur assimilation is regulated in a fashion similar to that of nitrate. When cells are faced with sulphur limiting conditions, a set of sulphur assimilatory genes is switched on. The expression of these genes is regulated by several transcriptional/translational feedback loops. Upon sulphur limitation, expression of the positive acting transcription factor CYS-3 is turned on. CYS-3 promotes the expression of two high affinity sulphate transporters, *cys-13* and *cys-14*, ensuring the uptake of sulphate into the hyphae. In addition, CYS-3 increases its own expression and promotes the transcription of the

negative acting element, *scon-2*. The SCON-2 protein inhibits the positive function of CYS-3 by binding to the *scon-2* binding sites (competitive inhibition), thus preventing further *cys-3* expression. A study by Onai and Nakashima showed that a mutation in *cys-9* gene encoding a NADPH-dependent THX reductase results in abnormal expression of the circadian conidiation rhythm in *Neurospora* [130]. In addition, genes involved in sulphur assimilation in *Arabidopsis* have been found to be circadianly regulated, and regulatory interactions between nitrogen and sulphur assimilatory pathways have been reported [107,132]. It was therefore hypothesised that *cys-3* and *scon-2* might be expressed in a circadian manner. Because *cys-3* and *scon-2* can display oscillatory (circadian) behaviour in a mathematical model of the *Neurospora* sulphur circuit, promoter-*luc* reporter strains were constructed (as described in section 3.1) to test for the presence of circadian rhythms. The reporter strains were characterized both under nitrate and ammonium conditions. Lastly, studies of relative *cys-3* mRNA levels in both the wt (*bd*) strain, as well as in the Δ*frq*Δ*nmr* KO mutants were performed.

3.8.1 Mathematical modelling of the Neurospora crassa sulphur regulatory circuit

Mathematical modelling is a valuable tool in circadian rhythm research, providing a kinetic and mechanistic description of a system. Kinetic models are quantitative sets of rate equations with defined parameters. Together, the differential equations, rate constants and other necessary parameters provide a quantitative description of a system. Despite the quantitative description, reaction kinetic models are a simplification of a particular system, most often including only the basic components. The model should ideally be able to predict the effects of environmental changes on the system. Biological systems often consist of a network of reactions, making them difficult to describe. Therefore

one breaks the system down into reactions describing the different network components.

The reaction kinetic model is shown in Figure 3.25 and includes the major contributors to the assimilation of sulphur (as described in Figure 1.11). The model does not describe the postulated inactivation of SCON-2 by SCON-1 under normal levels of sulphur, and does not explicitly show the activation of sulphate permease I and II (*cys-13* and *cys-14*), ARS and CSA.

Rate constants k_1, k_2 and k_3 correspond to *cys-3* mRNA transcription, degradation and translation, respectively, and k_4 and k_6 correspond to the degradation of cytosolic and nucleic CYS-3 protein. The transport of CYS-3 into the nucleus is represented by k_5. Similarly, k_7, k_8 and k_9 correspond to *scon-2* mRNA transcription, degradation and translation, respectively. Rate constants k_{10} and k_{12} correspond to the degradation of cytosolic and nucleic SCON-2 protein, respectively. The transport of SCON-2 into the nucleus is represented by k_{11}. The transcription and translation of the *scon-3* gene are represented by rate constants k_{13} and k_{15}, whereas rate constants k_{14}, k_{15} and k_{18} correspond to the degradation of *scon-3* mRNA, and that of cytosolic and nucleic SCON-3 protein, respectively. Transport of SCON-3 into the nucleus is represented by k_{17}, and k_{19}, k_{20} and k_{21} correspond to the formation, separation and degradation of the SCON-2/SCON-3 dimer. The formation of the CYS-3/CYS-3/SCON-2/SCON-3 complex is represented by k_{22}, and its separation and degradation by k_{23} and k_{24}. $K_{diss,1}$ represents the binding (dissociation constant) of CYS-3 on the *cys-3* promoter, resulting in the enhancement of its own expression. The inhibition of CYS-3 by SCON-2 is represented by $K_{diss,2}$ and, $K_{diss,3}$ corresponds to the binding of CYS-3 to the *scon-2* promoter. The parameters α, β, and γ refer to the cooperativeness of the binding events (number of binding sites).

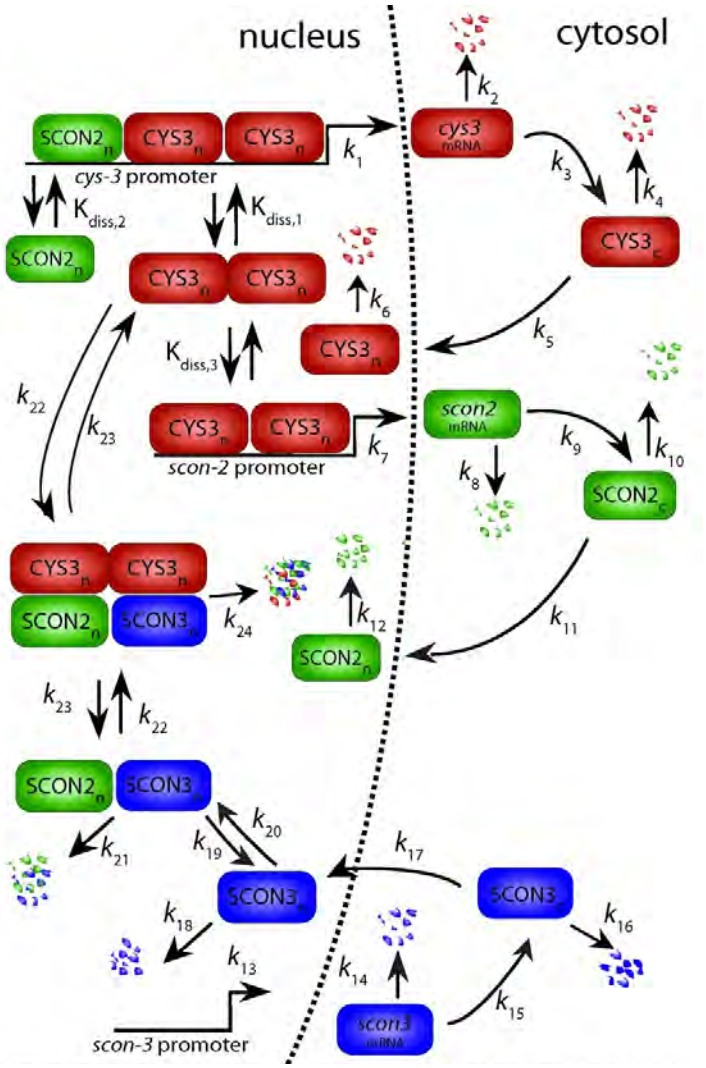

Figure 3.25. A reaction kinetic model for the *Neurospora crassa* sulphur regulatory circuit. The model is based on the experimental results currently available (described in Figure 1.11). Upon sulphur limitation, the transcription factor CYS-3 is expressed at elevated levels. CYS-3 mediates the expression of the sulphur controlled structural genes in addition to enhancing its own expression. Furthermore, CYS-3 promotes the expression of SCON-2, which acts to switch off the *cys-3* transcription by binding to the *cys-3* promoter and possibly entering into a complex with SCON-3, enhancing CYS-3 turnover. Rate constants for enzymatic processes and degradation rates are indicated.

In the equations describing the enzymatic reactions of the sulphur circuit model, the CYS-3/CYS-3/SCON-2/SCON-3 complex is abbreviated C3C3S2S3$_n$, and the SCON-2/SCON-3 complex as SCON2/3$_n$. The sulphur circuit model is based on the following rate equations:

1. $$\frac{d[cys3\text{mRNA}]}{dt} = \frac{k_1 \cdot [\text{CYS3}_n]^{\alpha}}{\text{K}_{\text{diss, 1}} \cdot \left(1 + \frac{[\text{SCON2}_n]^{\beta}}{\text{K}_{\text{diss, 2}}}\right) + [\text{CYS3}_n]^{\alpha}} - k_2 \cdot [cys3\text{mRNA}]$$

2. $$\frac{d[\text{CYS3}_c]}{dt} = k_3 \cdot [cys3\text{mRNA}] - (k_4 + k_5) \cdot [\text{CYS3}_c]$$

3. $$\frac{d[\text{CYS3}_n]}{dt} = k_5 \cdot [\text{CYS3}_c] - k_6 \cdot [\text{CYS3}_n] - k_{22} \cdot [\text{SCON2/3}_n] \cdot [\text{CYS3}_n]^2 + 2k_{23} \cdot [\text{C3C3S2S3}_n]$$

4. $$\frac{d[scon2\text{mRNA}]}{dt} = \left(\frac{k_7 \cdot [\text{CYS3}_n]^{\gamma}}{\text{K}_{\text{diss, 3}} + [\text{CYS3}_n]^{\gamma}}\right) - k_8 \cdot [scon2\text{mRNA}]$$

5. $$\frac{d[scon2\text{mRNA}]}{dt} = k_9 \cdot [scon2\text{mRNA}] - (k_{10} + k_{11}) \cdot [\text{SCON2}_c]$$

6. $$\frac{d[\text{SCON2}_n]}{dt} = k_{11} \cdot [\text{SCON2}_c] - k_{12} \cdot [\text{SCON2}_n] - k_{19} \cdot [\text{SCON3}_n] \cdot [\text{SCON2}_n]$$

7. $$\frac{d[scon3\text{mRNA}]}{dt} = k_{13} - k_{14} \cdot [scon3\text{mRNA}]$$

8. $$\frac{d[\text{SCON3}_c]}{dt} = k_{15} \cdot [scon3\text{mRNA}] - (k_{16} + k_{17}) \cdot [\text{SCON3}_c]$$

9. $$\frac{d[\text{SCON3}_n]}{dt} = k_{17} \cdot [\text{SCON3}_c] - k_{18} \cdot [\text{SCON3}_n] - k_{19} \cdot [\text{SCON3}_n] \cdot [\text{SCON2}_n] + k_{20} \cdot [\text{SCON2/3}_n]$$

10. $$\frac{d[\mathrm{SCON2/3_n}]}{dt} = k_{19}\cdot[\mathrm{SCON3_n}]\cdot[\mathrm{SCON2_n}] - (k_{20}+k_{21})\cdot[\mathrm{SCON2/3_n}] - k_{22}\cdot[\mathrm{SCON2/3_n}]\cdot[\mathrm{CYS3_n}]^2 + k_{23}\cdot[\mathrm{C3C3S2S3_n}]$$

11. $$\frac{d[\mathrm{C3C3S2S3_n}]}{dt} = k_{22}\cdot[\mathrm{SCON2/3_n}]\cdot[\mathrm{CYS3_n}]^2 - (k_{23}+k_{24})\cdot[\mathrm{C3C3S2S3_n}]$$

Table 3.5 shows the rate constants for each reaction step. It has been shown that CYS-3 is very stable under sulphur limiting conditions, with a half-life of over 4 h [127]. This corresponds to a degradation rate constant of approximately 0.2 h^{-1}. The rate of CYS-3 degradation was therefore set to 0.2 h^{-1}. The rest of the rate constants were varied until stable oscillations in CYS-3 and SCON-2 concentrations with a period of approximately 22 ½ h were achieved. The values for $K_{diss,1}$, $K_{diss,2}$ and $K_{diss,3}$ were set to 0.05, 0.01 and 1 respectively. CYS-3 has been reported to bind to DNA as a homodimer [119]. The number of CYS-3 molecules binding to the *cys-3* and *scon-2* promoters was therefore set to two. Interestingly, in order to obtain oscillations with an approximately 22 ½ h period, the number SCON-2 molecules binding to the *cys-3* promoter had to be set to six.

Table 3.5. Rate constants for the model outlined in Figure 3.25. This set of rate constants was chosen in order to allow for oscillations in CYS-3 and SCON-2 concentrations with a period of approximately 22 ½ h.

Rate constants, a.u. (h^{-1})							
k_1	0.50	k_7	1.00	k_{13}	0.20	k_{19}	0.10
k_2	0.50	k_8	0.50	k_{14}	0.30	k_{20}	0.90
k_3	0.60	k_9	1.00	k_{15}	0.50	k_{21}	0.10
k_4	0.20	k_{10}	0.50	k_{16}	0.40	k_{22}	1.00
k_5	0.50	k_{11}	1.00	k_{17}	1.00	k_{23}	0.10
k_6	0.30	k_{12}	0.60	k_{18}	0.50	k_{24}	10.00

Figure 3.26 shows the modelled levels of the CYS-3 and SCON-2 concentrations over a period of 4 days (96 h). The oscillations had an average period length of 22.77 h.

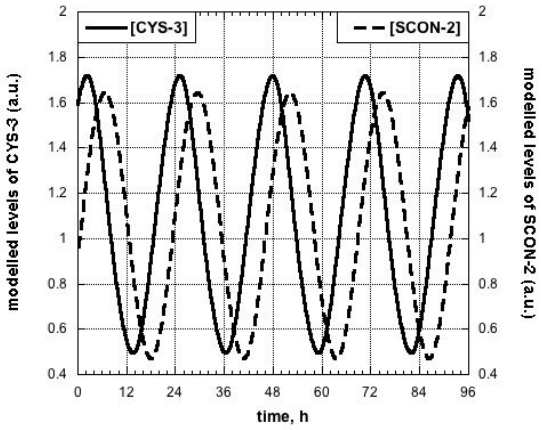

Figure 3.26. Modelled levels of CYS-3 and SCON-2 concentrations over a period of 4 days (96 h). The oscillations had an average period length of 22.77 h.

3.8.2 Real-time monitoring of cys-3 and scon-2 transcriptional activity in Neurospora crassa using luciferase reporter strains

Reporter strains in which the *cys-3* and *scon-2* promoters drive the expression of the LUCI protein, were used to study the transcriptional activity of *cys-3* and *scon-2*.

3.8.2.1 cys-3 transcriptional activity

Two strains were used in the study of *cys-3*: *cys-3-LUCI#1* and *cys-3-LUCI#5*. The strains were selected on the basis of their emission intensities and oscillatory pattern. Both strains were analyzed in liquid culture (as described in section 2.7.1.2) under 25 mM nitrate conditions for approximately 9 days (217 h). Figure 3.27 displays the results.

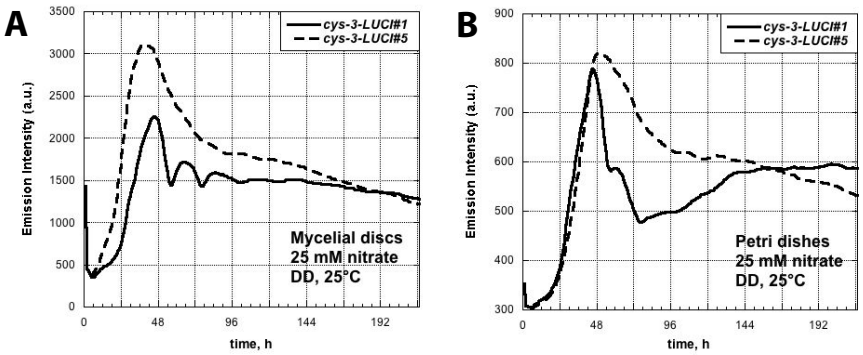

Figure 3.27. Liquid culture experiments performed with the *cys-3-LUCI#1* and *cys-3-LUCI#5* strains grown under 25 mM nitrate conditions in DD at 25°C. The average emission intensities from 3 mycelial discs are shown in panel A, and the emission intensities from the Petri dishes are shown in panel B. A picture of the last frame taken at the end of the experiment can be found in Figure 8.2, Appendix II.

Common for both *cys-3-LUCI* strains was an initial rise in the emission intensity, which continued for approximately 2 days. For strain *cys-3-LUCI#1*, this was followed by the development of oscillations with a period of approximately 20 h. This was not the case for *cys-3-LUCI#5*, which showed a steady decrease in emission intensity and development of dampened oscillations in the mycelial discs and whole Petri dish after 4 days (96 h). These dampened oscillations also appeared in the *cys-3-LUCI#1* dishes, and had a period of 18 h in both strains.

In light of the oscillatory behaviour seen in the mycelial discs, the *cys-3-LUCI#1* strain was assayed under 25 mM ammonium conditions. The results are shown in Figure 3.28. Oscillations in the emission intensity in both the mycelial discs as well as the whole Petri dishes were found to be present in the *cys-3-LUCI#1* strain grown under 25 mM ammonium conditions. The oscillations found in the mycelial discs had a period of approximately 22 h. This also seemed to be the case for the oscillations found in the cross sections of the whole Petri dishes.

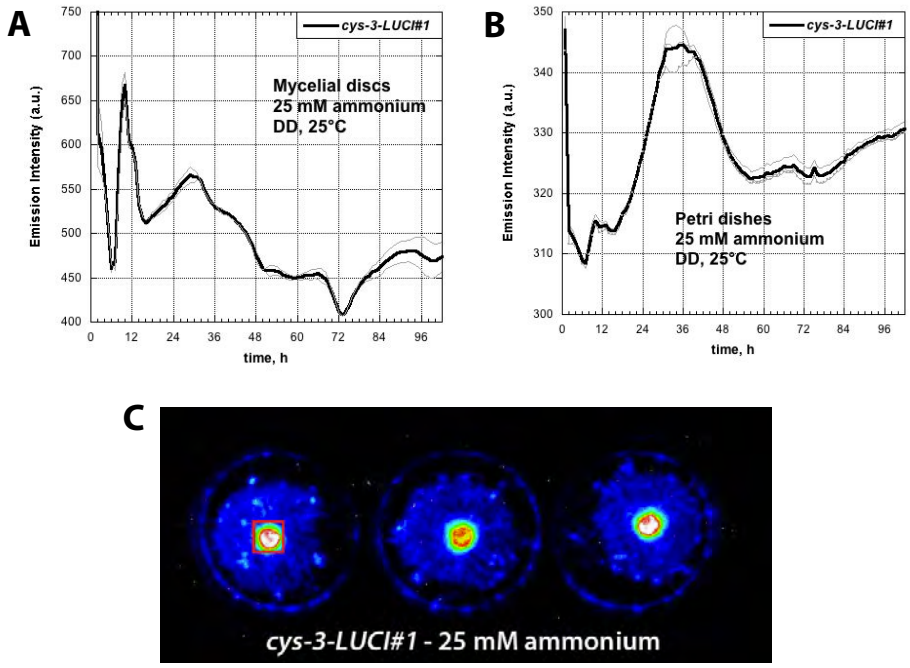

Figure 3.28. Liquid culture experiments performed with the *cys-3-LUCI#1* strain grown under 25 mM ammonium conditions in DD at 25°C. The average emission intensities from the three parallels are shown for the mycelial discs (panel A), and for the whole Petri dishes (panel B). Panel C shows a picture of the last frame taken at the end of the experiment. Colours represent luminescence intensity, white to red being brightest, and blue dimmest. A typical cross section of a mycelial disc used for the emission intensity measurements is shown as a red square.

Growth rate experiments were performed with both the *cys-3-LUCI#1* and *cys-3-LUCI#5* strains. The strains were assayed under both 25 mM nitrate and 25 mM ammonium conditions, and the *cys-3-LUCI#1* strains was found display the *bd* phenotype. The period length was determined to be 24.13±0.68 h in nitrate and 21.94±0.84 h in ammonium. Representative photographs from the growth rate experiments with the *cys-3-LUCI#1* strain are shown in Figure 3.29.

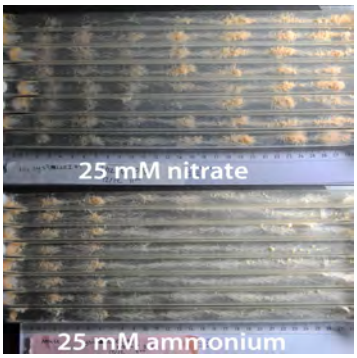

Figure 3.29. The sporulation rhythm of the *cys-3-LUCI#1* strain under 25 mM nitrate and 25 mM ammonium conditions. The average period length (n=2) was found to be 24.13±0.68 h when the strain was grown on nitrate, and 21.94±0.84 h when grown on ammonium. n refers to the number of experiments with six parallel race tubes.

As a final experiment, the *cys-3-LUCI#1* strain was assayed on race tubes containing luciferin under both 25 mM nitrate and 25 mM ammonium conditions. The tubes were monitored for 7 days (168 h), and the results are shown in Figure 3.30.

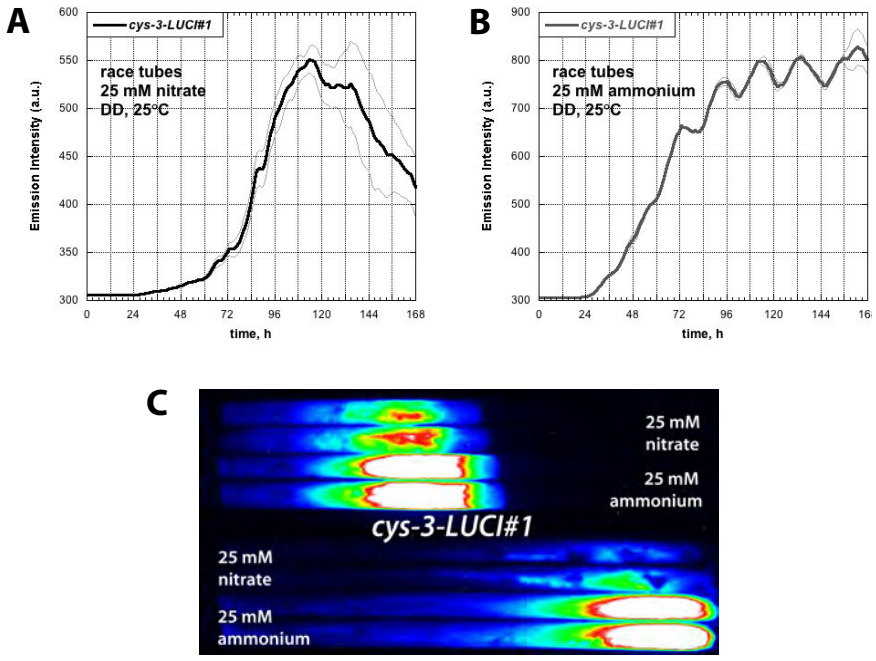

Figure 3.30. Race tube experiments performed with the *cys-3-LUCI#1* strain under 25 mM nitrate and 25 mM ammonium conditions. The average emitted intensities of two

parallel race tubes are shown for both nitrate (panel A) and ammonium conditions (panel B). Parallel race tubes are depicted in grey. Panel C shows pictures of frames taken at 90 h (upper part) and 168 h (lower part), approximately halfway through, and at the end of the experiment, respectively. Colours represent luminescence intensity, white to red being brightest, and blue dimmest.

No clear oscillations in the *cys-3-LUCI#1* emission intensity could be found when the strain was grown under 25 mM nitrate conditions, however, the strain displayed clear oscillations with a period of 21 h when grown on ammonium. In addition, the overall emission intensities were generally higher in ammonium.

3.8.2.2 scon-2 transcriptional activity

As for *cys-3*, two strains were used in the study of *scon-2*: *scon-2-LUCI#4* and *scon-2-LUCI#5*, both chosen based on their emission intensities. Both strains were analyzed in liquid culture (as described in section 2.7.1.2) under 25 mM nitrate conditions. The strains were monitored for 7 days (168 h). Figure 3.31 displays the results.

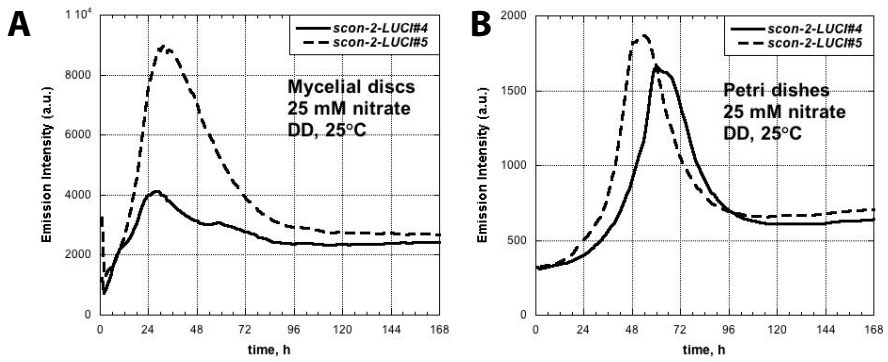

Figure 3.31. Liquid culture experiments performed with the *scon-2-LUCI#4* and *scon-2-LUCI#5* strains grown under 25 mM nitrate conditions in DD at 25°C. The average emission intensity from three mycelial discs is shown in panel A, and the emission intensity for the whole Petri dish in panel B. A picture of the last frame taken at the end of the experiment can be found in Figure 8.4, Appendix II.

No clear oscillations in the *scon-2-LUCI* mycelial discs could be seen, however smaller dampened oscillations appeared after 4 days (96 h).

The period length of these dampened oscillations could not be clearly determined, but was similar to that observed for the *cys-3-LUCI* strains grown under nitrate conditions (Figure 3.27).

In a final assay the *scon-2-LUCI* strains were assayed under 25 mM ammonium conditions for approximately 4 days (102 h). The results are shown in Figure 3.32.

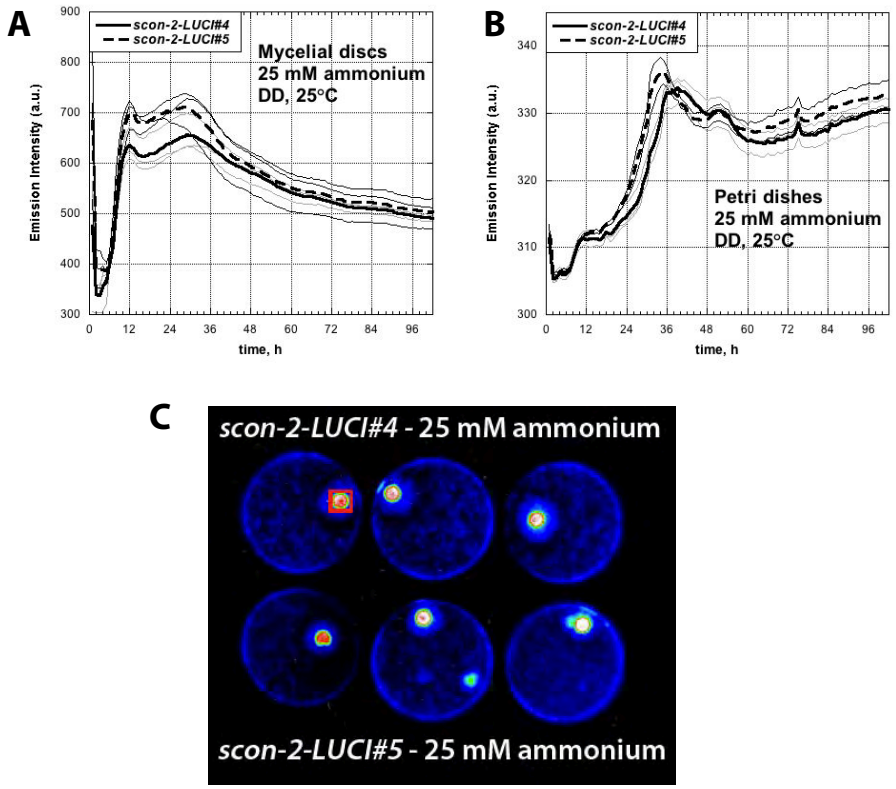

Figure 3.32. Liquid culture experiments performed with the *scon-2-LUCI#4* and *scon-2-LUCI#5* strains grown under 25 mM ammonium conditions in DD at 25°C. The average emission intensities from three parallels are shown for the mycelial discs (panel A), and for the whole Petri dishes (panel B). Panel C shows a picture of the last frame taken at the end of the experiment. Colours represent luminescence intensity, white to red being brightest, and blue dimmest. A typical cross section of a mycelial disc used for the emission intensity measurements is shown as a red square.

Both strains displayed a similar signal expression pattern. In the mycelial discs, oscillations in the emission intensity of approximately 18 h could be seen. In addition, smaller dampened oscillations with a period of 20 h appeared after approximately 2 days (48 h). These dampened oscillations were not evident in the analysis of the whole Petri dishes.

3.8.3 Real-time monitoring of cys-3 mRNA expression in Neurospora crassa using qPCR

3.8.3.1 cys-3 mRNA expression in the wild-type

To further assess if *cys-3* was expressed in oscillatory fashion as well as to determine the suitability of *luc* as a reporter for *cys-3* expression, relative *cys-3* mRNA expression experiments were performed with the wt (*bd*) strain grown both under 25 mM nitrate and 25 mM ammonium conditions. Time-course sampling was carried out as outlined in section 2.1.2, and qPCR was performed as described in section 2.6. Figure 3.33 shows the results.

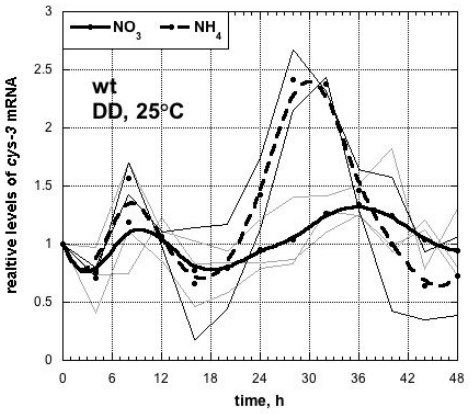

Figure 3.33. Relative levels of *cys-3* mRNA in the wt (*bd*) strain grown under nitrate and ammonium conditions in DD at 25°C. Curves fit to averaged experimental values are shown. Time t=0 represents the transfer of mycelial discs from LL to DD conditions, and from high to low sucrose medium as described in section 2.1.2. Results for the individual experiments are shown in grey (n=3) and black (n=2) for nitrate and ammonium conditions respectively.

Results showed that *cys-3* mRNA was indeed expressed in an oscillatory manner when grown both in nitrate and in ammonium. Two clear peaks could be seen for both conditions; the first at approximately 8 h. The second peak, however, appeared later when the strain was grown under nitrate conditions. In nitrate, the second peak appeared around 36 h, compared to 30 h in ammonium. Thus, *cys-3* mRNA expression levels were found to have a period of approximately 28 h in nitrate and 22 h in ammonium.

3.8.3.2 cys-3 mRNA expression in the ΔfrqΔnmr double knock-out strains

As interactions between nitrogen and sulphur assimilatory pathways have been reported in *Arabidopsis* [107,132], it was of interest to determine if *cys-3* mRNA levels in the Δ*frq*Δ*nmr* mutants differed from that of the wt (*bd*) strain. As described in section 3.7, a difference in the expression pattern of *nit-3* mRNA was observed between the banding and non-banding Δ*frq*Δ*nmr* double KO strains. Relative quantification of *cys-3* mRNA levels under nitrate conditions was therefore carried out for both the banding and the non-banding Δ*frq*Δ*nmr* mutants. The results are shown in Figure 3.34.

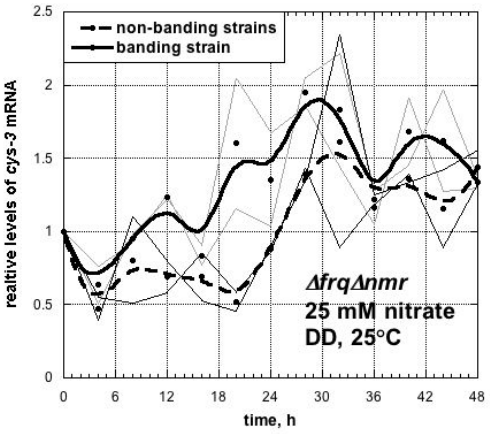

Figure 3.34. Relative levels of *cys-3* mRNA in the banding and non-banding *ΔfrqΔnmr* strains grown under nitrate conditions in DD at 25°C. Curves fit to averaged experimental values are shown. Time t=0 represents the transfer of mycelial discs from LL to DD conditions, and from high to low sucrose medium as described in section 2.1.2. Results for the individual experiments are shown in grey (n=2) and black (n=2) for the banding and non-banding strains respectively.

Comparable to that of *nit-3*, a difference *cys-3* mRNA expression between the banding and non-banding Δ*frq*Δ*nmr* strains could be observed. The non-banding strains displayed oscillations with a period of approximately 22 h, while the oscillations in the banding strain were markedly distinct. For this strain, four peaks could be identified at 12, 21, 29 and 42 h, resulting in apparent short period oscillations (10 h) in *cys-3* mRNA.

4 Discussion

4.1 Construction of the Neurospora luciferase reporter strains

4.1.1 Cloning strategy

One of the goals of this thesis was to study the circadian organization of nitrogen metabolism in *Neurospora crassa*. Time-course data taken every 4 h showed clear limitations to observe the nature of NR activity and *nit-3* mRNA oscillations. Moreover, preliminary analyses of a *nit-3-luc* reporter strain (*nit-3(2.6)-LUCI*) kindly provided by Professor Luis F. Larrondo (Santiago, Chile), indicated that the *luc* reporter activity did not concur with results obtained by qPCR, or by measuring NR activity (Figure 4.1). The *nit-3(2.6)-LUCI* reporter strain had a very long promoter sequence inserted (the 2.6 kb sequence upstream from the *nit-3* start codon). It was therefore of interest to determine if the length of the promoter sequence inserted would affect *luc* expression. In this respect, new *luc* reporter strains with truncated versions of the 2.6 kb *nit-3* promoter sequence were constructed.

To devise a cloning strategy suitable for the construction of the *nit-3-LUCI*, *cys-3-LUCI*, *wc-1-LUCI*, and *scon-2-LUCI* reporter constructs, the *lucI* [136] sequence was modified. This resulted in an alanine to proline mutation at the fourth amino acid of the LUC sequence. The crystal structure of LUC (as determined by Conti *et. al.* [150]) gave no indication of the involvement of the first four amino acids in substrate binding or secondary structures. Moreover, the same trend in the signal emission pattern as observed for *nit-3(2.6)-LUCI* was found in the promoter-*lucI* transformants.

A previous study of the *nit-3* promoter revealed a high level of consensus between the WCC binding site in the *frq* promoter (the C-box [56]), and the most distal NIT-2 binding site in the *nit-3* promoter. In addition, four putative GATA sites were found upstream from the NIT-2 and NIT-4 binding sites. These findings together with NR activity data for a *wc-1*^{KO}, suggested a role for WCC in *nit-3* regulation [83]. Therefore, reporter constructs in which the *luc* and *lucI* genes were expressed by the *wc-1* promoter were made. Attempts to express these constructs in *Neurospora* were however unsuccessful.

4.1.2 Expression in Neurospora crassa

The stable expression of the promoter-*luc* reporter constructs in *Neurospora* was achieved by electroporation of conidia using a standard protocol for transformation (section 2.4). Attempts were made to optimize experimental conditions, however, an overall very low transformation efficiency was observed (Table 3.1). The low transformation efficiency could be attributed to the large size of the DNA insertions [143,144].

In addition, transformants expressing an identical promoter-*luc* reporter construct varied considerably in their emission intensities (refer to Appendix II). Conidia have one to several haploid nuclei, those with two being the most frequent [27]. Most likely, the presence of both transformed and untransformed nuclei accounts for the differences in the emission signal.

4.1.3 Comparing the luciferase reporter gene sequences

Two *Neurospora* optimized *luc* sequences (*NcLUC* and *lucI*) were used in the construction of the promoter-*luc* reporter constructs, in hope to determine if the presence of the *ccg-2* intron in *lucI* [136] would affect the reporter signal. Only one transformant expressing the intron-less *luc*

sequence was obtained. The *nit-3-NcLUC* strain was extremely slow growing and exhibited a very low emission signal (Figure 3.8). Moreover, attempts to construct a strain in which the 2 kb *nit-3* promoter sequence expressed the *lucI* sequence, were unsuccessful, and no comparison of the emission signal from the two *luc* reporter genes could be made.

4.2 Luciferase expression in a negative control strain

As shown in Figure 3.10 and Figure 3.11, *luc* activity was observed in the *LUCI#16* negative control strain, *LUCI#16* (transformed with only the *lucI* sequence). The promoter-*luc* reporter constructs were targeted to the *Neurospora his-3* locus, and integrated at an unmapped 3'-prime segment (downstream of the *his-3* coding sequence) through homologues recombination. *his-3* is a complex multidomain structural gene encoding histidinol dehydrogenase, phosphoribosyl-ATP-pyrophosphohydrolase and phosphoribosyl-AMP cyclohydrolase [108]. These enzymes are needed for histidine biosynthesis, and *his-3* mutants require the addition of histidine for growth. The mechanisms regulating *his-3* expression are not clear. It could be speculated that elements involved in *his-3* control promote the expression of *luc*, independent of the presence of an inserted promoter.

Nitrate is a secondary nitrogen source in *Neurospora*, and in the presence of glutamine, the genes involved in the assimilation of nitrate are repressed [86,87]. In the absence of ammonium when nitrate or nitrite is present, nitrate repression is lifted (de-repressed) and nitrate is assimilated. De-repression and induction of various genes (*nit-2*, *nit-4*) by nitrate has been shown to be necessary for *nit-3* expression [90]. Thus, no signal, or possibly a low and sporadic background emission would be expected for the *nit-3*Δ*-LUCI#3* strain under ammonium conditions. However, contrary to the expectations, distinct oscillations

in *luc* activity as well as high emission levels were observed (Figure 3.6). These observations may be explained by a promoter-independent expression of *luc* through an unknown mechanism.

4.3 Factors influencing luciferase reporter system in Neurospora

The *luc* reporter strains for the *nit-3*, *cys-3*, and *scon-2* were studied in both liquid culture as well as on race tubes, and observations indicated that the *luc* reporter signal was affected by several other factors in addition to promoter activity.

4.3.1 Nitrate, oxygen and reactive oxygen species

For all *luc* reporter strains studied, a difference in the *luc* emission pattern under nitrate and ammonium conditions was observed. As was the case for *nit-3(2.6)-LUCI* (Figure 4.1, panel B), the phase and period length of the oscillations in *nit-3-LUCI#3* did not concur with qPCR experiments (Figure 4.1, panel A). The same was found to be true for the *cys-3-LUCI* strains when grown in nitrate (Figure 3.27 and Figure 3.33). Interestingly, the *nit-3* mRNA rhythm appears to be in anti-phase with the *luc* activity. The reason for this peculiar behaviour is not understood.

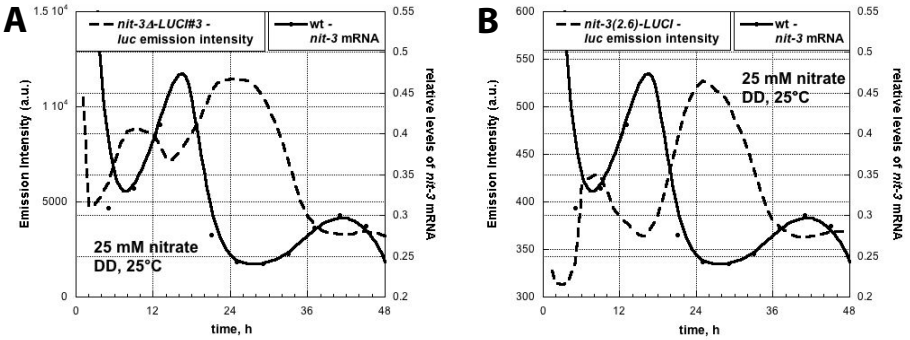

Figure 4.1. Comparison of relative levels of *nit-3* mRNA in the wt (*bd*) strain, and *luc* emission activity in the *nit-3-LUCI#3* and *nit-3(2.6)-LUCI* reporter strains grown under 25 mM nitrate conditions. Panel A shows the comparison between the wt and *nit-3-LUCI#3*, and panel B shows the comparison between the wt and *nit-3(2.6)-LUCI*.

Surprisingly, as shown in Figure 4.2, when *cys-3-LUCI#1* was grown using ammonium as the nitrogen source, the oscillations in wt *cys-3* mRNA levels and the *luc* emission pattern were found to be in phase! In both cases, the oscillations had a period of approximately 22 h, which was the same as the period length of the wt and *cys-3-LUCI#1* sporulation rhythm (as determined in separate growth tube experiments (Figure 3.30 and Table 3.3)).

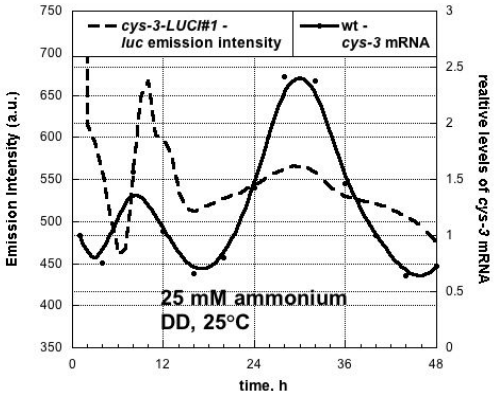

Figure 4.2. Comparison of relative levels of *cys-3* mRNA in the wt (*bd*) strain, and the *luc* emission activity in the *cys-3-LUCI#1* reporter strain grown in 25 mM ammonium.

These findings indicate that the *luc* expression signal is somehow influenced by the presence of nitrate. Nitrate has been reported to be a

strong inhibitor of the *luc* bioluminescent reaction [151,152]. In liquid culture when nitrate is present, the reporter signal emission pattern showed the same trend over the course of the first days in all *luc* reporter strains studied; a steep rise in signal emission was followed by a rapid decline. These observations may, at least in part, be explained by an inhibitory effect of nitrate on the *luc* reporter signal.

The *luc* bioluminescent reaction is dependent on molecular oxygen and ATP as well as luciferin [150]. A study performed by van Leeuwen and colleagues, showed that *luc* activity *in planta* can be related to the promoter activity of the reporter gene only when the activity is measured under substrate equilibrium conditions [153]. The availability of luciferin, ATP and oxygen should therefore remain constant during the period over which *luc* activity is monitored. In liquid culture, the oscillations in *luc* activity in the *nit-3*Δ*-LUCI#1* and *nit-3(2.6)-LUCI* mycelial discs faded after approximately 48-60 h (Figure 3.3, section 3.2.1.1 and Figure 8.6, Appendix II). The cause for this may be that liquid culture conditions are static, and the mycelial discs may rapidly be affected by the consumption of oxygen.

Furthermore, findings indicate that NR can utilize molecular oxygen as an electron acceptor, forming superoxide anion radicals (O_{2^-}) [154,155]. Superoxide is toxic to living cells, and leads to oxidative stress and cell damage. Due to the sensitivity of the *luc* bioluminescent reaction to oxygen levels, the formation of reactive oxygen species (ROS) in nitrate conditions may influence the *luc* activity rhythm. ROS formation may be under circadian control, and have a different oscillatory pattern in anti-phase with *nit-3* and *cys-3* expression.

4.3.2 Expression in a banding background

When the *nit-3*Δ*-LUCI#3* and *nit-3(2.6)-LUCI* strains were grown on 25 mM nitrate medium in race tubes, a substantial dampening of the oscillatory behaviour was observed for *nit-3(2.6)-LUCI* compared to

*nit-3*Δ*-LUCI#3* (Figure 4.3). Moreover, oscillations in the *luc* reporter signal were found in only one of the two *cys-3-LUCI* reporter strains studied (*cys-3-LUCI#1*), despite that the strains expressed identical promoter-*luc* constructs (Figure 3.27). Upon closer examination, it was found that both *nit-3*Δ*-LUCI#3* and *cys-3-LUCI#1*, displayed the *bd* phenotype, and that the oscillations observed were due to the sporulation rhythm.

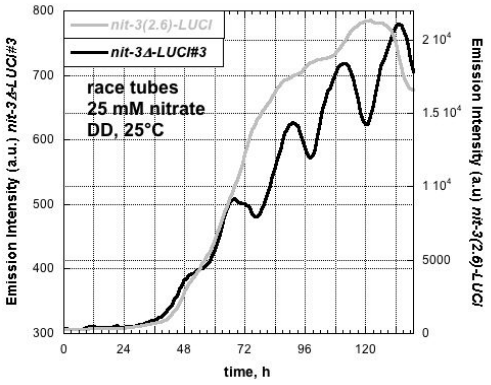

Figure 4.3. Comparison of the banding *nit-3*Δ*-LUCI#3* and non-banding *nit-3(2.6)-LUCI* reporter strains grown on race tubes on 25 mM nitrate medium.

The *Neurospora* conidiation rhythm is expressed much more clearly in the *bd* mutant than in the wt strains, and under more varied conditions [32]. In the wt strains, the conidiation rhythm is obscured by high CO_2 concentrations [156]. The *ras-1* mutation causing the *bd* phenotype renders the strain about 200-fold less sensitive to the CO_2 effect, and it has been shown that regulators of conidiation are elevated in *ras-1* mutant [32,33].

Microarray data (P. Ruoff - unpublished results) show that several genes involved in conidiation are elevated under nitrate conditions. It could be thought that the oscillations in the negative control strain, as well as the difference in *luc* expression between banding and non-banding reporter strains, could be attributed to *luc* being influenced by "metabolic growth". The oscillations observed under ammonium conditions in the *nit-3*Δ*-LUCI#3* strain appear to coincide with the

formation of conidia. Metabolic influences may explain the phase differences observed under nitrate and ammonium conditions (Figure 3.7), as well as the oscillations in the *LUCI#16* negative control strain on race tubes when ammonium was used as the nitrogen source (Figure 3.11).

In liquid culture the decline in emission intensity (described in section 4.3.1) is followed by the appearance of small amplitude oscillations in the *luc* activity. These dampened oscillations were found under nitrate and ammonium conditions, and appeared after approximately 2-4 days. The oscillations were seen in all strains, and had close to the same period length (approximately 20 h). In experiments with the *LUCI#16* and *nit-3*Δ-*LUCI#1* strains, mycelial discs were incubated in LL for 36, 24, 12, and 0 h before transfer to DD and the recording of *luc* activity (Figure 3.3 and Figure 3.10). Results showed that the appearance of the first peak in the emission intensity could be related to the growth of the mycelial disc, i.e. the longer the incubation in LL, the more biological mass was formed, and the peak in emission intensity as well as the onset of the dampened oscillations, appeared earlier. Moreover, the oscillations were more distinct in areas with newly formed hyphae compared to in the mycelial discs (Figure 8.3, Appendix II).

In experiments performed with the *nit-3(2.6)-LUCI* strain, histidine was added to 25 mM nitrate medium (Figure 3.5 and Figure 3.9). On race tubes, histidine addition seemed to abolish the oscillations in *luc* activity, and a decrease in the signal emission levels as well as in sporulation was observed. Upon histidine addition in liquid culture, signal emission levels rose following the first 48 h, however showed a steady decline during the following days. Histidine has been shown to repress NR activity [145], and such an inhibition would account for the findings. Under ammonium nitrate conditions, a large supply of nitrogen is available through ammonium, and conditions favour overall growth and sporulation. When only nitrate is present, and histidine

inhibits NR, the consequence is lower NR activity and apparently less sporulation.

Thus, oscillations in *luc* activity might in some cases be due to a general metabolic (and therefore circadian) influence on *luc* expression, where the reporter signal reflects the overall metabolic activity, including ROS.

4.4 Luciferase as a reporter in Neurospora crassa

The findings discussed above indicate that the *luc* reporter signal is influenced by several factors besides promoter activity. It appears that the *nit-3 luc*-signal, for example, is in part due to the promoter activity, which is reflected in the higher *luc* reporter signal when grown under nitrate compared to ammonium conditions (Figure 3.6). The presence of small amplitude oscillations with a period of approximately 20 h in both the *luc* strains and the negative control, indicate that circadian regulated metabolic intermediates, possibly by ROS, may modulate the *luc* signal.

In a study by van Gooch *et. al.* [136], *frq* and *ccg-2* promoters were shown to drive an oscillatory *luc* expression in good agreement with race tube data. These experiments were performed with normal Vogel's medium where NR is down-regulated, probably avoiding modulation of the *luc* activity by reactive intermediates such as NR-generated superoxide (O_2^-) and other ROS.

The influence of nitrate on the *luc* reporter system limits its use in the study of nitrate assimilation, however the system might be applicable in the case of *cys-3* as well as *scon-2*. Regardless, the potential influences of oxygen and reactive metabolic intermediates needs further study.

4.5 The effect of nitrate on the sporulation rhythm in the wild-type, *frq*^{10} and Δ*frq*Δ*nmr* knock-out strains

The *frq*^{10} phenotype was originally characterized using Vogel's medium containing ammonium nitrate [82]. Under these conditions, conidiation was shown to be arrhythmic during the first days of growth on race tubes, with rhythmic banding appearing after 5-7 days. The *frq*^{10} and Δ*frq*Δ*nmr#37* KO strains were assayed on race tubes both under sole nitrate and sole ammonium conditions (Table 3.3). Interestingly, both strains showed rhythmic sporulation after approximately 2 days when grown on sole nitrate medium (Figure 3.15). Rhythmic banding could not be observed on pure ammonium medium for either strain. These observations indicate that nitrate may exert an effect on the sporulation rhythm. Analyses of the *luc* reporter strains showed a difference in the reporter signal emission pattern between banding and non-banding strains, as well as a difference between nitrate and ammonium conditions in a *bd* background. In addition, an increase in the period length in nitrate compared to ammonium was observed for the *cys-3-LUCI#1* strain (Figure 3.29). Furthermore, increased sporulation in nitrate compared to ammonium medium was observed for the wt (*bd*) strain (results not shown).

The *bd* allele results from a Thr791 point mutation in the *ras-1* gene [33]. The gene is member of the *ras* supergene family encoding highly conserved G-proteins important for signal transduction pathways regulating growth and differentiation [108]. An increase in conidiation has been observed when the *bd* strain is grown under nitrate conditions (results not shown). Microarray experiments (P. Ruoff - unpublished results) imply that this may be due to an increase in levels of oxidative stress. NR has been implicated in the production of superoxide, a radical toxic to living cells and a cause of oxidative stress [154,155]. Moreover, a variety of studies indicate that activated RAS protein can

cause elevations in cellular levels of ROS, and it has been shown that manipulation of ROS levels can influence the appearance of circadian banding [33]. This strongly suggests a link between RAS signalling and the formation of ROS in promoting asexual band development. These findings taken together would explain the presence of a sporulation rhythm in the *frq*^{10} and Δ*frq*Δ*nmr#37* KO strains under nitrate conditions, and the modulation of the *luc* rhythm.

The growth rate and period lengths of the wt, *frq*^{10} and Δ*frq*Δ*nmr#37* KO strains were determined at 20°, 25°, and 30°C, both under nitrate and ammonium conditions (Table 3.3). An increased growth rate for ammonium compared to nitrate conditions was observed for all strains. This was found to be the case at all three temperatures, although the difference was not as evident at 30°C. The slightly reduced growth rate and the slightly elevated period length in nitrate medium can be explained by nitrate assimilation, during which more energy is needed for the production of ammonium, resulting in a slightly slower free-running clock. This would in addition explain why the period lengths in nitrate decrease with increasing temperature. At lower temperature, the overall metabolism is slower, resulting in longer period lengths. When the temperature is increased, the metabolism speads up and the period lengths decrease.

In the wt, the sporulation rhythm on sole ammonium should be temperature compensated [71]. Results showed however, that the period lengths did differ more than expected between the three temperatures (Table 3.3). The standard deviation calculated for 20°, and 30°C was high, thus the difference would not be significant.

4.6 Understanding the NR oscillator

When grown in sole nitrate medium, endogenous oscillations in NR activity have been found in the wt strain, as well as in the *frq*^{9}, *frq*^{10},

and *wc-1*^{KO} mutants [83]. Kinetic models describing the NR transcriptional/translational feedback circuit have been constructed [83,84,157]. One model, described in the study by Christensen, showed good correlation with experimentally achieved data for period length and predicted temperature compensation of the NR activity rhythm [83]. Bioinformatics data from the same study revealed the presence of potential GATA sites in the *nit-3* promoter, possibly implicating the WCC in the regulation of the NR negative feedback loop. These findings were incorporated into a second model, coupling the FRQ/WCC to the NR negative feedback circuit through the addition of WCC binding to the *nit-3* promoter [157]. Consistent with the experimental data, the coupled model predicted sustained oscillations in NR activity levels both in the wt, as well as in a *frq*, and an *nmr* KO mutant.

The NMR protein is involved in the repression of NR by interacting with the transcription factor NIT-2 [158]. *Neurospora nmr* mutants display elevated levels of NR and NiR due to greater enzyme concentrations [137]. During the work presented in this thesis, *frq* and *nmr* double KO mutants were made to determine if the oscillations in NR activity were abolished. Surprisingly, oscillations in NR activity were also observed in these double KO strains. The coupled reaction kinetic model was used to describe NR activity levels in a *ΔfrqΔnmr* KO mutant, however no oscillations were observed. This is due to the mode of construction of the model where both the FRQ/WCC and the NR negative feedback loops were broken. It was therefore hypothesized that the oscillations observed in the *ΔfrqΔnmr* double KO mutants are due to other control mechanisms than just repression by NMR.

Molecular homeostatic controllers can be described by a control engineering view of integral control. Many physiologically important compounds are under tight homeostatic regulation where internal concentrations are adapted at certain levels, despite environmental

disturbances. The control engineering approach has shown that homeostasis in a controlled variable can be obtained by means of integral control [159]. The induction of NR by nitrate and removal of nitrate by NR can be considered as the first step in nitrate assimilation. This simplified version of a feedback loop can be represented as a homeostatic control motif, which can lead to robust homeostatic behaviour [159]. This type of feedback motif has been termed an outflow controller, and such a structure can show nitrate homeostasis (to avoid oxidative stress) and circadian oscillations even in the absence of NMR [160]. Furthermore, it appears that the homeostatic oscillations in nitrate concentrations can be modulated by NMR, creating an additional negative feedback loop (P. Ruoff - unpublished results). If this is the case, then the increase in NR activity and *nit-3* transcript levels in the Δ*frq*Δ*nmr* double KO mutants compared to the wt (*bd*) strain (Figure 3.23 and Figure 3.24) would be due to loss of repression by NMR. Support for this view is given by the fact that the NR oscillatory activity in the Δ*frq*Δ*nmr* KO mutants is significantly higher than in the wt (nmr^+) strains. Furthermore, the oscillations could be attributed to the homeostatic regulation of nitrate concentrations, and are therefore found even when the negative feedback by *frq* and *nmr* is broken.

4.7 Regulation of the Neurospora crassa sulphur circuit

4.7.1 Reaction kinetic model predictions

A mathematical model of the regulation of the *Neurospora* sulphur circuit had been made (Figure 3.25). The model was constructed by the cooperative efforts of I. W. Jolma (Stavanger) and R. E. Spee (Wageningen), and had been based on the information currently available from experimental studies. Central to the regulation of the

sulphur circuit in *Neurospora* are the positive acting *cys-3* and negative acting *scon-2* genes [115,116]. The CYS-3 protein turns on the expression of the sulphur circuit structural genes to take up sulphur in the form of sulphate. In addition, CYS-3 promotes its own expression by binding to the *cys-3* promoter [120]. *scon-2* expression is also dependent on CYS-3 [122], and together, the CYS-3 and SCON-2 proteins are assumed to make up the core regulatory elements in the sulphur circuit.

When sulphur is readily available, the half-lives of CYS-3 and *cys-3* mRNA have been reported to be 5 and 10 min, respectively. Under sulphur limiting conditions however, CYS-3 was found to be much more stable with a half-life greater than 4 h [127]. This corresponds to a rate constant of approximately 0.2 h^{-1}, which was used in the model calculations to describe the rate of CYS-3 degradation (k_4).

CYS-3 dimerization has been shown to be required for DNA binding [119]. The *cys-3* and *scon-2* promoters contain three and four putative CYS-3 binding sites, respectively [120,122]. A study by Tyson *et. al.* suggests that protein dimerization may play an essential role in the generation of circadian rhythms in *Drosophila* [161]. Furthermore, SCON-2 is hypothesized to bind to the *cys-3* promoter to inhibit *cys-3* transcription. SCON-3 has been found to interact with SCON-2, possibly contributing to CYS-3 degradation. The model was therefore made to incorporate CYS-3 dimerization as well as the influence of SCON-2 and SCON-3 on the CYS-3 turnover rate. The model is nevertheless greatly simplified in the sense that it describes an enzymatically catalyzed processes as first- and second-order reactions[24]. Moreover, as is the case for kinetic models, the modelled oscillations are dependent on the rate constants. These values will vary

[24] First-order reactions depend on the concentration of only one reactant. Second-order reactions depend on the concentrations of two reactants.

according to the structure of the model, and therefore may not necessarily reflect true values.

A high number (six) of SCON-2 molecules binding to the *cys-3* promoter was found to be necessary in establishing oscillations with a 22 ½ h period length. This appears mechanistically unrealistic, and could indicate that other molecules are involved in CYS-3 inhibition. SCON-3 forms part of the *Neurospora* SCF complex, which targets proteins for degradation by the proteasome. It could be argued that additional proteins involved in the proteasomal degradation pathway may influence CYS-3 degradation, exerting their effects through SCON-3. The SCF complex is also involved in degradation of FRQ and is thus in the regulation of the FRQ/WCC oscillator [51].

4.7.2 Experimental results

qPCR experiments showed the existence of clear oscillations in *cys-3* mRNA transcript levels in the *Neurospora* wt strain. Furthermore, the oscillations were observed both under nitrate and ammonium conditions (Figure 3.33). However, a difference in the period length between the two nutritional conditions was found. A study by Koprivova and colleagues demonstrates that sulphate reduction is regulated by nitrogen in *Arabidopsis* [132]. In addition, it has been shown that genes in *Arabidopsis* encoding sulphate and nitrate transporters peak coordinately toward the end of the night [107]. Under nitrate conditions, an increase in the period length of the oscillations seen in *cys-3* transcript levels was observed. This could indicate the existence of a link between the nitrate and sulphur assimilatory pathways also in *Neurospora*.

The *cys-3* mRNA expression pattern in the Δ*frq*Δ*nmr* double KO strains was also studied. As for *nit-3*, a difference in *cys-3* expression between the banding and non-banding strains was found (Figure 3.34). *cys-3* levels in the non-banding strains resemble that of the wt strain

found under nitrate conditions, however with a shorter period length. *cys-3* levels in the banding strain were different from the non-banding mutants, and it therefore seems likely that the *ras-1* mutation somehow influences *cys-3* expression. If this is only the case for nitrate is unknown, as no *cys-3* expression experiments with the Δ*frq*Δ*nmr* double KO grown in ammonium, have been performed.

The period length of the oscillations in *cys-3* mRNA levels under ammonium conditions, showed good correlation with the period length calculated in the study of the sulphur circuit reaction kinetic model. Moreover, the model predicted a phase shift in the oscillations in CYS-3 and SCON-2 concentration, CYS-3 reaching its highest levels 4 h prior to SCON-2. Considering the speculative model for the regulation of the *Neurospora* sulphur circuit regulation (Figure 1.11), such a phase shift is predicted, and reflects the CYS-3-promoteded expression of SCON-2, and the following inhibition of CYS-3 by and SCON-2. Thus, *cys-3* mRNA levels would be expected to peak prior to that of *scon-2*. Results from the experiments with *scon-2-luc* reporter strains indicate a phase shift of approximately 4 h between the oscillations in *cys-3* and *scon-2* activity. However, further qPCR experiments need to be carried out for comparison.

Though simplified, the sulphur circuit reaction kinetic model highlights the importance of CYS-3 degradation in the determination of the period length. Moreover, the model is indicative of other inhibition mechanisms than that of competitive binding by SCON-2. Thus, this quantitative model could be said to provide qualitative information about the *Neurospora* sulphur regulatory circuit.

5 Conclusions and future perspectives

In nature, *Neurospora crassa*'s ability to make use of secondary nitrogen sources would increase fitness. Based on the number of elements involved in the assimilation pathway, the ability to utilize nitrate and nitrite must be important. Much is known about the genes involved in nitrate assimilation, but more work remains in order to determine the importance of the NR oscillatory system in the *Neurospora* circadian system. The effect of homeostatic regulation of nitrate concentration is found in plants and its possible role in the control of the NR system needs to be elucidated. The use of firefly *luc* as a reporter would be a valuable tool in such studies, however work presented in this thesis revealed that the reporter activity is modulated in the presence of nitrate and does not reflect corresponding qPCR data. Further study of the potential influence of oxygen and metabolic intermediates on reporter activity is needed, and the usefulness of alternative *luc* genes, from for example *Renilla*, could be assessed.

Model predictions and qPCR experiments have revealed an oscillatory expression of *cys-3*, indicating a possible circadian regulation of the *Neurospora* sulphur circuit. To determine whether or not the oscillations in *cys-3* mRNA levels are truly circadian, or merely just an output of the *Neurospora* clock, *cys-3* oscillations ought to be studied in a *frq* KO strain. It would also be of interest to determine whether or not the oscillations are temperature compensated. Finally, qPCR studies of *scon-2* mRNA levels are needed in order to understand the possible circadian regulation of *cys-3* and *scon-2*.

6 References

[1] Roenneberg, T. and Merrow, M. (2001). Seasonality and photoperiodism in fungi. J Biol Rhythms 16, 403-14.

[2] Jolma, I.W., Laerum, O.D., Lillo, C. and Ruoff, P. (2010). Circadian oscillators in eukaryotes. Wiley Interdiscip Rev Syst Biol Med 2, 533-49.

[3] Simonneaux, V. and Ribelayga, C. (2003). Generation of the melatonin endocrine message in mammals: a review of the complex regulation of melatonin synthesis by norepinephrine, peptides, and other pineal transmitters. Pharmacol Rev 55, 325-95.

[4] Huang, T.C., Tu, J., Chow, T.J. and Chen, T.H. (1990). Circadian rhythm of the prokaryote *Synechococcus* sp. RF-1. Plant Physiol 92, 531-3.

[5] Grobbelaar, N., Huang, T.-C., Lin, H.-Y. and Chow, T.-J. (1986). Dinitrogen-fixing endogenous rhythm in *Synechococcus* RF-1. FEMS Microbiol Lett 37, 173-177.

[6] Baker, C.L., Loros, J.J. and Dunlap, J.C. (2011). The circadian clock of *Neurospora crassa*. FEMS Microbiol Rev

[7] Toh, K.L., Jones, C.R., He, Y., Eide, E.J., Hinz, W.A., Virshup, D.M., Ptacek, L.J. and Fu, Y.H. (2001). An hPer2 phosphorylation site mutation in familial advanced sleep phase syndrome. Science 291, 1040-3.

[8] Mansour, H.A., Monk, T.H. and Nimgaonkar, V.L. (2005). Circadian genes and bipolar disorder. Ann Med 37, 196-205.

[9] Jolma, I.W., Falkeid, G., Bamerni, M. and Ruoff, P. (2006). Lithium leads to an increased FRQ protein stability and to a partial loss of temperature compensation in the *Neurospora* circadian clock. J Biol Rhythms 21, 327-34.

[10] Gachon, F. and Firsov, D. (2011). The role of circadian timing system on drug metabolism and detoxification. Expert Opin Drug Metab Toxicol 7, 147-58.

[11] Zhou, F., He, X., Liu H., Zhu, Y., Jin, T., Chen, C., Qu, F., Li, Y., Bao, G., Chen, Z. and Xing, J. (2011). Functional polymorphisms of circadian positive feedback regulation genes and clinical outcome of Chinese patients with resected colorectal cancer. Cancer

[12] Dunlap, J.C., Loros, J.J., Colot, H.V., Mehra, A., Belden, W.J., Shi, M., Hong, C.I., Larrondo, L.F., Baker, C.L., Chen, C.H., Schwerdtfeger, C., Collopy, P.D., Gamsby, J.J. and Lambreghts, R. (2007). A circadian clock in *Neurospora*: how genes and proteins cooperate to produce a sustained, entrainable, and compensated biological oscillator with a period of about a day. Cold Spring Harb Symp Quant Biol 72, 57-68.

[13] Correa, A. and Bell-Pedersen, D. (2002). Distinct signaling pathways from the circadian clock participate in regulation of rhythmic conidiospore development in *Neurospora crassa*. Eukaryot Cell 1, 273-80.

[14] Crosthwaite, S.K., Loros, J.J. and Dunlap, J.C. (1995). Light-induced resetting of a circadian clock is mediated by a rapid increase in *frequency* transcript. Cell 81, 1003-12.

[15] Liu, Y., Merrow, M., Loros, J.J. and Dunlap, J.C. (1998). How temperature changes reset a circadian oscillator. Science 281, 825-9.

[16] Ouyang, Y., Andersson, C.R., Kondo, T., Golden, S.S. and Johnson, C.H. (1998). Resonating circadian clocks enhance fitness in cyanobacteria. Proc Natl Acad Sci U S A 95, 8660-4.

[17] Ruoff, P., Behzadi, A., Hauglid, M., Vinsjevik, M. and Havas, H. (2000). pH homeostasis of the circadian sporulation rhythm in clock mutants of *Neurospora crassa*. Chronobiol Int 17, 733-50.

References

[18] de Paula, R.M., Vitalini, M.W., Gomer, R.H. and Bell-Pedersen, D. (2007). Complexity of the *Neurospora crassa* circadian clock system: multiple loops and oscillators. Cold Spring Harb Symp Quant Biol 72, 345-51.

[19] Lillo, C., Meyer, C. and Ruoff, P. (2001). The nitrate reductase circadian system. The central clock dogma contra multiple oscillatory feedback loops. Plant Physiol 125, 1554-7.

[20] Liu, Y. and Bell-Pedersen, D. (2006). Circadian rhythms in *Neurospora crassa* and other filamentous fungi. Eukaryot Cell 5, 1184-93.

[21] Meijer, J.H., Michel, S., Vanderleest, H.T. and Rohling, J.H. (2010). Daily and seasonal adaptation of the circadian clock requires plasticity of the SCN neuronal network. Eur J Neurosci 32, 2143-51.

[22] Albrecht, U. and Eichele, G. (2003). The mammalian circadian clock. Curr Opin Genet Dev 13, 271-7.

[23] Correa, A., Lewis, Z.A., Greene, A.V., March, I.J., Gomer, R.H. and Bell-Pedersen, D. (2003). Multiple oscillators regulate circadian gene expression in *Neurospora*. Proc Natl Acad Sci U S A 100, 13597-602.

[24] Bell-Pedersen, D., Cassone, V.M., Earnest, D.J., Golden, S.S., Hardin, P.E., Thomas, T.L. and Zoran, M.J. (2005). Circadian rhythms from multiple oscillators: lessons from diverse organisms. Nature Reviews Genetics 6, 544-56.

[25] Roenneberg, T. and Merrow, M. (2001). Circadian systems: different levels of complexity. Philos Trans R Soc Lond B Biol Sci 356, 1687-96.

[26] Perkins, D.D. (1992). *Neurospora*: the organism behind the molecular revolution. Genetics 130, 687-701.

[27] Davies, R.H. (2000). *Neurospora*. Contributions of a Model Organism, Oxford University Press

[28] Lowry, R.J., Durkee, T.L. and Sussman, A.S. (1967). Ultrastructural studies of microconidium formation in *Neurospora crassa*. J Bacteriol 94, 1757-63.

[29] Pandit, A. and Maheshwari, R. (1996). Life-history of *Neurospora intermedia* in a sugar cane field. Journal of Biosciences 21, 57-79.

[30] Pittendrigh, C.S., Bruce, V.G., Rosensweig, N.S. and Rubin, M.L. (1959). Growth patterns in *Neurospora*: A biological clock in *Neurospora*. Nature 184, 169-170.

[31] Chang, B. and Nakashima, H. (1997). Effects of light-dark cycles on the circadian conidiation rhythm in Neurospora crassa. Journal of Plant Research 110, 449-453.

[32] Sargent, M.L. and Woodward, D.O. (1969). Genetic determinants of circadian rhythmicity in *Neurospora*. J Bacteriol 97, 861-6.

[33] Belden, W.J., Larrondo, L.F., Froehlich, A.C., Shi, M., Chen, C.H., Loros, J.J. and Dunlap, J.C. (2007). The band mutation in *Neurospora crassa* is a dominant allele of *ras-1* implicating RAS signaling in circadian output. Genes Dev 21, 1494-505.

[34] Feldman, J.F. and Hoyle, M.N. (1973). Isolation of circadian clock mutants of *Neurospora crassa*. Genetics 75, 605-13.

[35] Galagan, J.E., Calvo, S.E., Borkovich, K.A., Selker, E.U., Read, N.D., Jaffe, D., FitzHugh, W., Ma, L.J., Smirnov, S., Purcell, S., Rehman, B., Elkins, T., Engels, R., Wang, S., Nielsen, C.B., Butler, J., Endrizzi, M., Qui, D., Lanakiev, P., Bell-Pedersen, D., Nelson, M.A., Washburne, M.W., Selitrennikoff, C.P., Kinsey, J.A., Braun, E.L., Zelter, A., Schulte, U., Kothe, G.O., Jedd, G., Mewes, W., Staben, C., Marcotte, E., Greenberg, D., Roy, A., Foley, K., Naylor, J., Thomann, N.S., Barrett, R., Gnerre, S., Kamal, M., Kamvysselis, M., Mauceli, E., Bielke, C., Rudd, S., Frishman, D., Krystofova, S., Rasmussen, C., Metzenberg, R.L., Perkins, D.D., Kroken, S., Cogoni, C., Macino, G., Catcheside, D., Li, W., Pratt, R.J., Osmani, S.A., DeSouza, C.P.C., Glass, L., Orbach, M.J., Berglund, J.A., Voelker, R., Yarden, O., Plamann, M., Seiler, S., Dunlap, J.C., Radford, A., Aramayo, R., Natvig, D.O., Alex,

L.A., Mannhaupt, G., Ebbole, D.J., Freitag, M., Paulsen, I., Sachs, M.S., Lander, E.S., Nusbaum, C. and Birren, B. (2003). The genome sequence of the filamentous fungus *Neurospora crassa*. Nature 422, 859-68.

[36] Perkins, D.D. and Turner, B.C. (1988). *Neurospora* from natural populations: Towards the population biology of a haploid eukaryote. Exp Mycol 12, 91-131.

[37] Beadle, G.W. and Tatum, E.L. (1941). Genetic Control of Biochemical Reactions in *Neurospora*. Proc Natl Acad Sci U S A 27, 499-506.

[38] Sulzman, F.M., Ellman, D., Fuller, C.A., Moore-Ede, M.C. and Wassmer, G. (1984). *Neurospora* circadian rhythms in space: a reexamination of the endogenous-exogenous question. Science 225, 232-4.

[39] Jinhu, G. and Yi, L. (2010). Molecular mechanism of the *Neurospora* circadian oscillator. Protein Cell 1, 331-41.

[40] Lowry, J.A. and Atchley, W.R. (2000). Molecular evolution of the GATA family of transcription factors: conservation within the DNA-binding domain. J Mol Evol 50, 103-15.

[41] Aronson, B.D., Johnson, K.A., Loros, J.J. and Dunlap, J.C. (1994). Negative feedback defining a circadian clock: autoregulation of the clock gene *frequency*. Science 263, 1578-84.

[42] Cheng, P., He, Q., Wang, L. and Liu, Y. (2005). Regulation of the *Neurospora* circadian clock by an RNA helicase. Genes Dev 19, 234-41.

[43] Crosthwaite, S.K., Dunlap, J.C. and Loros, J.J. (1997). *Neurospora wc-1* and *wc-2*: transcription, photoresponses, and the origins of circadian rhythmicity. Science 276, 763-9.

[44] Cheng, P., Yang, Y. and Liu, Y. (2001). Interlocked feedback loops contribute to the robustness of the *Neurospora* circadian clock. Proc Natl Acad Sci U S A 98, 7408-13.

[45] Froehlich, A.C., Liu, Y., Loros, J.J. and Dunlap, J.C. (2002). White Collar-1, a circadian blue light photoreceptor, binding to the *frequency* promoter. Science 297, 815-9.

[46] He, Q. and Liu, Y. (2005). Molecular mechanism of light responses in *Neurospora*: from light-induced transcription to photoadaptation. Genes Dev 19, 2888-99.

[47] Cheng, P., Yang, Y., Heintzen, C. and Liu, Y. (2001). Coiled-coil domain-mediated FRQ-FRQ interaction is essential for its circadian clock function in *Neurospora*. EMBO J 20, 101-8.

[48] He, Q., Cha, J., Lee, H.C., Yang, Y. and Liu, Y. (2006). CKI and CKII mediate the FREQUENCY-dependent phosphorylation of the WHITE COLLAR complex to close the *Neurospora* circadian negative feedback loop. Genes Dev 20, 2552-65.

[49] Schafmeier, T., Haase, A., Kaldi, K., Scholz, J., Fuchs, M. and Brunner, M. (2005). Transcriptional feedback of *Neurospora* circadian clock gene by phosphorylation-dependent inactivation of its transcription factor. Cell 122, 235-46.

[50] Guo, J., Cheng, P., Yuan, H. and Liu, Y. (2009). The exosome regulates circadian gene expression in a posttranscriptional negative feedback loop. Cell 138, 1236-46.

[51] He, Q., Cheng, P. and Liu, Y. (2005). The COP9 signalosome regulates the *Neurospora* circadian clock by controlling the stability of the SCF^{FWD-1} complex. Genes Dev 19, 1518-31.

[52] He, Q., Cheng, P., Yang, Y., Wang, L., Gardner, K.H. and Liu, Y. (2002). White collar-1, a DNA-binding transcription factor and a light sensor. Science 297, 840-3.

[53] Linden, H. (2002). Circadian rhythms. A white collar protein senses blue light. Science 297, 777-8.

[54] Cheng, P., Yang, Y., Wang, L., He, Q. and Liu, Y. (2003). WHITE COLLAR-1, a multifunctional *Neurospora* protein involved in the circadian feedback loops, light sensing, and transcription repression of *wc-2*. J Biol Chem 278, 3801-8.

References

[55] Belden, W.J., Loros, J.J. and Dunlap, J.C. (2007). Execution of the circadian negative feedback loop in *Neurospora* requires the ATP-dependent chromatin-remodeling enzyme CLOCKSWITCH. Mol Cell 25, 587-600.

[56] Froehlich, A.C., Loros, J.J. and Dunlap, J.C. (2003). Rhythmic binding of a WHITE COLLAR-containing complex to the *frequency* promoter is inhibited by FREQUENCY. Proc Natl Acad Sci U S A 100, 5914-9.

[57] Ballario, P., Talora, C., Galli, D., Linden, H. and Macino, G. (1998). Roles in dimerization and blue light photoresponse of the PAS and LOV domains of *Neurospora crassa* white collar proteins. Mol Microbiol 29, 719-29.

[58] Ballario, P., Vittorioso, P., Magrelli, A., Talora, C., Cabibbo, A. and Macino, G. (1996). White collar-1, a central regulator of blue light responses in *Neurospora*, is a zinc finger protein. EMBO J 15, 1650-7.

[59] Collett, M.A., Garceau, N., Dunlap, J.C. and Loros, J.J. (2002). Light and clock expression of the *Neurospora* clock gene *frequency* is differentially driven by but dependent on WHITE COLLAR-2. Genetics 160, 149-58.

[60] Denault, D.L., Loros, J.J. and Dunlap, J.C. (2001). WC-2 mediates WC-1-FRQ interaction within the PAS protein-linked circadian feedback loop of *Neurospora*. EMBO J 20, 109-17.

[61] Lee, K., Dunlap, J.C. and Loros, J.J. (2003). Roles for WHITE COLLAR-1 in circadian and general photoperception in *Neurospora crassa*. Genetics 163, 103-14.

[62] Kaldi, K., Gonzalez, B.H. and Brunner, M. (2006). Transcriptional regulation of the *Neurospora* circadian clock gene *wc-1* affects the phase of circadian output. EMBO Rep 7, 199-204.

[63] Neiss, A., Schafmeier, T. and Brunner, M. (2008). Transcriptional regulation and function of the *Neurospora* clock gene *white collar-2* and its isoforms. EMBO Rep 9, 788-94.

[64] Huang, G., Chen, S., Li, S., Cha, J., Long, C., Li, L., He, Q. and Liu, Y. (2007). Protein kinase A and casein kinases mediate sequential phosphorylation events in the circadian negative feedback loop. Genes Dev 21, 3283-95.

[65] Cha, J., Chang, S.S., Huang, G., Cheng, P. and Liu, Y. (2008). Control of WHITE COLLAR localization by phosphorylation is a critical step in the circadian negative feedback process. EMBO J 27, 3246-55.

[66] Hong, C.I., Ruoff, P., Loros, J.J. and Dunlap, J.C. (2008). Closing the circadian negative feedback loop: FRQ-dependent clearance of WC-1 from the nucleus. Genes Dev 22, 3196-204.

[67] Cheng, P., Yang, Y., Gardner, K.H. and Liu, Y. (2002). PAS domain-mediated WC-1/WC-2 interaction is essential for maintaining the steady-state level of WC-1 and the function of both proteins in circadian clock and light responses of *Neurospora*. Mol Cell Biol 22, 517-24.

[68] de Paula, R.M., Lewis, Z.A., Greene, A.V., Seo, K.S., Morgan, L.W., Vitalini, M.W., Bennett, L., Gomer, R.H. and Bell-Pedersen, D. (2006). Two circadian timing circuits in *Neurospora crassa* cells share components and regulate distinct rhythmic processes. J Biol Rhythms 21, 159-68.

[69] Li, S. and Lakin-Thomas, P. (2010). Effects of *prd* circadian clock mutations on FRQ-less rhythms in *Neurospora*. J Biol Rhythms 25, 71-80.

[70] Schneider, K., Perrino, S., Oelhafen, K., Li, S., Zatsepin, A., Lakin-Thomas, P. and Brody, S. (2009). Rhythmic conidiation in constant light in *vivid* mutants of *Neurospora crassa*. Genetics 181, 917-31.

[71] Aronson, B.D., Johnson, K.A. and Dunlap, J.C. (1994). Circadian clock locus *frequency*: protein encoded by a single open reading frame defines period length and temperature compensation. Proc Natl Acad Sci U S A 91, 7683-7.

[72] Colot, H.V., Loros, J.J. and Dunlap, J.C. (2005). Temperature-modulated alternative splicing and promoter use in the circadian clock gene *frequency*. Mol Biol Cell 16, 5563-71.

[73] Diernfellner, A., Colot, H.V., Dintsis, O., Loros, J.J., Dunlap, J.C. and Brunner, M. (2007). Long and short isoforms of *Neurospora* clock protein FRQ support temperature-compensated circadian rhythms. FEBS Lett 581, 5759-64.

[74] Garceau, N.Y., Liu, Y., Loros, J.J. and Dunlap, J.C. (1997). Alternative initiation of translation and time-specific phosphorylation yield multiple forms of the essential clock protein FREQUENCY. Cell 89, 469-76.

[75] Liu, Y., Garceau, N.Y., Loros, J.J. and Dunlap, J.C. (1997). Thermally regulated translational control of FRQ mediates aspects of temperature responses in the *Neurospora* circadian clock. Cell 89, 477-86.

[76] Kramer, C., Loros, J.J., Dunlap, J.C. and Crosthwaite, S.K. (2003). Role for antisense RNA in regulating circadian clock function in *Neurospora crassa*. Nature 421, 948-52.

[77] Liu, Y. (2005). Analysis of posttranslational regulations in the *Neurospora* circadian clock. Methods Enzymol 393, 379-93.

[78] Baker, C.L., Kettenbach, A.N., Loros, J.J., Gerber, S.A. and Dunlap, J.C. (2009). Quantitative proteomics reveals a dynamic interactome and phase-specific phosphorylation in the *Neurospora* circadian clock. Mol Cell 34, 354-63.

[79] Mehra, A., Shi, M., Baker, C.L., Colot, H.V., Loros, J.J. and Dunlap, J.C. (2009). A role for casein kinase 2 in the mechanism underlying circadian temperature compensation. Cell 137, 749-60.

[80] Diernfellner, A.C., Querfurth, C., Salazar, C., Hofer, T. and Brunner, M. (2009). Phosphorylation modulates rapid nucleocytoplasmic shuttling and cytoplasmic accumulation of *Neurospora* clock protein FRQ on a circadian time scale. Genes Dev 23, 2192-200.

[81] Lee, K., Loros, J.J. and Dunlap, J.C. (2000). Interconnected feedback loops in the *Neurospora* circadian system. Science 289, 107-10.

[82] Loros, J.J. and Feldman, J.F. (1986). Loss of temperature compensation of circadian period length in the *frq-9* mutant of *Neurospora crassa*. J Biol Rhythms 1, 187-98.

[83] Christensen, M.K. (2007) A *frequency*-independent nitrate reductase rhythm in *Neurospora crassa*. PhD thesis. University of Stavanger.

[84] Christensen, M.K., Falkeid, G., Loros, J.J., Dunlap, J.C., Lillo, C. and Ruoff, P. (2004). A nitrate-induced *frq*-less oscillator in *Neurospora crassa*. Journal of Biological Rhythms 19, 280-286.

[85] Li, S., Motavaze, K., Kafes, E., Suntharalingam, S. and Lakin-Thomas, P. (2011). A new mutation affecting FRQ-less rhythms in the circadian system of *Neurospora crassa*. PLoS Genet 7, e1002151.

[86] Fu, Y.H. and Marzluf, G.A. (1987). Molecular cloning and analysis of the regulation of *nit-3*, the structural gene for nitrate reductase in *Neurospora crassa*. Proc Natl Acad Sci U S A 84, 8243-7.

[87] Marzluf, G.A. (1997). Genetic regulation of nitrogen metabolism in the fungi. Microbiol Mol Biol Rev 61, 17-32.

[88] Borkovich, K.A., Alex, L.A., Yarden, O., Freitag, M., Turner, G.E., Read, N.D., Seiler, S., Bell-Pedersen, D., Paietta, J., Plesofsky, N., Plamann, M., Tanrikulu, M.G-., Schulte, U., Mannhaupt, G., Nargang, F.E., Radford, A., Selitrennikoff, C., Galagan, J.E., Dunlap, J.C., Loros, J.J., Catcheside, D., Inoue, H., Aramayo, R., Polymenis, M., Selker, E.U., Sachs, M.S., Marzluf, G.A., Paulsen, I., Davis, R., Ebbole, D.J., Zelter, A., Kalkman, E.R., O'Rourke, R., Bowring, F., Yeadon, J., Ishii, C., Suzuki, K., Sakai, W. and Pratt, R. (2004). Lessons from the genome sequence of

Neurospora crassa: tracing the path from genomic blueprint to multicellular organism. Microbiol Mol Biol Rev 68, 1-108.

[89] Gao-Rubinelli, F. and Marzluf, G.A. (2004). Identification and characterization of a nitrate transporter gene in *Neurospora crassa*. Biochem Genet 42, 21-34.

[90] Fu, Y.H. and Marzluf, G.A. (1988). Metabolic control and autogenous regulation of *nit-3*, the nitrate reductase structural gene of *Neurospora crassa*. J Bacteriol 170, 657-61.

[91] Campbell, W.H. and Kinghorn, K.R. (1990). Functional domains of assimilatory nitrate reductases and nitrite reductases. Trends Biochem Sci 15, 315-9.

[92] Exley, G.E., Colandene, J.D. and Garrett, R.H. (1993). Molecular cloning, characterization, and nucleotide sequence of *nit-6*, the structural gene for nitrite reductase in *Neurospora crassa*. J Bacteriol 175, 2379-92.

[93] Fu, Y.H. and Marzluf, G.A. (1990). *nit-2*, the major positive-acting nitrogen regulatory gene of *Neurospora crassa*, encodes a sequence-specific DNA-binding protein. Proc Natl Acad Sci U S A 87, 5331-5.

[94] Fu, Y.H. and Marzluf, G.A. (1990). *nit-2*, the major nitrogen regulatory gene of *Neurospora crassa*, encodes a protein with a putative zinc finger DNA-binding domain. Mol Cell Biol 10, 1056-65.

[95] Xiao, X. and Marzluf, G.A. (1996). Identification of the native NIT2 major nitrogen regulatory protein in nuclear extracts of *Neurospora crassa*. Genetica 97, 153-63.

[96] Fu, Y.H. and Marzluf, G.A. (1987). Characterization of *nit-2*, the major nitrogen regulatory gene of *Neurospora crassa*. Mol Cell Biol 7, 1691-6.

[97] Feng, B. and Marzluf, G.A. (1996). The regulatory protein NIT4 that mediates nitrate induction in *Neurospora crassa* contains a complex tripartite activation domain with a novel leucine-rich, acidic motif. Curr Genet 29, 537-48.

[98] Fu, Y.H., Feng, B., Evans, S. and Marzluf, G.A. (1995). Sequence-specific DNA-binding by NIT4, the pathway-specific regulatory protein that mediates nitrate induction in *Neurospora*. Mol Microbiol 15, 935-42.

[99] Yuan, G.F., Fu, Y.H. and Marzluf, G.A. (1991). *nit-4*, a pathway-specific regulatory gene of *Neurospora crassa*, encodes a protein with a putative binuclear zinc DNA-binding domain. Mol Cell Biol 11, 5735-45.

[100] Feng, B. and Marzluf, G.A. (1998). Interaction between major nitrogen regulatory protein NIT2 and pathway-specific regulatory factor NIT4 is required for their synergistic activation of gene expression in *Neurospora crassa*. Mol Cell Biol 18, 3983-90.

[101] Mo, X. and Marzluf, G.A. (2003). Cooperative action of the NIT2 and NIT4 transcription factors upon gene expression in *Neurospora crassa*. Curr Genet 42, 260-7.

[102] Chiang, T.Y. and Marzluf, G.A. (1995). Binding affinity and functional significance of NIT2 and NIT4 binding sites in the promoter of the highly regulated *nit-3* gene, which encodes nitrate reductase in *Neurospora crassa*. J Bacteriol 177, 6093-9.

[103] Premakumar, R., Sorger, G.J. and Gooden, D. (1980). Repression of nitrate reductase in *Neurospora* studied by using L-methionine-DL-sulfoximine and glutamine auxotroph gln-1b. J Bacteriol 143, 411-5.

[104] Tomsett, A.B., Dunn-Coleman, N.S. and Garrett, R.H. (1981). The regulation of nitrate assimilation in *Neurospora crassa*: the isolation and genetic analysis of *nmr-1* mutants. Mol Gen Genet 182, 229-33.

[105] Young, J.L., Jarai, G., Fu, Y.H. and Marzluf, G.A. (1990). Nucleotide sequence and analysis of NMR, a negative-acting regulatory gene in the nitrogen circuit of *Neurospora crassa*. Mol Gen Genet 222, 120-8.

[106] Fu, Y.H., Young, J.L. and Marzluf, G.A. (1988). Molecular cloning and characterization of a negative-acting nitrogen regulatory gene of *Neurospora crassa*. Mol Gen Genet 214, 74-9.

[107] Harmer, S.L., Hognesch, J.B., Straume, M., Chang, H-S., Han, B., Zhu, T., Wang, Z., Kreps, J.A. and Kay, S.A. (2000). Orchestrated transcription of key pathways in *Arabidopsis* by the circadian clock. Science 290, 2110-3.

[108] Perkins, D.D., Radford, A. and Sachs, M.S. (2001) The *Neurospora* Compendium. Chromosomal Loci. Academic Press

[109] Marzluf, G.A. (1997). Molecular genetics of sulfur assimilation in filamentous fungi and yeast. Annu Rev Microbiol 51, 73-96.

[110] Jarai, G. and Marzluf, G.A. (1991). Sulfate transport in *Neurospora crassa*: regulation, turnover, and cellular localization of the CYS-14 protein. Biochemistry 30, 4768-73.

[111] Ketter, J.S., Jarai, G., Fu, Y.H. and Marzluf, G.A. (1991). Nucleotide sequence, messenger RNA stability, and DNA recognition elements of *cys-14*, the structural gene for sulfate permease II in *Neurospora crassa*. Biochemistry 30, 1780-7.

[112] Marzluf, G.A. (1970). Genetic and biochemical studies of distinct sulfate permease species in different developmental stages of *Neurospora crassa*. Arch Biochem Biophys 138, 254-63.

[113] Ketter, J.S. and Marzluf, G.A. (1988). Molecular cloning and analysis of the regulation of *cys-14*+, a structural gene of the sulfur regulatory circuit of *Neurospora crassa*. Mol Cell Biol 8, 1504-8.

[114] Fu, Y.H., Paietta, J.V., Mannix, D.G. and Marzluf, G.A. (1989). *cys-3*, the positive-acting sulfur regulatory gene of *Neurospora crassa*, encodes a protein with a putative leucine zipper DNA-binding element. Mol Cell Biol 9, 1120-7.

[115] Paietta, J.V. (1989). Molecular cloning and regulatory analysis of the arylsulfatase structural gene of *Neurospora crassa*. Mol Cell Biol 9, 3630-7.

[116] Paietta, J.V. (1990). Molecular cloning and analysis of the *scon-2* negative regulatory gene of *Neurospora crassa*. Mol Cell Biol 10, 5207-14.

[117] Fu, Y.H. and Marzluf, G.A. (1990). *cys-3*, the positive-acting sulfur regulatory gene of *Neurospora crassa*, encodes a sequence-specific DNA-binding protein. J Biol Chem 265, 11942-7.

[118] Kanaan, M.N. and Marzluf, G.A. (1993). The positive-acting sulfur regulatory protein CYS-3 of *Neurospora crassa*: nuclear localization, autogenous control, and regions required for transcriptional activation. Mol Gen Genet 239, 334-44.

[119] Paietta, J.V. (1995). Analysis of CYS-3 regulator function in *Neurospora crassa* by modification of leucine zipper dimerization specificity. Nucleic Acids Res 23, 1044-9.

[120] Coulter, K.R. and Marzluf, G.A. (1998). Functional analysis of different regions of the positive-acting CYS-3 regulatory protein of *Neurospora crassa*. Curr Genet 33, 395-405.

[121] Hanson, M.A. and Marzluf, G.A. (1973). Regulation of a sulfur-controlled protease in *Neurospora crassa*. J Bacteriol 116, 785-9.

[122] Kumar, A. and Paietta, J.V. (1995). The *sulfur controller-2* negative regulatory gene of *Neurospora crassa* encodes a protein with beta-transducin repeats. Proc Natl Acad Sci U S A 92, 3343-7.

[123] Li, Q. and Marzluf, G.A. (1996). Determination of the *Neurospora crassa* CYS-3 sulfur regulatory protein consensus DNA-binding site: amino-acid substitutions in the CYS-3 bZIP domain that alter DNA-binding specificity. Curr Genet 30, 298-304.

References

[124] Li, Q., Zhou, L. and Marzluf, G.A. (1996). Functional *in vivo* studies of the *Neurospora crassa cys-14* gene upstream region: importance of CYS-3-binding sites for regulated expression. Mol Microbiol 22, 109-17.

[125] Kanaan, M.N. and Marzluf, G.A. (1991). Mutational analysis of the DNA-binding domain of the CYS-3 regulatory protein of *Neurospora crassa*. Mol Cell Biol 11, 4356-62.

[126] Paietta, J.V. (1992). Production of the CYS-3 regulator, a bZIP DNA-binding protein, is sufficient to induce sulfur gene expression in *Neurospora crassa*. Mol Cell Biol 12, 1568-77.

[127] Tao, Y. and Marzluf, G.A. (1998). Synthesis and differential turnover of the CYS-3 regulatory protein of *Neurospora crassa* are subject to sulfur control. J Bacteriol 180, 478-82.

[128] Sizemore, S.T. and Paietta, J.V. (2002). Cloning and characterization of *scon-3+*, a new member of the *Neurospora crassa* sulfur regulatory system. Eukaryot Cell 1, 875-83.

[129] Kumar, A. and Paietta, J.V. (1998). An additional role for the F-box motif: gene regulation within the *Neurospora crassa* sulfur control network. Proc Natl Acad Sci U S A 95, 2417-22.

[130] Onai, K. and Nakashima, H. (1997). Mutation of the *cys-9* gene, which encodes thioredoxin reductase, affects the circadian conidiation rhythm in *Neurospora crassa*. Genetics 146, 101-10.

[131] Lepisto, A., Kangasjarvi, S., Luomala, E.M., Brader, G., Sipari, N., Keranen, M., Keinanen, M. and Rintamaki, E. (2009). Chloroplast NADPH-thioredoxin reductase interacts with photoperiodic development in *Arabidopsis*. Plant Physiol 149, 1261-76.

[132] Koprivova, A., Suter, M., den Camp, R.O., Brunold, C. and Kopriva, S. (2000). Regulation of sulfate assimilation by nitrogen in *Arabidopsis*. Plant Physiol 122, 737-46.

[133] Robertson, J.B., Stowers, C.C., Boczko, E. and Johnson, C.H. (2008). Real-time luminescence monitoring of cell-cycle and respiratory oscillations in yeast. Proc Natl Acad Sci U S A 105, 17988-93.

[134] Morgan, L.W., Greene, A.V. and Bell-Pedersen, D. (2003). Circadian and light-induced expression of luciferase in *Neurospora crassa*. Fungal Genet Biol 38, 327-32.

[135] Hastings, J.W. and Johnson, C.H. (2003). Bioluminescence and chemiluminescence. Methods Enzymol 360, 75-104.

[136] Gooch, V.D., Mehra, A., Larrondo, L.F., Fox, J., Touroutoutoudis, M., Loros, J.J. and Dunlap, J.C. (2008). Fully codon-optimized luciferase uncovers novel temperature characteristics of the *Neurospora* clock. Eukaryot Cell 7, 28-37.

[137] Dunn-Coleman, N.S., Tomsett, A.B. and Garrett, R.H. (1981). The regulation of nitrate assimilation in *Neurospora crassa*: biochemical analysis of the *nmr-1* mutants. Mol Gen Genet 182, 234-9.

[138] Colot, H.V., Gyungsoon, P., Turner, G.E., Ringelberg, C., Crew, C.M., Litvinkova, L., Weiss, R.L., Borkovich, K.A. and Dunlap, J.C. (2006). A high-throughput gene knockout procedure for *Neurospora* reveals functions for multiple transcription factors. Proc Natl Acad Sci U S A 103, 10352-7.

[139] Horowitz, N.H. (1947). Methionine synthesis in *Neurospora*: The isolation of cystathionine. J Biol Chem 171, 255-264.

[140] Vogel, A. (1956). A convenient growth medium for *Neurospora* (medium N). Microbial Genetics Bulletin 13, 42-43.

[141] Westergaard, M. and Mitchell, H.K. (1947). *Neurospora* V. A synthetic medium favoring sexual reproduction. Am. J. Bot. 34, 573-577.

[142] Lillo, C. (1983). Studies of diurnal variations of nitrate reductase activity in barley leaves using various assay methods. Physiol Plant 57, 357-362.

[143] Margolin, B.S., Freitag, M. and Selker, E.U. (2000). Improved plasmids for gene targeting at the *his-3* locus of *Neurospora crassa* by electroporation. Fungal Genetics Newsletter 44

[144] Aramayo, R. and Metzenberg, R.L. (1996). Gene replacements at the *his-3* locus of *Neurospora crassa*. Fungal Genetics Newsletter 43, 9-13.

[145] Subramanian, K.N., Padmanaban, G. and Sarma, P.S. (1968). The regulation of nitrate reductase and catalase by amino acids in *Neurospora crassa*. Biochim Biophys Acta 151, 20-32.

[146] Lillo, C. (1984). Circadian rhythms of nitrate reductase activity in barley leaves. Physiol Plant 61, 219-223.

[147] Lillo, C. and Ruoff, P. (1989). An unusually rapid light-induced nitrate reductase mRNA pulse and circadian oscillations. Naturwissenschaften 76, 526-8.

[148] Pilgrim, M.L., Caspar, T., Quail, P.H. and McClung, C.R. (1993). Circadian and light-regulated expression of nitrate reductase in *Arabidopsis*. Plant Mol Biol 23, 349-64.

[149] Ramalho, C.B., Hastings, J.W. and Colepicolo, P. (1995). Circadian oscillation of nitrate reductase activity in *Gonyaulax polyedra* is due to changes in cellular protein levels. Plant Physiol 107, 225-31.

[150] Conti, E., Lloyd, L.F., Akins, J., Franks, N.P. and Brick, P. (1996). Crystallization and preliminary diffraction studies of firefly luciferase from *Photinus pyralis*. Acta Crystallogr D Biol Crystallogr 52, 876-8.

[151] Denburg, J.L. and McElroy, W.D. (1970). Anion inhibition of firefly luciferase. Arch Biochem Biophys 141, 668-75.

[152] Leitao, J.M. and Esteves da Silva, J.C. Firefly luciferase inhibition. J Photochem Photobiol B 101, 1-8.

[153] van Leeuwen, W., Hagendoorn, M.J.M., Ruttink, T., van Poecke, R.M., van Der Plas, L.H. and van Der Krol, A.R. (2000). The use of the luciferase reporter system for *in planta* gene expression studies. Plant Mol Biol Rep 18, 143a-143t.

[154] Ruoff, P. and Lillo, C. (1990). Molecular oxygen as electron acceptor in the NADH-nitrate reductase system. Biochem Biophys Res Commun 172, 1000-5.

[155] Barber, M.J. and Kay, C.J. (1996). Superoxide production during reduction of molecular oxygen by assimilatory nitrate reductase. Arch Biochem Biophys 326, 227-32.

[156] Sargent, M.L. and Kaltenborn, S.H. (1972). Effects of medium composition and carbon dioxide on circadian conidiation in *Neurospora*. Plant Physiol 50, 171-5.

[157] Spee, R.E. (2009). Modelling circadian rhythms in *Neurospora crassa*. Bachelor thesis. Wageningen University/University of Stavanger.

[158] Pan, H., Feng, B. and Marzluf, G.A. (1997). Two distinct protein-protein interactions between the NIT2 and NMR regulatory proteins are required to establish nitrogen metabolite repression in *Neurospora crassa*. Mol Microbiol 26, 721-9.

[159] Ni, X.Y., Drengstig, T. and Ruoff, P. (2009). The control of the controller: molecular mechanisms for robust perfect adaptation and temperature compensation. Biophysical Journal 97, 1244-53.

[160] Huang, Y. (2011). Negative feedback leading to nitrate homeostasis and oscillatory nitrate assimilation in plants and fungi. Bachelor thesis. University of Stavanger.

[161] Tyson, J.J., Hong, C.I., Thron, C.D. and Novak, B. (1999). A simple model of circadian rhythms based on dimerization and proteolysis of PER and TIM. Biophysical Journal 77, 2411-7.

References

7 Appendix I – Molecular biology

7.1 Gene, promoter and primer sequences

Table 7.1. The promoter sequences used in the construction of the *Neurospora crassa luciferase* reporter constructs. The gene sequences can be found in the *Neurospora crassa* database (Broad Institute)[25].

Gene	Accession number	Promoter sequence
nit-3	NCU05298.5	2000 bp upstream from the *nit-3* start codon
*nit-3*Δ	NCU05298.5	1568 bp upstream from the *nit-3* start codon
wc-1	NCU02356.5	2223 bp upstream from the *wc-1* start codon in addition to the first 200 bp of the *wc-1* ORF
cys-3	NCU03536.5	1885 bp upstream from the *cys-3* start codon
scon-2	NCU08563.5	2106 bp upstream from the *scon-2* start codon

Table 7.2. Primers used to confirm the Δ*frq*Δ*nmr* knock out genotypes.

Gene	Forward primer (5'→3')	Reverse primer (5'→3')	Annealing temperature
frq	AGAAGAAGCTGGTTGTCCGA	TCCGACCATTCTTATCCGAG	60°C
nmr	ACTTTCTATGGCGACGAGGA	GCCTCCAACTGGATTCGATA	60°C
hph[26]	GACAGAAGATGATATTGAAGGAGC	GATTTCAGTAACGTTAAGTGGA	65°C

[25] http://www.broadinstitute.org/annotation/genome/neurospora/MultiHome.html

[26] http://www.fgsc.net/neurosporaprotocols/How%20to%20create%20gene%20knockouts%20in%20Neurospora.pdf

Appendix I

Table 7.3. Primers used to amplify the *lucI* gene and the *nit-3*, *wc-1*, *cys-3* and *scon-2* promoter sequences. EcoRI restriction site in red, BamHI restriction site in green, XbaI site in blue, NotI restriction site in orange, and AscI restriction site in purple. The annealing temperatures, cycle number and target vectors are indicated.

Gene/ promoter	Forward primer (5'-3')	Reverse primer (5'-3')	Annealing temperature	Cycles	Target vector
lucI	ATCGGAATTCATGGAGGATC CCAAGAACATCAAGAAAGGC CCCGC	CGATTCTAGACTACTAGATCA GAGCTTGGAC	63.5°C	35	pBM61
nit-3 (*lucI*)	ATCGGAATTCACACCTGCAG ATCCTGCTGG	CTTGGGATCCTCCATGATGAT GCTCGTGAGGTA	63°C	35	pLUCI
nit-3Δ (*lucI*)	ATCGGAATTCCCGCCGCCTC CTCCTCCTCC	CTTGGGATCCTCCATGATGAT GCTCGTGAGGTA	64.5°C	35	pLUCI
wc-1 (*lucI*)	ATCGGAATTCCCTGTGATGT TCTCGACCGC	CTTGGGATCCTCCATATGCCG GCATTGCGAT	63°C	35	pLUCI
cys-3 (*lucI*)	ATCGGAATTCGAGAGGAAGA CGCTT	CTTGGGATCCTCCATTTTGAC GATGGTTTG	67°C	30	pLUCI
scon-2 (*lucI*)	ATCGGAATTCGGGAGGCATG CTGTGGTCAG	CTTGGGATCCTCCATGTTGGT GACGCTGTT	67°C	30	pLUCI
nit-3 (*NcLUC*)	ATCGGCGGCCGCACACCTGC AGATCCTGCTGG	CGATGGCGCGCCGATGATGCT CGTGAGGTAGG	63°C	35	pRMP62
nit-3Δ (*NcLUC*)	ATCGGCGGCCGCCCGCCGCC TCCTCCTCCTCC	CGATGGCGCGCCCGATGATGCT CGTGAGGTAGG	64.5°C	35	pRMP62
wc-1 (*NcLUC*)	ATCGGCGGCCGCCCTGTGAT GTTCTCGACCGC	CGATGGCGCGCCCATGCCGGCA TTGCGATGCTG	63°C	35	pRMP62
cys-3 (*NcLUC*)	ATCGTCTAGAAAGAAACCCC TCCTGGCGGGGCGGGAC	CGATGCGGGCCGCTTTGACGAT GGTTTGTGTGGTGTTGTC	67°C	30	pRMP62

Table 7.4. Restriction endonucleases used in the cloning of the promoter-*luciferase* reporter constructs. The enzymes were obtained from New England Biolabs (NEB). All restriction reactions were carried out at 37°C.

Enzyme	Recognition site (5'→3')	Buffer	BSA
AscI	GG^CGCGCC	NEB 4	-
AseI	AT^TAAT	NEB 3	-
BamHI	G^GATCC	NEB 3	+
EcoRI	G^AATTC	NEB U	-
NdeI	CA^TATG	NEB 4	+
NotI	GC^GGCCGC	NEB 4	+
SpeI	A^CTAGT	NEB 4	+
XbaI	T^CTAGA	NEB 4	+

Appendix I

Figure 7.1. Allignment of the *Neurospora crassa* optimized intron-containing (*lucI*) and the intron-less (*NcLUC*) *luciferase* sequences. The *ccg-2* intron is highlighted in red. The alignment was done using ClustalW2[27].

```
lucI    ATGGAGGACGCCAAGAACATCAAGAAGGGCCCCGCCCCCTTCTACCCCCTCGAGGACGGC 60
NcLUC   ATGGAGGACGCCAAGAACATCAAGAAGGGCCCCGCCCCCTTCTACCCCCTCGAGGACGGC 60
        ************************************************************

lucI    ACCGCCGGCGAGCAGCTCCACAAGGCCATGAAGCGCTACGCCCTCGTCCCCGGCACCATC 120
NcLUC   ACCGCCGGCGAGCAGCTCCACAAGGCCATGAAGCGCTACGCCCTCGTCCCCGGCACCATC 120
        ************************************************************

lucI    GCCTTCGTAGGTTTCCTCCAGCTCTCGCCTCCAGCACCCGAGGCACATCTCGGGCATCTT 180
NcLUC   GCCTTC------------------------------------------------------ 126
        ******

lucI    CACAACAACAGACACTGACATCTCATTCTCACAGACCGACGCCCACATCGAGGTCAACAT 240
NcLUC   ----------------------------------ACCGACGCCCACATCGAGGTCGACAT 152
                                           ********************.****

lucI    CACCTACGCCGAGTACTTCGAGATGTCCGTCCGCCTCGCCGAGGCCATGAAGCGCTACGG 300
NcLUC   CACCTACGCCGAGTACTTCGAGATGTCCGTCCGCCTCGCCGAGGCCATGAAGCGCTACGG 212
        ************************************************************

lucI    CCTCAACACCAACCACCGCATCGTCGTCTGCTCCGAGAACTCCCTCCAGTTCTTCATGCC 360
NcLUC   CCTCAACACCAACCACCGCATCGTCGTCTGCTCCGAGAACTCCCTCCAGTTCTTCATGCC 272
        ************************************************************

lucI    CGTCCTCGGCGCCCTCTTCATCGGCGTCGCCGTCGCCCCCGCCAACGACATCTACAACGA 420
NcLUC   CGTCCTCGGCGCCCTCTTCATCGGCGTCGCCGTCGCCCCCGCCAACGACATCTACAACGA 332
        ************************************************************

lucI    GCGCGAGCTCCTCAACTCCATGAACATCTCCCAGCCCACCGTCGTCTTCGTCTCCAAGAA 480
NcLUC   GCGCGAGCTCCTCAACTCCATGGGCATCTCCCAGCCCACCGTCGTCTTCGTCTCCAAGAA 392
        **********************..************************************

lucI    GGGCCTCCAGAAGATCCTCAACGTCCAGAAGAAGCTCCCCATCATCCAGAAGATCATCAT 540
NcLUC   GGGCCTCCAGAAGATCCTCAACGTCCAGAAGAAGCTCCCCATCATCCAGAAGATCATCAT 452
        ************************************************************

lucI    CATGGACTCCAAGACCGACTACCAGGGCTTCCAGTCCATGTACACCTTCGTCACCTCCCA 600
NcLUC   CATGGACTCCAAGACCGACTACCAGGGCTTCCAGTCCATGTACACCTTCGTCACCTCCCA 512
        ************************************************************

lucI    CCTCCCCCCCGGCTTCAACGAGTACGACTTCGTCCCCGAGTCCTTCGACCGCGACAAGAC 660
NcLUC   CCTCCCCCCCGGCTTCAACGAGTACGACTTCGTCCCCGAGTCCTTCGACCGCGACAAGAC 572
        ************************************************************

lucI    CATCGCCCTCATCATGAACTCCTCCGGCTCCACCGGCCTCCCCAAGGGCGTCGCCCTCCC 720
```

[27] http://www.ebi.ac.uk/Tools/msa/clustalw2/

```
NcLUC  CATCGCCCTCATCATGAACTCCTCCGGCTCCACCGGCCTCCCCAAGGGCGTCGCCCTCCC 632
       ************************************************************

lucI   CCACCGCACCGCCTGCGTCCGCTTCTCCCACGCCCGCGACCCCATCTTCGGCAACCAGAT 780
NcLUC  CCACCGCACCGCCTGCGTCCGCTTCTCCCACGCCCGCGACCCCATCTTCGGCAACCAGAT 692
       ************************************************************

lucI   CATCCCCGACACCGCCATCCTCTCCGTCGTCCCCTTCCACCACGGCTTCGGCATGTTCAC 840
NcLUC  CATCCCCGACACCGCCATCCTCTCCGTCGTCCCCTTCCACCACGGCTTCGGCATGTTCAC 752
       ************************************************************

lucI   CACCCTCGGCTACCTCATCTGCGGCTTCCGCGTCGTCCTCATGTACCGCTTCGAGGAGGA 900
NcLUC  CACCCTCGGCTACCTCATCTGCGGCTTCCGCGTCGTCCTCATGTACCGCTTCGAGGAGGA 812
       ************************************************************

lucI   GCTCTTCCTCCGCTCCCTCCAGGACTACAAGATCCAGTCCGCCCTCCTCGTCCCCACCCT 960
NcLUC  GCTCTTCCTCCGCTCCCTCCAGGACTACAAGATCCAGTCCGCCCTCCTCGTCCCCACCCT 872
       ************************************************************

lucI   CTTCTCCTTCTTCGCCAAGTCCACCCTCATCGACAAGTACGACCTCTCCAACCTCCACGA 1020
NcLUC  CTTCTCCTTCTTCGCCAAGTCCACCCTCATCGACAAGTACGACCTCTCCAACCTCCACGA 932
       ************************************************************

lucI   GATCGCCTCCGGCGGCGCCCCCCTCTCCAAGGAGGTCGGCGAGGCCGTCGCCAAGCGCTT 1080
NcLUC  GATCGCCTCCGGCGGCGCCCCCCTCTCCAAGGAGGTCGGCGAGGCCGTCGCCAAGCGCTT 992
       ************************************************************

lucI   CCACCTCCCCGGCATCCGCCAGGGCTACGGCCTCACCGAGACCACCTCCGCCATCCTCAT 1140
NcLUC  CCACCTCCCCGGCATCCGCCAGGGCTACGGCCTCACCGAGACCACCTCCGCCATCCTCAT 1052
       ************************************************************

lucI   CACCCCCGAGGGCGACGACAAGCCCGGCGCCGTCGGCAAGGTCGTCCCCTTCTTCGAGGC 1200
NcLUC  CACCCCCGAGGGCGACGACAAGCCCGGCGCCGTCGGCAAGGTCGTCCCCTTCTTCGAGGC 1112
       ************************************************************

lucI   CAAGGTCGTCGACCTCGACACCGGCAAGACCCTCGGCGTCAACCAGCGCGGCGAGCTCTG 1260
NcLUC  CAAGGTCGTCGACCTCGACACCGGCAAGACCCTCGGCGTCAACCAGCGCGGCGAGCTCTG 1172
       ************************************************************

lucI   CGTCCGCGGCCCCATGATCATGTCCGGCTACGTCAACAACCCCGAGGCCACCAACGCCCT 1320
NcLUC  CGTCCGCGGCCCCATGATCATGTCCGGCTACGTCAACAACCCCGAGGCCACCAACGCCCT 1232
       ************************************************************

lucI   CATCGACAAGGACGGCTGGCTCCACTCCGGCGACATCGCCTACTGGGACGAGGACGAGCA 1380
NcLUC  CATCGACAAGGACGGCTGGCTCCACTCCGGCGACATCGCCTACTGGGACGAGGACGAGCA 1292
       ************************************************************

lucI   CTTCTTCATCGTCGACCGCCTCAAGTCCCTCATCAAGTACAAGGGCTACCAGGTCGCCCC 1440
NcLUC  CTTCTTCATCGTCGACCGCCTCAAGTCCCTCATCAAGTACAAGGGCTACCAGGTCGCCCC 1352
       ************************************************************

lucI   CGCCGAGCTCGAGTCCATCCTCCTCCAGCACCCCAACATCTTCGACGCCGGCGTCGCCGG 1500
NcLUC  CGCCGAGCTCGAGTCCATCCTCCTCCAGCACCCCAACATCTTCGACGCCGGCGTCGCCGG 1412
       ************************************************************

lucI   CCTCCCCGACGACGACGCCGGCGAGCTCCCCGCCGCCGTCGTCGTCCTCGAGCACGGCAA 1560
NcLUC  CCTCCCCGACGACGACGCCGGCGAGCTCCCCGCCGCCGTCGTCGTCCTCGAGCACGGCAA 1472
       ************************************************************
```

Appendix I

```
lucI   GACCATGACCGAGAAGGAGATCGTCGACTACGTCGCCTCCCAGGTCACCACCGCCAAGAA 1620
NcLUC  GACCATGACCGAGAAGGAGATCGTCGACTACGTCGCCTCCCAGGTCACCACCGCCAAGAA 1532
       ************************************************************

lucI   GCTCCGCGGCGGCGTCGTCTTCGTCGACGAGGTCCCCAAGGGCCTCACCGGCAAGCTCGA 1680
NcLUC  GCTCCGCGGCGGCGTCGTCTTCGTCGACGAGGTCCCCAAGGGCCTCACCGGCAAGCTCGA 1592
       ************************************************************

lucI   CGCCCGCAAGATCCGCGAGATCCTCATCAAGGCCAAGAAGGGCGGCAAGTCCAAGCTCTG 1740
NcLUC  CGCCCGCAAGATCCGCGAGATCCTCATCAAGGCCAAGAAGGGCGGCAAGATCGCCGTCTG 1652
       ************************************************: *..  ****

lucI   ATCTAG 1746
NcLUC  A----- 1653
       *
```

7.2 Vector maps

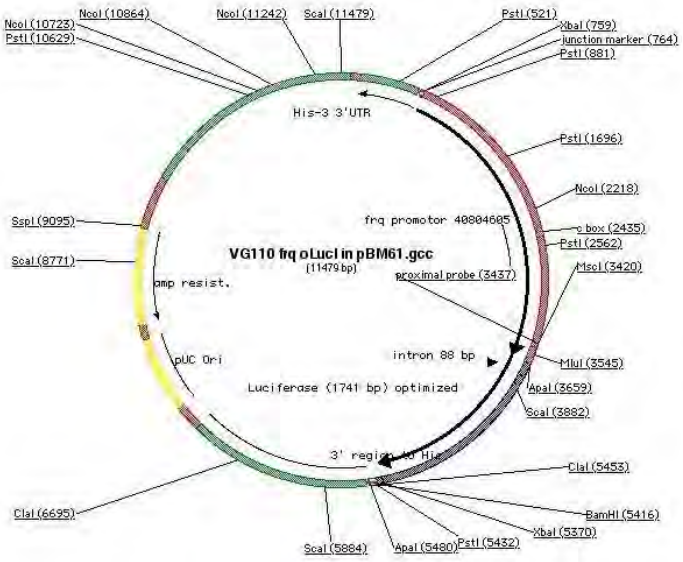

Figure 7.2. Map and restriction sites of the pVG110 vector [136]. The vector is designed for *his-3*-targeted integration in *Neurospora crassa*. Contains the *Neurospora* optimized *lucI* gene sequence [136]. The vector was obtained from the FGSC.

Appendix I

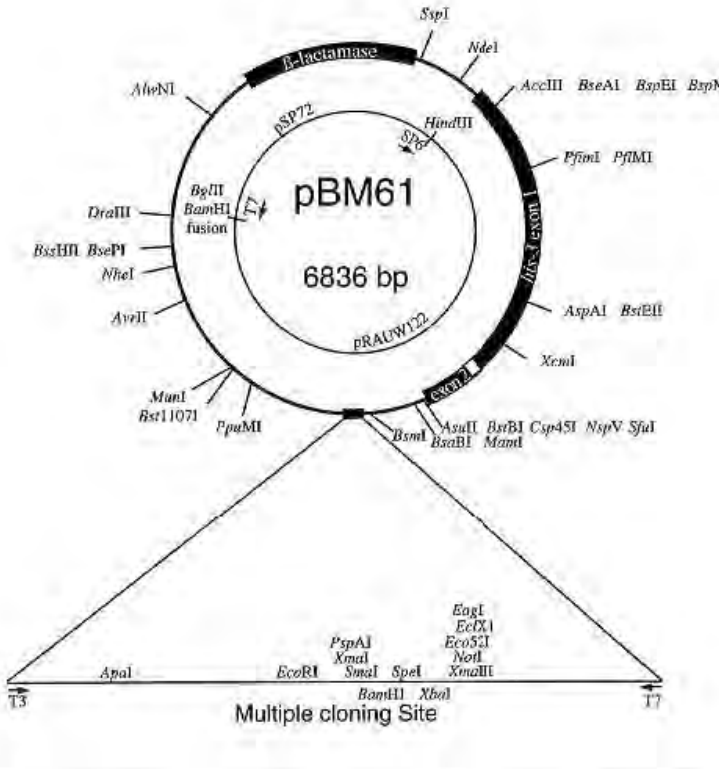

Figure 7.3. Map and restriction sites of the pBM61 vector [143]. The vector is designed for integration at the *his*-3 locus of *Neurospora crassa*. Recognition sites for single-cutting restriction endonucleases in the multiple cloning site are indicated. The vector was obtained from the FGSC.

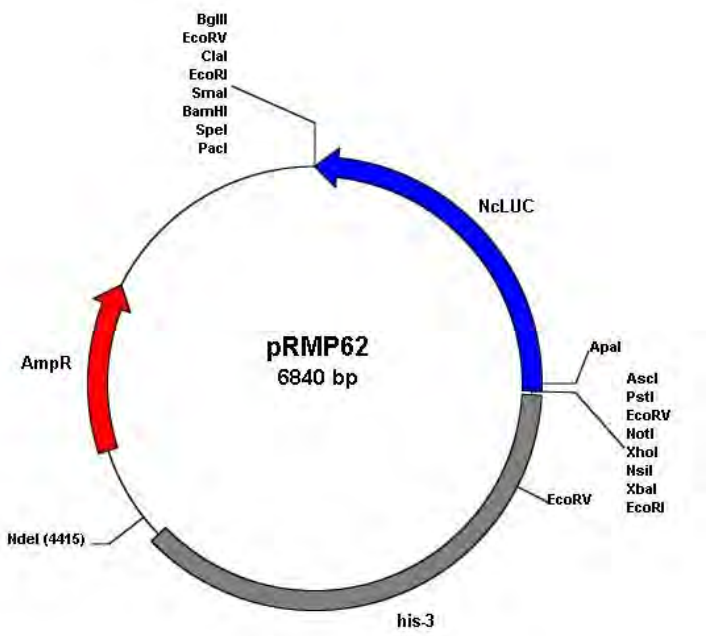

Figure 7.4. Map and restriction sites of the pRMP62 vector. The vector is designed for expression of the codon-optimized *luciferase* (*NcLUC*) in *Neurospora crassa*, and engineered for *his-3* targeted. Unique cloning sites are XbaI, NotI and AscI. The vector was kindly provided by Professor Deborah Bell-Pedersen (Department of Biology, Texas A&M University, USA)

8 Appendix II – Characterization of the promoter-*luciferase* reporter strains

8.1 Characterization of the promoter-LUCI reporter strains

Table 3.1 (section 3.1.3) overviews the *Neurospora* promoter-LUCI reporter strains constructed. All transformants were characterized in liquid culture as described in section 2.7.1.2 and 2.7.2. The strains were inoculated in high sucrose Vogel's medium with 25 mM nitrate as the sole nitrogen source and incubated in LL conditions for 36 h. Following incubation, 1-3 mycelial discs were punched out and transferred to 20 ml low sucrose Vogel's medium with 25 mM nitrate and 25 μM of luciferin added. The signal intensities and oscillatory patterns were assessed. The strains displaying the highest signal intensity were selected for further studies.

8.1.1 The LUCI negative control strains

The construct pLUCI containing solely the *Neurospora* optimized intron-containing *lucI* gene sequences (no promoter inserted) was transformed as a negative control. Four positive transformants designated *LUCI#4*, *LUCI#13*, *LUCI#15* and *LUCI#16* were obtained. Figure 8.1 shows the results from the experiment carried out with the *LUCI* reporter strains. Due to its intensity levels and oscillatory behaviour, the *LUCI#16* strain was chosen for further studies. The results are presented in section 3.3.1.

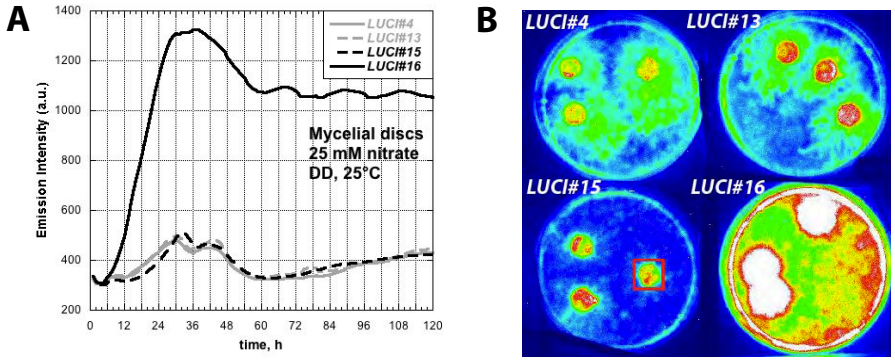

Figure 8.1. Liquid culture experiment performed with the *LUCI#4, LUCI#13, LUCI#15* and *LUCI#16* negative control strains. Mycelial discs grown in Vogel's medium containing 25 mM nitrate and 25 µM luciferin were transferred to DD conditions and then monitored for 120 h. The average emission intensity from the mycelial discs for each of the four strains is shown in panel A. Panel B shows a picture of the last frame taken at the end of the experiment. Colours represent luminescence intensity, white to red being brightest, and blue dimmest. A typical cross section of a mycelial disc shown as a red square.

8.1.2 The cys-3-LUCI reporter strains

The p*cys-3*-LUCI plasmid contained a DNA sequence stretching 1885 bp upstream from the start codon of the *cys-3* gene. The sequence was inserted in front of the intron-containing *Neurospora* optimized *lucI* gene. The transformations yielded the four positive transformants designated *cys-3-LUCI#1*, *cys-3-LUCI#2*, *cys-3-LUCI#3* and *cys-3-LUCI#5*. Figure 8.2 shows the results from the experiment carried out with the *cys-3-LUCI* strains. Due to their intensity levels and oscillatory behaviours, the strains *cys-3-LUCI#1* and *cys-3-LUCI#5* were chosen for further studies. The results are presented in section 3.8.2.1.

The appearance of small amplitude oscillations in *luc* activity in liquid culture was observed in all *luc* reporter strains, under both nitrate and ammonium conditions. The dampened oscillations were more distinct in areas with newly formed hyphae compared to the entire mycelial disc. This is exemplified using the *cys-3-LUCI#5* strain in Figure 8.3.

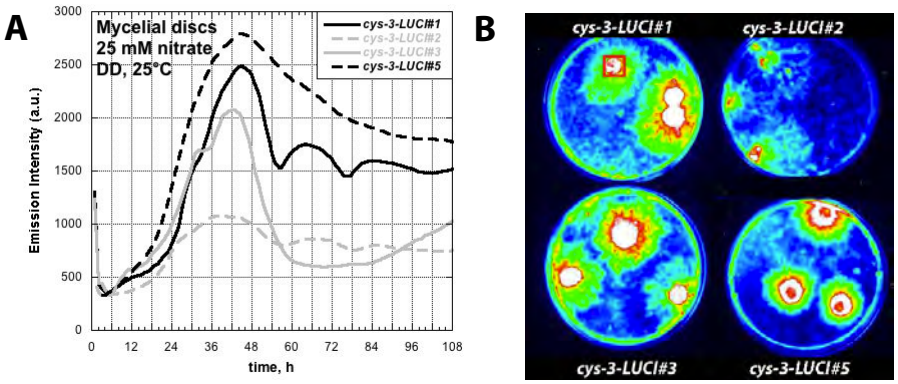

Figure 8.2. Liquid culture experiment performed with the *cys-3-LUCI#1*, *cys-3-LUCI#2*, *cys-3-LUCI#3* and *cys-3-LUCI#5* strains Mycelial discs grown in Vogel's medium containing 25 mM nitrate and 25 µM luciferin were transferred to DD conditions and then monitored for 108 h. The average emission intensity from the mycelial discs for each of the four strains is shown in panel A. Panel B shows a picture of the last frame taken at the end of the experiment. Colours represent luminescence intensity, white to red being brightest, and blue dimmest. A typical cross section of a mycelial disc is shown as a red square.

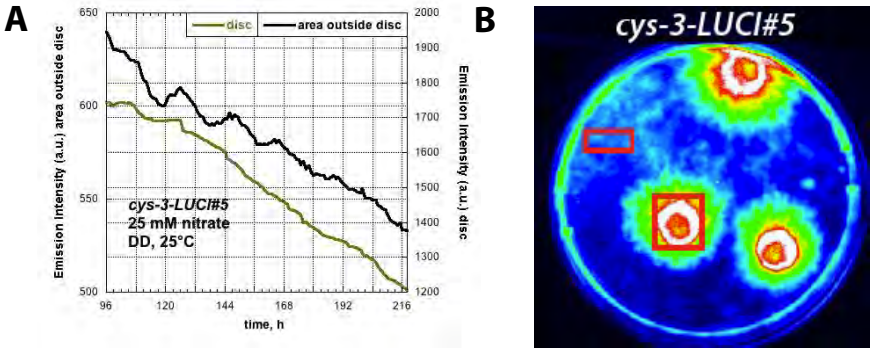

Figure 8.3. Small amplitude oscillations in *luc* activity in the *cys-3-LUCI#5* strain. Panel A shows the emission intensity from 96-218 h in the *cys-3-LUCI#5* mycelial disc, and an area outside of the disc. The areas corresponding to the graphs shown in panel A are indicated in panel B with red squares.

8.1.3 The scon-2-LUCI reporter strains

The p*scon-2*-LUCI plasmid contained a DNA sequence stretching 2106 bp upstream from the *scon-2* start codon. The sequence was inserted in front of the intron-containing *Neurospora* optimized *lucI* gene. The transformations yielded the six positive transformants designated *scon-2-LUCI#1*, *scon-2-LUCI#2*, *scon-2-LUCI#3*, *scon-2-LUCI#4*, *scon-2-LUCI#5* and *scon-2-LUCI#6*. Figure 8.4 shows the results from the experiment carried out with the *scon-2-LUCI* strains. Due to their intensity levels and oscillatory behaviours, the strains *scon-2-LUCI#4* and *scon-2-LUCI#5* were chosen for further studies. The results are presented in section 3.8.2.2.

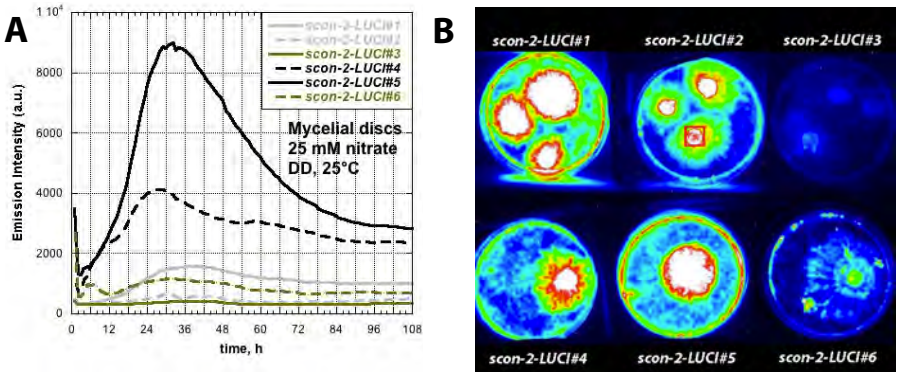

Figure 8.4. Liquid culture experiment performed with the *scon-2-LUCI#1*, *scon-2-LUCI#2*, *scon-2-LUCI#3*, *scon-2-LUCI#4*, *scon-2-LUCI#5* and *scon-2-LUCI#6* strains. Mycelial discs igrown n Vogel's medium containing 25 mM nitrate and 25 µM luciferin were transferred to DD conditions and then monitored for 108 h. The emission intensity from the mycelial discs is shown in panel A (the average of three mycelail discs is shown for *scon-2-LUCI#1*, *scon-2-LUCI#2* and *scon-2-LUCI#3*). Panel B shows a picture of the last frame taken at the end of the experiment. Colours represent luminescence intensity, white to red being brightest, and blue dimmest. A typical cross section of a mycelial disc is shown as a red square.

8.1.4 The nit-3Δ-LUCI reporter strains

The p*nit-3Δ*-LUCI plasmid contained a DNA sequence stretching 1568 bp upstream from the *nit-3* start codon. The sequence was inserted in

front of the intron-containing *Neurospora* optimized *lucI* gene. The transformations yielded the two positive transformants designated *nit-3Δ-LUCI#1* and *nit-3Δ-LUCI#3*. Figure 8.5, panels A and B, shows the results from the experiments performed with the *nit-3Δ-LUCI* strains. Due to its intensity levels and oscillatory behaviour, the strain *nit-3Δ-LUCI#3* was chosen for further studies. The results are presented in sections 3.2.1.1 and 3.2.2.1.

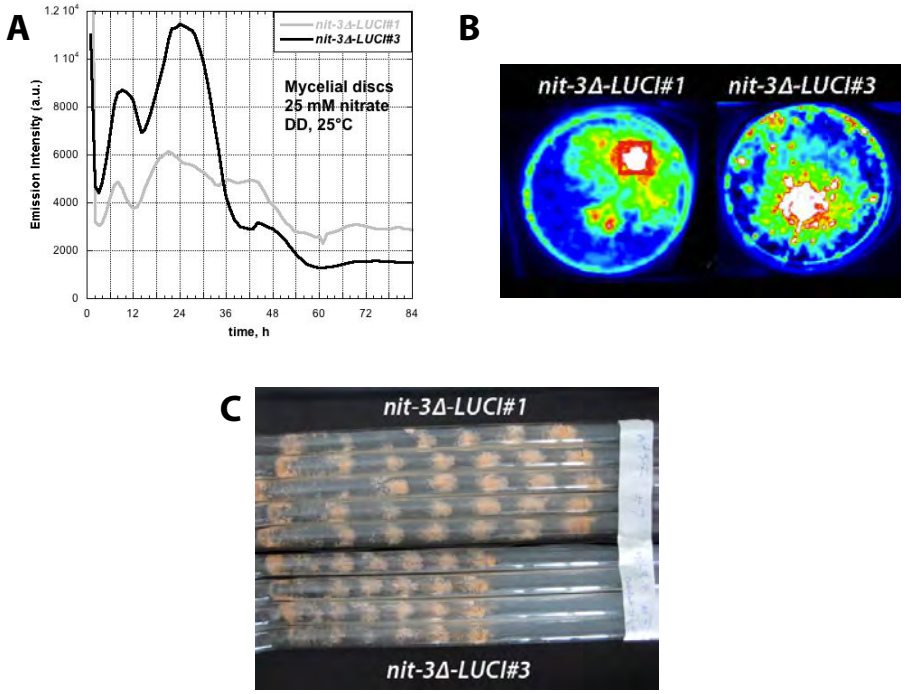

Figure 8.5. Liquid culture experiment performed with the *nit-3Δ-LUCI#1* and *nit-3Δ-LUCI#3* strains. Mycelial discs in Vogel's medium containing 25 mM nitrate and 25 µM luciferin were transferred to DD conditions and monitored for 84 h. The emission intensity from each mycelial discs is shown in panel A. Panel B shows a picture of the last frame taken at the end of the experiment. Colours represent luminescence intensity, white to red being brightest, and blue dimmest. A typical cross section of a mycelial disc used for the emission intensity measurements is shown as a red square. Panel C shows a representative photograph of the growth rate experiment performed with the *nit-3Δ-LUCI#1* and *nit-3Δ-LUCI#3* strains under 25 mM nitrate conditions. The experiment was performed by I. W. Jolma.

Both the *nit-3Δ-LUCI#1* and *nit-3Δ-LUCI#3* strains displayed the *bd* phenotype. The strains were assayed on race tubes under 25 mM nitrate conditions and the growth rates and period lengths were determined. Five parallel race tubes were set up for each strain, and a representative photograph is shown in Figure 8.5, panel C. The *nit-3Δ-LUCI#1* and *nit-3Δ-LUCI#3* growth rates were 3.92±0.21 and 2.75±0.09 cm/day, respectively. The period length was determined to be 22.27±0.31 h for the *nit-3Δ-LUCI#1* strain, and 23.1±0.97 h for *nit-3Δ-LUCI#3*.

8.1.5 Characterization of the nit-3(2.6)-LUCI strain

The *nit-3(2.6)-LUCI* strain was kindly provided by Professor Luis F. Larrondo (Santiago, Chile). The strain was transformed with a DNA sequence stretching 2.6 kb upstream from the *nit-3* start codon, was inserted in front of the intron-containing *Neurospora* optimized *lucI* gene. The strain was inoculated in high sucrose Vogel's medium with 25 mM nitrate as the sole nitrogen source and incubated in LL conditions for 36 h. Following incubation, 1, 2 and 3 mycelial discs were transferred to 20 ml low sucrose Vogel's medium with 25 mM nitrate and 25 μM of luciferin added. The dishes were transferred to DD conditions and monitored for approximately 7 days (169 h). Figure 8.6 shows the result of the experiment.

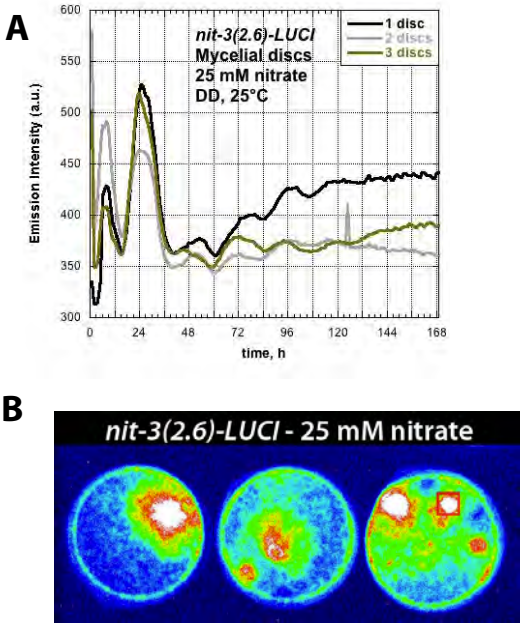

Figure 8.6. Liquid culture experiments performed with the *nit-3(2.6)-LUCI* strain under 25 mM nitrate conditions. The emission intensities of 1 mycelial disc, as well as the average intensity for 2 and 3 discs, are shown in panel A. Panel B shows a picture of the last frame taken at the end of the experiment. Colours represent luminescence intensity, white to red being brightest, and blue dimmest. A typical cross section of a is shown as a red square.

8.2 Characterization of the nit-3-NcLUC reporter strain

The p*nit-3*-NcLUC plasmid contained a DNA sequence stretching 2 kb upstream from the *nit-3* start codon. The sequence was inserted in front of the intron-less *Neurospora* optimized *NcLUC* gene. The sole transformant obtained, designated *nit-3-NcLUC*, was a very slow growing with a very low emission intensity levels. The strain was assayed in both liquid culture under 25 mM nitrate conditions, as well as on race tubes containing 25 mM nitrate and 25 mM ammonium.

8.2.1 Growth in liquid culture

The *nit-3-NcLUC* strain was inoculated in high sucrose Vogel's medium and incubated in LL at 30°C for 60 h. Following incubation, one mycelial disc was punched out and transferred to 20 ml low

sucrose Vogel's medium with 25 µM of luciferin added. The dishes were placed back in LL conditions for 36, 24, 12 and 0 h before transfer to DD (section 2.7.1.2). Two parallels were set up for each time-point, and the dishes were monitored for approximately 6 days (138 h). Figure 8.7 shows the results from the experiment.

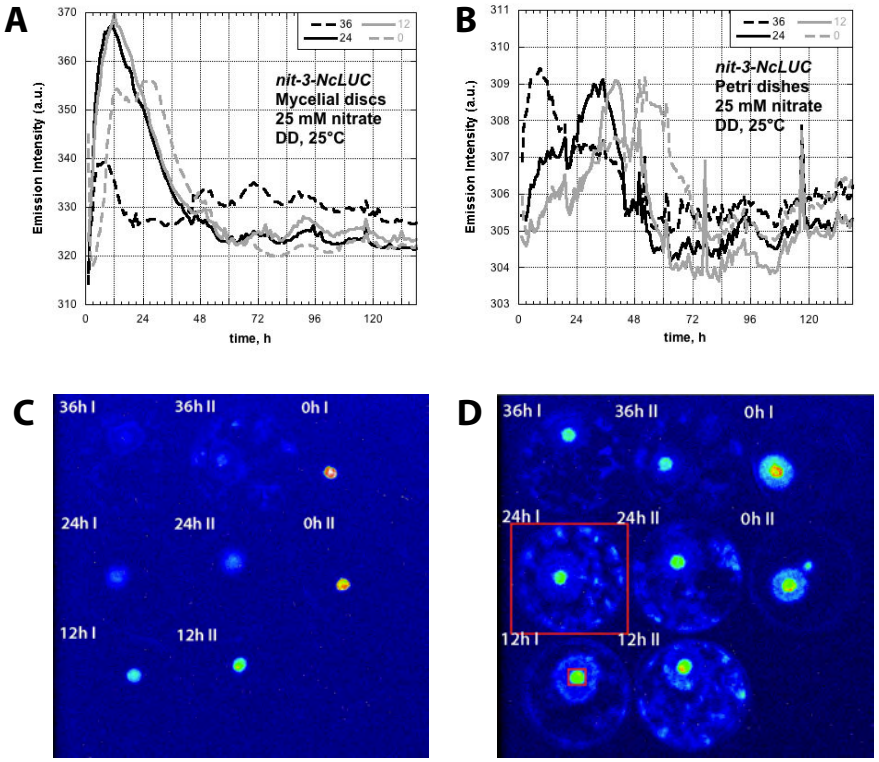

Figure 8.7. Liquid culture experiments performed with the *nit-3-NcLUC* strain in 25 mM nitrate. The average emission intensities of two parallels are shown for the mycelial discs (panel A) and whole Petri dishes (panel B). Panel C shows a picture of the first frame of the experiment taken immediately after transfer to DD. Panel D shows a picture of the frame taken 36 h after transfer to DD. Colours represent luminescence intensity, white to red being brightest, and blue dimmest. Typical cross sections of a Petri dish and a mycelial disc are shown red squares, and hours of incubation in LL are indicated.

8.2.2 Growth on race tubes

A total of twelve race tubes were made (section 2.7.1.3), one half with 25 mM nitrate, and the other half with 25 mM ammonium. Following inoculation, the race tubes were immediately transferred to DD conditions. The emission intensity was monitored for approximately 10 days (250 h). Emission intensity levels were very low with high background. Figure 8.8 shows the result of the experiment.

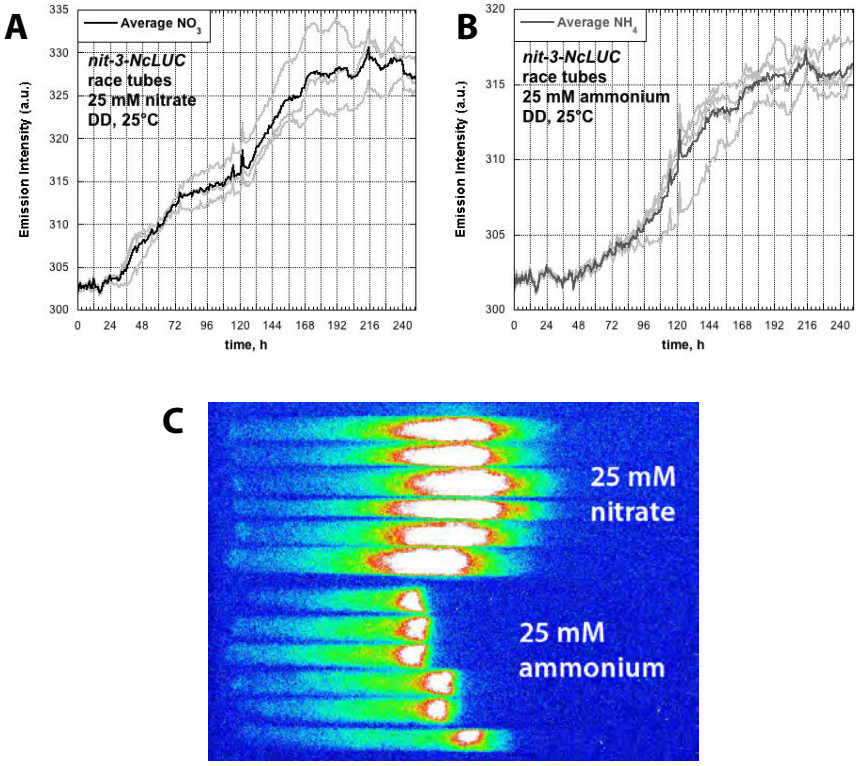

Figure 8.8. Race tube experiments performed with the *nit-3-NcLUC* strain under 25 mM nitrate and 25 mM ammonium conditions. Panels A and B show the average emission intensity in nitrate and ammonium, respectively. Individual race tubes are shown in grey. Panel C shows a picture of the last frame taken at the end of the experiment. Colours represent luminescence intensity, white to red being brightest, and blue dimmest.

Appendix II

9 Appendix III – Experimental validation of the *cys-3* primers used for qPCR

For the comparative C_t method to be valid, experiments to ensure that the assay is indeed quantifying the target gene must be performed. The amplication efficiency of the target primers and of the primers for the endogenous control must be approximately equal. This is tested by using template concentrations covering an area where the expected level of the genes will occur, creating a standard curve for each primer set. The amplification efficiency of the *nit-3* and *L6* primer pairs had previously been determined [83].

The amplication efficiency of the *cys-3* primer pair was determined. The standard curves for the *cys-3* and *L6* primer pairs are shown in Figure 9.1.

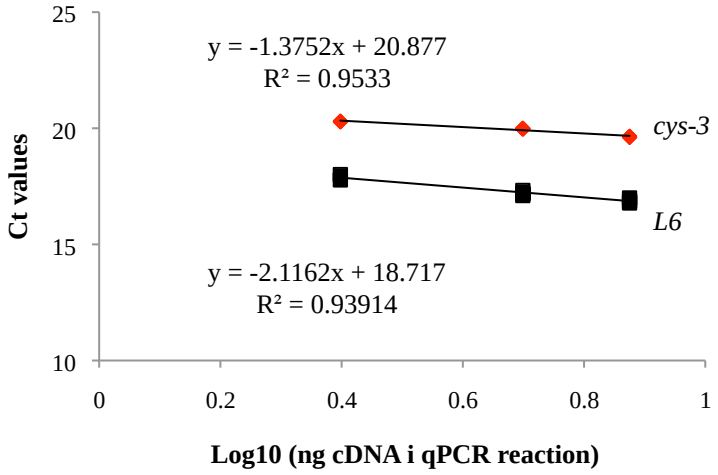

Figure 9.1. Primer efficiency test. The standard curves for the *cys-3* and the *L6* primer pairs.